# Impacts of ENSO on coastal South African Sea

# Surface Temperatures


## Submitted by Belinda Nhesvure

## Supervised by: Prof Mathieu Rouault




**A research report submitted to the Faculty of Science, University of Cape Town, in partial fulfilment of the requirements for the degree of Master of Science in Physical Oceanography**

**Cape Town, 2020**

**DECLARATION**

I, Belinda Nhesvure, declare that this research report is my own work except as indicated in the references and acknowledgements. It is submitted in partial fulfilment of the requirements for the degree of Master of Science in Physical Oceanography at the University of Cape Town. It has not been submitted before for any degree or examination in this or any other university.

Signed by candidate

Belinda Nhesvure

Signed at ……CAPE TOWN……

On the ……11th……. day of ……May ..... 2020

## DEDICATION

This thesis is dedicated to my father Tias Nhesvure who taught me the value of pursuing education and working hard and my mother Phelistus Nhesvure for her endless love, support and encouragement. To my friends and family whose support and encouragement is greatly appreciated. I dedicate this thesis to my husband Tafadzwa and my little baby Munesu Ryan, I love you. Finally, to the Lord Almighty for always answering my prayers and having His mercies grace upon me throughout the journey of my life. Thank you, God.

## ACKNOWLEDGEMENTS

.
I would like to thank my funders throughout this entire project namely ACCESS, Nansen Tutu Center, and NRF SARChI chair on Ocean Atmosphere interaction. This work was supported by EU H2020 TRIATLAS project under the grant agreement 817578. Special thanks to my Supervisor Professor Mathieu Rouault who guided me in this process and encouraged me to work hard, never giving up on me. I would like to thank Serge Tomety, for helping me develop my data analysis skills and for the countless hours spent teaching me to master Matlab. Also, thanks to Department of Oceanography staff members and students who helped me in various ways big and small. Finally, I would also like to thank Professor John Field for helping me with the write up of my thesis and his feedback and corrections.

**ABSTRACT**

The impact of El Niño Southern Oscillation (ENSO) on the Southern African inland climate is well documented and provides skill in the seasonal forecast of rainfall but little is known of the impact of ENSO on the ocean surrounding South Africa. The aim of this study is to assess the impact of ENSO on sea surface temperatures around the coast of South Africa and to calculate SST trends around the coast. I start by updating the study of Rouault et al (2010) on the very topic with an additional 10 years of data and two additional newer datasets which allow sampling closer to the coast where wind-driven upwelling is more active. The new high-resolution ERA 5 reanalyzed climate dataset is also used to look at the atmospheric forcing of sea surface temperatures by ENSO. As in Rouault et al. (2010), I study five similar three-degree-long coastal regions around South Africa, namely: West Coast, South Coast, Port Elizabeth/Port Alfred, Transkei, Kwazulu-Natal and a larger offshore Agulhas Current area domain. Three SST datasets are evaluated in this study: the 1˚x1˚ Optimal Interpolation sea surface temperature (OI SST) used by Rouault et al (2010), the 0.25˚x 0.25˚ Optimal Interpolation SST and the 4 km x 4 km Advanced Very High-Resolution Radiometer (AVHRR) Pathfinder SST version 5.3. The 0.25˚x 0.25˚ OI SST resolves SST anomalies better in these coastal regions as compared to 1˚x1˚ OISST. The difference in results among the three products concerning trends and correlation with ENSO is a cause for concern. The 4 km x 4 km AVHRR Pathfinder allows for SST to be extracted even closer to the coast but missing values are numerous and hamper the use of this dataset for ENSO composites and trend analyses. Results show a significant positive correlation with El Niño in summer at the monthly scale, reaching a maximum correlation of 0.45 at 3 months lag. Correlation is the highest in late summer. There is a negative correlation in the Agulhas Current area, opposite to those with ENSO and West Coast. The impact of ENSO on the coast of South Africa, West Coast and South Coast is due to change in surface wind speed with weaker upwelling favorable during El Niño leading to warmer than normal coastal water SST and stronger than normal South-easterly winds during la Niña leading to cooler than normal coastal water. The wind perturbation is part of largescale basin-wide perturbations in the tropical Atlantic, in the South Atlantic high-pressure atmospheric system and in the westerly wind pattern of the midlatitude to the south. Non-ENSO related impact can be as important as ENSO related SST perturbation and is also linked to large scale perturbations in the South Atlantic. There is no relation between the strength of ENSO and the strength of the perturbation, and some ENSO events do not lead to the expected canonical warming or cooling. The large-scale SST perturbations seem to be caused by anomalous surface turbulent flux of latent and sensible heat and abnormal wind speed and direction. This study opens the possibility of seasonal forecasting of SST in the South Benguela upwelling system because of the positive lag

correlation between ENSO and SST with ENSO leading SST.

## CHAPTER 1: INTRODUCTION

South Africa has 3 600 km of coastline and 275 000 km2 of ocean shelf area. Most fish are found on the shelf. Fisheries contribute significantly to the South African economy according to the Food and Agriculture Organization of the United Nation (www.fao.org), 100 000 persons are employed in the fishery related economy with about 1 500 000 recreational fishermen. The main fishes are anchovy, hakes and pilchard which are offshore species found in the upwelling region of the Benguela Current (Mead et al. 2013; Blamey et al. 2014; Kainge et al. 2020). Whale- and shark-watching are also an important contribution to the coastal economy especially with nearshore fish species, crayfish or abalone becoming scarcer due to overfishing and poaching and maybe climatic changes (Mead et al. 2013; Blamey et al. 2014). Aquaculture does not contribute much to the fishery economy but could in future play an important role. South Africa waters are one of the most productive areas in the world due to the wind-driven upwelling of nutrient rich water along the west coast in the Southern Benguela Current (Hutchings et al. 2009; Veitch et al. 2009). Once it reaches the upper ocean where there is enough sun and photosynthesis can occur, the nutrients help the growth of phytoplankton which is eaten by zooplankton the main source of food for small fish Small fish are then eaten by big fish and the excrement and decaying material of all those living creatures produce nutrients which sink to the bottom of the shelf unless upwelling brings them back to the surface. The Benguela Current is an eastern boundary current along with the Humboldt Current the California Current and the Canary Current, all wind driven upwelling systems. In the Benguela the wind is mostly southerly and upwelling favorable in summer. In brief, due to the Coriolis Effect, the resulting effect of the southerly wind that flows along the coast is to push the surface water away from the coast and because the ocean needs to stay flat some water must replace that westward moving water and it can only come upwards vertically along the coast which acts as a wall. The coast also reduces wind speed by friction creating a wind stress curl that also creates upwelling. For that matter, Sea Surface Temperature (SST) is a good indication of the strength of the upwelling. The stronger the southerly wind component, the colder the upwelling in most of the Benguela Current. In winter in the Southern Benguela the wind is mostly north-westerly and is not upwelling favorable (Hutchings et al., 2009). In their study, Rouault et al. (2010) found that El Niño warmed the coastal waters in the western region of the South African coast due to weaker upwelling favorable south easterly winds, while La Niña was associated with a cooling and stronger south-easterly winds. The change of wind was linked to shifts in the atmospheric high-pressure system over the South Atlantic (Dufois and

Rouault, 2012). Recently Duncan et al. (2020) have linked La Niña to intense upwelling events along the south coast of South Africa. On a seasonal to interannual time scale, predictability of rainfall in South Africa is made possible because of the influence of the El Niño–Southern Oscillation (ENSO). ENSO has had a significant effect on rainfall and temperature variability over the Southern African region. Many studies have shown that interannual variability in rainfall is influenced by ENSO in the austral summer with El Niño generally but not all the time creating drought in the summer region of Southern Africa and La Niña leading to above rainfall there (Fauchereau et al., 2003, Rouault and Richard, 2003, 2005, Pohl et al., 2010, Crétat et al., 2012, to name a few) . Less was done to link ENSO to regional coastal ocean (Rouault et al., 2010, Dufois and Rouault, 2012, Blamey et al., 2014, Duncan et al., 2020)). Rouault et al. (2009, 2010), updated by Blamey et al. (2014) indicate that since the 1980s the Agulhas Current and the coastal region adjacent to the Agulhas current (Kwazulu-Natal and Transkei has warmed up significantly while the West Coast, South Coast and coastal area up to Port Alfred to the east has cooled down. This hypothesis has been found to be linked to a migration of cold-water species from west to east and a migration of warm- water and tropical species from east to west (Blamey et al., 2014). However, Blamey et al. (2014) indicate serious problems in the validity of the SST dataset around Southern Africa for trend studies.

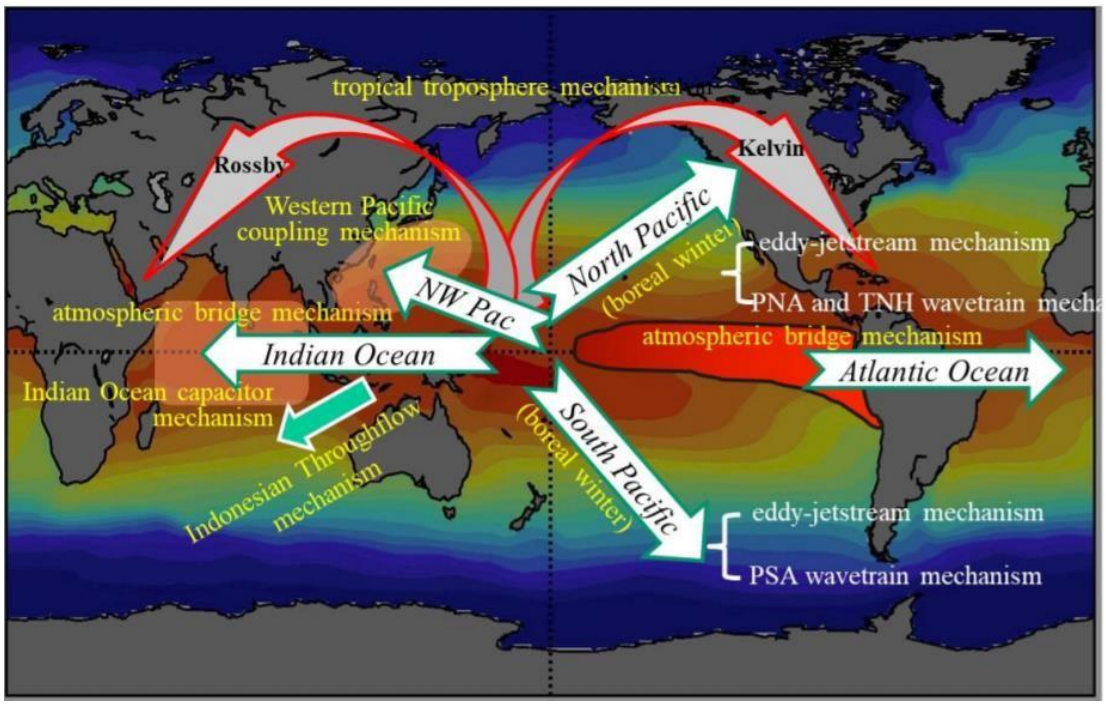


*Figure 1. Major teleconnection mechanisms driving global ENSO effects. Adapted from 'El Niño- Southern Oscillation and Its Impact' (The Changing Climate, 2018, Geosciences, p.45)*

ENSO consists of 3 phases namely El Niño, La Niña and the ENSO neutral phase. El Niño, which means "Christ Child" (Dijkstra, 2006) in Spanish, has no global definition although it has been widely used by many authors. Philander (1990) defined El Niño as "a combination of

anomalously warm sea temperature, stronger than usual southward coastal current, high rainfall and floods in Ecuador as well as in northern Peru". Ocean- atmosphere interaction is an essential part of El Niño and La Niña events. Sea level atmospheric pressure tends to be lower in the eastern Pacific and higher in the western Pacific during an El Niño, while the opposite tends to occur during a La Niña. The Southern Oscillation (SO) is characterized by an interannual fluctuation in atmospheric pressure between the tropical Pacific (eastern and western parts), characterised by weakening and strengthening of the easterly trade winds. The warm phase of ENSO is known as El Niño and the cold phase La Niña. The tropical tropospheric warming mechanism and tropical cooling mechanism are responsible for spreading ENSO signals to other ocean basins by propagation of Kelvin and Rossby waves in the tropical troposphere (Chiang and Sobel, 2001). Warming and cooling caused by El Niño and La Niña first cause changes in temperatures in the troposphere over the tropical central-eastern Pacific (Yulaeva and Wallace, 1994). SST changes the atmospheric pressure and by a domino effect changes the global atmospheric circulation poleward by modification of the Hadley Circulation and along the Equator by modification of the Walker Circulation. This also changes the SST in the Atlantic and Indian Oceans which in turn can modify the Hadley and Walker Circulations; change in the Hadley Circulation will also change the westerly circulation, poleward of the main high-pressure system in those three oceans (Wang et al., 2017). ENSO is known for its impact on the interannual rainfall variability in Southern Africa (Dieppois et al., 2015). ENSO causes drier than normal conditions during an El Niño and wetter than normal conditions during a La Niña event in the summer rainfall regions. Philippon et al.(2012) analysed the relationship between ENSO and South African winter rainfall using daily rainfall data for the period 1950–1999 and they found that the May, June and July seasonal rainfall amount showed a positive correlation with the Niño3.4 index that became significant after the so-called 1976/1977 climate regime shift. Since South Africa's highly variable climate is influenced by broad patterns in the ocean and the atmosphere above it, some of these patterns are not only more obvious than others but they are also predictable; we call these our climate drivers. There is predictability in the seasonal to interannual variability of climate due to the influence of ENSO (Landman and Mason, 2001, Landman et al., 2019) which tends to start months before the austral summer. EL Niño also matures during the austral summer having therefore the strongest influence on the atmosphere and rainfall of the Pacific. The austral summer is the main upwelling season and main summer rainfall season in Southern Africa. For the most part, seasonal rainfall forecasting skill is a result of these models' ability to capture the influence of the ENSO events over the region (Johnston et al., 2004). Predictability may be improved by the development of state-of-the-art Earth System models or coupled ocean-atmosphere interaction models. Recent forecasts have shown skill in predicting above- or below-normal rainfall and temperature for the coming season mostly

during ENSO periods (Landman et al., 2019). This has been exploited operationally by weather services in southern Africa for the prediction of rainfall and droughts. Correlation between ENSO and rainfall is in the same order of magnitude as correlation with SST found by Rouault et al. (2010) and Rouault and Dufois (2012). There is a need for further research on southern African seasonal climate anomalies for forecasting purposes and therefore further research is required on the impacts of ENSO on the seasonal to interannual variability of SST which has not attracted the same attention as rainfall. ENSO already provides the opportunity to forecast rainfall in Southern Africa and provides a learning opportunity for societal application (Landman et al., 2019).

The aim of this study is to better understand the impact of ENSO on South Africa coastal regions at different lags and update SST trend analyses done so far in the region. This may open the road to operational forecasting of SST in South Africa. New long-term datasets starting in 1982 allow us to study the ocean domain closer to the coast where the upwelling is more active; these are now available from Rouault et al. (2010) who used 1˚x 1˚resolution Optimally Interpolated (OI) SST (Reynolds et al., 2002); 0.25˚x 0.25˚OI SST has now been available since 1982, at the beginning of the satellite era. A new version of 4 x 4 km resolution AVHRR Pathfinder SST (Pathfinder SST Version 5.3) is also now available. The three datasets will be compared and used for trend detection to update Rouault et al. (2010) with 10 more years data available now to study the impact of ENSO on the coast in more detail. The closer to the coast in a coastal upwelling area, the cooler the water and the more important the wind effect. Most of the productivity is found very close to the coast and that is why it is so important to monitor changes close to the coast. Also missing data in OI SST due to clouds and sunglint is filled up by interpolating data in a 300 km radius so it is hoped that the 0.25˚ x 0.25˚ OI SST is more accurate. Pathfinder SST does not use interpolation for missing data at all so has a lot of missing data. The study complements and updates previous analyses on ocean climate change and variability around the coast of South Africa (Rouault et al., 2010, Dufois and Rouault (2012), Blamey et al., 2014). No lag correlation study was done, and little was done to find out the origin of the correlation with ENSO and mechanisms behind it, or the atmospheric forcing underpinning it. Here I will use new high resolution ERA-5 reanalysed climate data to look at large scale wind speed, geopotential height and surface air-sea turbulent flux of latent and sensible heat to link the coastal change to basin-wide scale perturbations during El Niño and La Niña events in all of the South and Tropical Atlantic Ocean.

The outline of the study is as follows: the introduction chapter is followed by a data and methods chapter. The results chapter starts with a comparison of the annual cycle of the three

datasets. It is followed by an SST trend analysis for the region. This prompts me to detrend the data for the rest of the study that focuses on monthly and seasonal anomalies of SST by means of time series analyses in the 6 domains and latitude-longitude regional charts analysis at the seasonal scale. I first focus on the average of February, March and April (FMA), the late summer season, following Rouault et al (2010). Composite El Niño and La Niña charts are compiled to look at the average or canonical effect of El Niño and La Niña on the region and in the South Atlantic. Interesting summer (FMA) season years are singled out and studied. A lag correlation is then done for all six domains for all summer months and the two OI SST datasets only. At last I use ERA-5 reanalysis climate data to look at mechanisms behind the change of SST during El Niño and la Niña in early summer, late summer and for all summer and to investigate whether the coastal changes are part of a large- scale signal. A discussion chapter follows as there are many issues to discuss in the data used, the methodology used and the literature. A conclusion chapter closes the study.

## CHAPTER 2: DATA AND METHODS

### 2.1 Study Area and Sampling Method

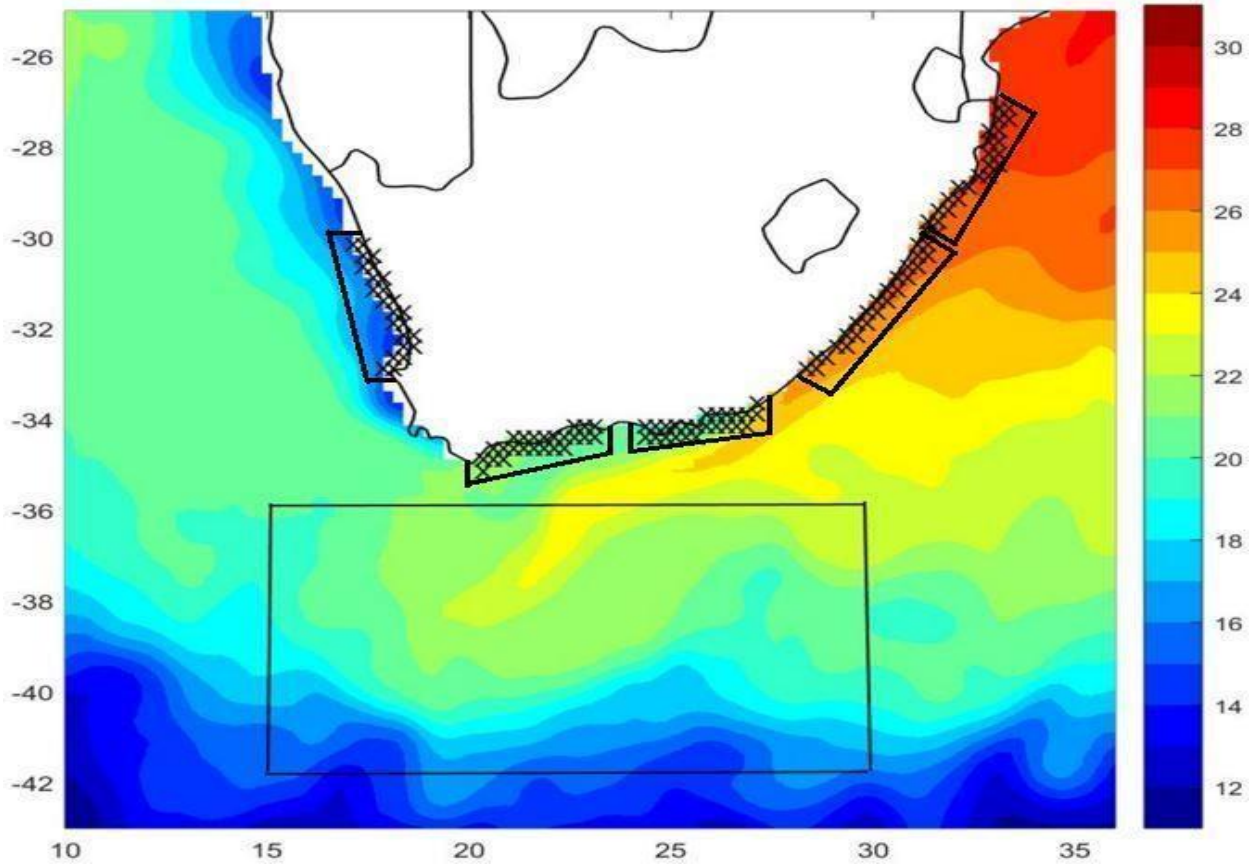


*Figure 2. Location of the 6 domains studies used by Rouault et al (2010) and this study for 1˚ x1˚ OI SST (solid line) and data points(crosses) used with 0.25˚x0.25˚ OI SST dataset. From west to east: West Coast, South Coast, Port Elizabeth/Port Alfred, Transkei Kwazulu-Natal and Agulhas Retroflection domain (rectangle). The mean 0.25 ˚x0.25˚ austral summer OI SST is plotted in color.*

The six domains chosen for this study are from west to east: West Coast, South Coast, Port Elizabeth/Port Alfred (PE/PA), Transkei, Kwazulu-Natal and the Agulhas Current. The sampling method used for this study is the same as in Rouault et al. (2010). Each domain along the coast has approximately the same width of 3° but varies in offshore extent according to dataset. The Agulhas Current system domain is extracted from 36° to 42° South and 15° to 30° East. It is interesting to note from Figure 2 that this the Agulhas Retroflection domain is more centred on the retroflection region than the core of the Agulhas Current system and that the 0.25° x 0.25° OI SST allows sampling the Agulhas current better than the 1˚x 1˚OI SST that misses the core of the current (Rouault et Lutjeharms, 2003, Rouault et al., 2003). When using the 1° x 1° OI SST the domain is of course 1° exactly as in Rouault et al. (2010) and correspond to 3 OI SST points per coastal domain included in the solid line of Figure 2. When using the 0.25° x 0.25° OI SST, it is 0.5° to get closer to the coast. The 0.25° x 0.25° OI SST

represents the upwelling better that the 1° x 1° OI SST with cooler water inshore but still an underestimation of near coastal water when compared with high resolution climatology (Dufois and Rouault, 2012, Pfaff et al., 2019). When using the 4 km x 4 km AVHRR pathfinder dataset the domain is still 0.125 ° wide, about 25 km wide, because of the large number of missing data near the coast. This also will be discussed.

## 2.1 Data

The rationale behind choice of 0.25° x 0.25° OI SST and Pathfinder SST is that they are the only products available from 1982 with higher resolution than 1° x 1° OI SST, an important requirement for climatological and trend purposes. The spatial extent of higher resolution datasets is reduced towards the coast to allow sampling closer to the coast where upwelling is more active and changes in wind speed should have more effect on SST. This should improve the results of Rouault et al. (2010) especially trends should be clearer and correlation with ENSO stronger. What prompted Rouault to take those domains was just that one dataset of low resolution was available at that time and the regions were systematically taken to encompass all the South African coastline with domains of the same dimension separated by 1 degree. The new datasets follow the same coastal length but are closer to the coast.

### 2.1.1 NOAA Optimum Interpolated (OI) Sea Surface Temperature

Two of the SST datasets used in this study were obtained from the National Oceanic and Atmospheric Administration (NOAA). These datasets were created using a combination of estimation from the Advanced Very High-Resolution Radiometer (AVHRR) instrument flying on various consecutive NOAA satellites and observations from ships and buoys averaged on a regular global grid with missing data filled up by interpolation. The 1°x1° Optimum Interpolation (OI) SST version 2 dataset, also called Reynolds SST (Reynolds et al. 2002) is available at NOAA. The SST monthly means have a resolution of 1°x1° on a global grid and are available from 1982 to the last month. The 0.25°x0.25° OI SST dataset (Reynolds et al. (2007) ; Banzon et al. (2016) ) is available as daily anomalies in near real time and is downloaded from: https://www.ncei.noaa.gov/data/sea-surface-temperature- optimum-interpolation/access/ . Both datasets are widely used and have limitations in coastal upwelling regions near the coast (Dufois et al., 2012, Blamey et al., 2014, Meneghesso et al., 2020) but not many SST datasets are available for a period long enough for climate studies. I am using data from 1982 to 2017 in those studies that compare datasets, and the up to 2019 in the latest part of the study when I only use the 0.25°x0.25° OI SST.

### 2.1.1 4x4 km resolution AVHRR SST Data

Due to its high spatial resolution and ability to show SSTs along coastal areas, I also used the AVHRR Pathfinder SST version 5.3 obtained from: https://data.nodc.noaa.gov/cgi-bin/iso?id=gov.noaa.nodc:AVHRR_Pathfinder-NCEI-L3C-v5.3.

The 4km resolution SST dataset, which is generated using the same polar orbiting NOAA satellites, is available from 1981 to 2017. The data are twice daily (day and night) and are produced by the NOAA National Center for Environmental Information (NCEI); monthly means are calculated from these daily values. The 4x4 km resolution AVHRR SST dataset has some limitations as it contains sparse values and some missing data due to adverse weather conditions such as cloud cover; regions with high SST gradients are also sometimes discarded which is a problem in upwelling regions leading to a warm bias (Dufois et al., 2012, Smit et al., 2013, Meneghesso et al., 2020).

### 2.1.2 Climate Index

The seasonal (February, March, April) Ocean Niño Index is used in this study to highlight El Niño and La Niña events from 1982 to 2017. The Oceanic Niño Index (ONI) is one of the primary indices used for monitoring ENSO. It is calculated by averaging SST anomalies in the Niño-3.4 region from 5S to 5N and 170W to 120W. A 3-month time average anomaly from the running mean is then calculated. El Niño and La Niña are classified based on exceeding SST anomalies above a threshold in the east-central equatorial Pacific Ocean; SST anomalies equal to or greater than 0.5°C in the Niño-3.4 indicate ENSO warm phase (El Niño) conditions while anomalies less than –0.5°C indicate cool phase (La Niña) conditions, whilst anomalies in between these thresholds are known as neutral conditions. ONI is a well-used index and the region Niño3.4 which is in the warm water of the Pacific away from the coast has been used to correlate the Southern African Climate to ENSO on numerous occasions (Fauchereau et al., 2003, Rouault and Richard, 2003, 2005, Pohl et al., 2010, Crétat et al , 2012). The ONI index used here is available in gridded format and was obtained from the CPCP NCEP web site at https://origin.cpc.ncep.noaa.gov/products/analysis_monitoring/ensostuff/ONI_v5.php.

### 2.1.3 ERA 5 reanalysis

A reanalysis is like a weather forecast run retrospectively using historical observations and satellite estimates assimilated in a state-of-the-art model. ERA 5 is the latest reanalysed climate dataset. It gives monthly estimates of many atmospheric, land and oceanic climate

and weather variables. Data is provided on a 30km grid and there are 137 levels in the atmosphere. ERA 5 replaces the ERA Interim reanalysis that not updated anymore. Several problems in the region at the surface using the ERA Interim were pointed out by Imbol Nkwinkwa et al (2019) leading to underestimation of surface wind along the coast and above the Agulhas Current. The first reanalyses were of 2.5-degree resolution such as NCEP 1 and 2 and ERA 40. Newer reanalyses CFSR, ERA Interim, MERRA and JERA have a third of a degree grid. Data used are 1000 hPa and 850 hPa geopotential heights which characterised the atmospheric pressure near the surface and around 1500 m respectively. These are good heights for studying high pressure systems and low-pressure systems other than cut-off lows. I use wind speed and direction at these two heights, the air-sea turbulent flux of latent heat, also called turbulent flux of moisture and the air sea turbulent flux of sensible heat.

### 2.2 Method

Using the three SST datasets, I assess the variability of Pathfinder SST for the period 1982 to 2017. Although OI SST data are available in almost real time, Pathfinder SST is only available until 2017. The annual cycle is calculated by doing simple monthly means and monthly standard deviations. Trends are simply calculated using a linear trend which is like fitting a straight line in a dataset and calculating the slope of the line. Data are presented in degree Celsius per decade (10 years). Monthly temperature anomalies are calculated by subtracting the mean monthly 1982 to 2017 climatology of a particular month and dividing the results by the standard deviation of the same month to normalise the time series so 1 corresponds to 1 standard deviation above normal and -1 correspond to 1 standard below normal. 66.6 % of the data are found within 1 and -1 standard deviation. Data are linearly detrended in order to remove a long-term trend. This is the same method used by Rouault et al. (2010). To assess the effects of ENSO on SST during the austral summer season, which is known to be the peak of El Niño and La Niña events (Cai et al. 2014), seasonal charts (3-month averages) are plotted to give an overview and to show spatial patterns of SST normalised seasonal anomalies (normalised this time by the standard deviation of that season) around South Africa for the period of study. I use mainly FMA (mean of February, March and April) and OND (mean of October, November and December). I use the ONI time series for ENSO to find the correlation between ENSO and SST at monthly and seasonal scales. Composite seasonal anomalies are calculated for FMA and OND and ONDJFMA using all Niño or La Niña years active in the austral summer for El Niño or La Niña seasonal composites and subtracting the corresponding climatological seasonal mean and then dividing by the standard deviation of the same season to normalise the composites. These give the average or canonical effects of El

Niño or La Niña for selected seasons. Lag correlations are also calculated at different times of the month in order to find which months and which domains have the best correlation with ENSO and at what lag.

## CHAPTER 3: RESULTS

### 3.1 Annual Cycle and Trends

Figure 3 shows the annual cycle of sea surface temperatures in the 6 domains which are calculated by averaging all SSTs of all the months from 1982 to 2017, which is 36 years or 36 points. Note that the coastal domains are 3 degree long but 1 degree wide for the 1 x 1˚ OI SST, 0.5˚for the 0.25 x 0.25˚OI SST and 0.25˚for Pathfinder SST.

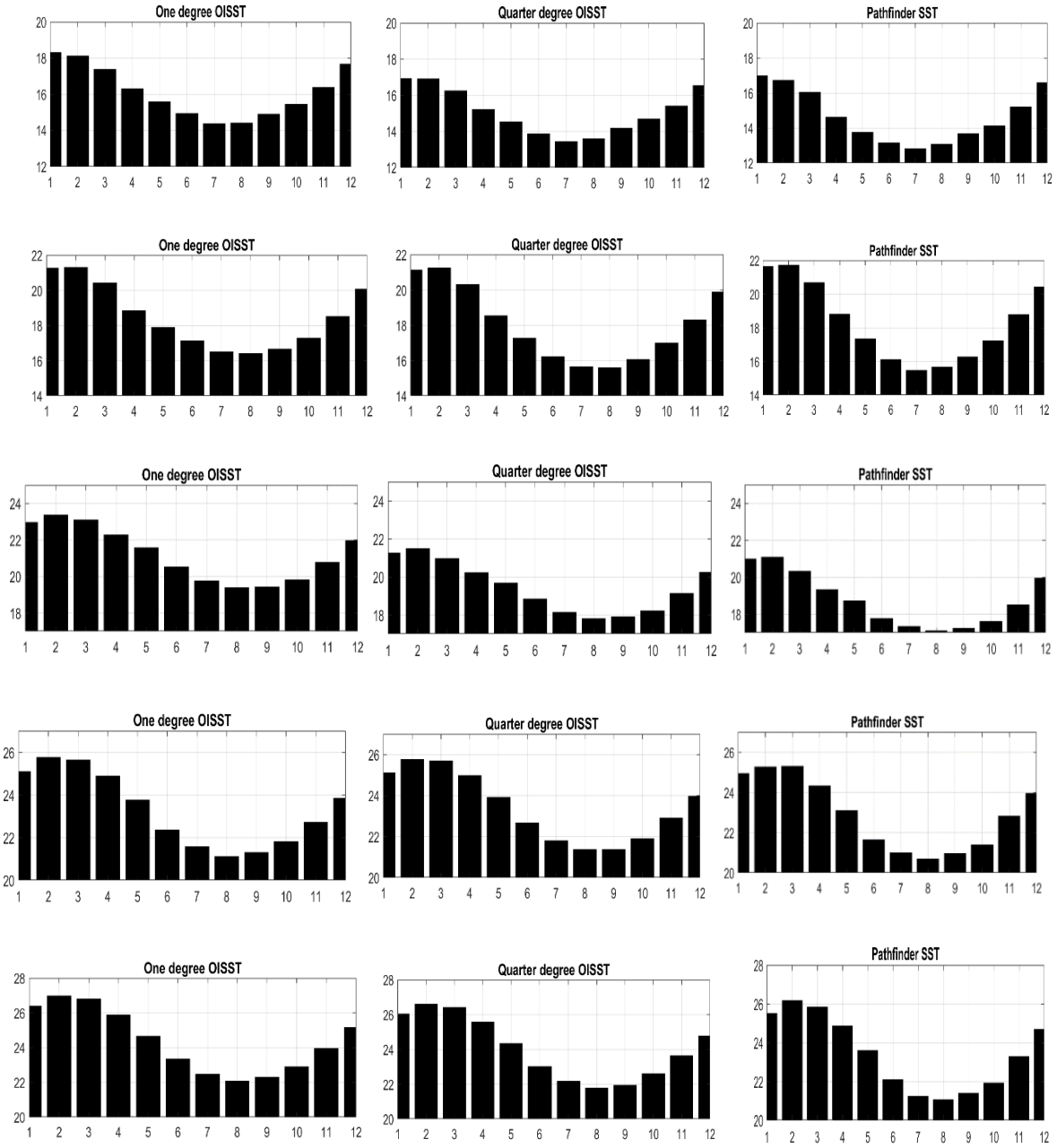

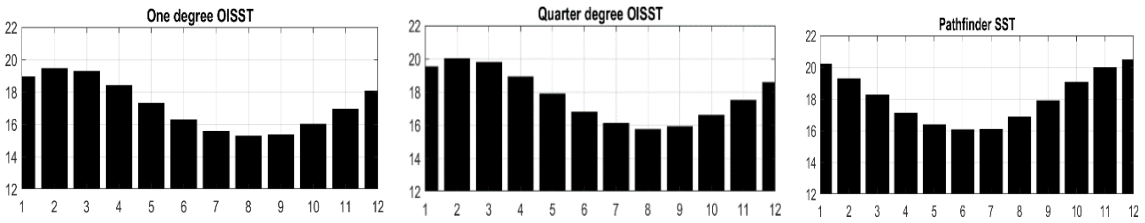


*Figure 3: Mean January to December 1982-2017 annual cycle of sea surface temperature (°C) for each region (top to bottom) for 1X1° OI SST, 0.25°X0.25° OI SST and 4x4 km resolution AVHRR SST (left to right). From top to bottom: West Coast, South Coast, Port Elizabeth/Port Alfred, Transkei, KwaZulu-Natal and the Agulhas Current system domain. X-axis is the month of the year.*

SSTs are clearly warmer for 1 x 1˚OI SST and cooler for Pathfinder SST which makes sense since the water is cooler near the coast than offshore in an upwelling region. We note that in the West Coast upwelling region near the coast the water should be cooler in summer when the upwelling favorable south-easterly wind is stronger, and warmer in winter when north-westerly wind dominates (Dufois and Rouault, 2012, Pfaff et al., 2019). However, to get close to the coast one needs to use 500-meter resolution MODIS SST that is only available since 2000 and full of missing values. Pathfinder SST has also a warm bias near the coast as does AVHRR which is the basis for producing OI SST (Dufois et al., 2012, Meneghesso et al., 2016). Due to the large offshore extend of the upwelling and the large scale forcing, Rouault et al (2010) argued that calculated anomalies represent anomalous events well even though the absolute values are not perfect The annual cycles across all the regions present a similar pattern where maximum temperatures are in October to March and minimum temperatures in the months of June, July and August. In the West Coast region, maximum temperatures occur in January and range from 16 degrees to 18 degrees in the 3 datasets analysed, whilst minimum temperatures range from 12 degrees to 14 degrees in July. The SSTs follow the solar radiation annual cycle and do not follow the upwelling season which is more intense in summer and should lead to cooler SSTs at that time. However, the minimum summer SST only occurs within 10 km of the coast (Dufois and Rouault, 2012, Pfaff et al., 2019). The South Coast, Port Elizabeth/ Port Alfred, Transkei, Kwazulu-Natal and Agulhas Current regions have maximum temperatures ranging from 20 to 28 degrees among the three datasets (1x 1˚ OI SST, 0.25 x 0.25˚ OI SST and Pathfinder SST) and minimum temperatures recorded in these 5 regions range from 16 degrees to 22 degrees. The South Coast annual cycle does not show much difference among the three datasets, although the Pathfinder SST has warmer maxima in summer than the OI SST, which is odd since that region also experiences wind-driven upwelling in summertime. The PE/PA annual cycle has the largest differences between datasets because the 1 x 1˚OI SST is probably affected by the temperature of the Agulhas Current and the Pathfinder SST can better capture the dynamic coastal upwelling of Port Alfred. In PE/PA and South Coast the coast at time in summer can have wind-driven upwelling

when the wind is easterly and upwelling favorable. The annual cycles of OI SST in Transkei and Kwazulu-Natal, which are in the Agulhas Current have the same characteristics as Pathfinder SST, with Pathfinder SST having lower temperatures probably because it is less affected by the Agulhas Current. Being a large domain there is little difference between datasets for the Agulhas Current domain although the pathfinder SST has a maximum at a different time than the OI SST datasets.

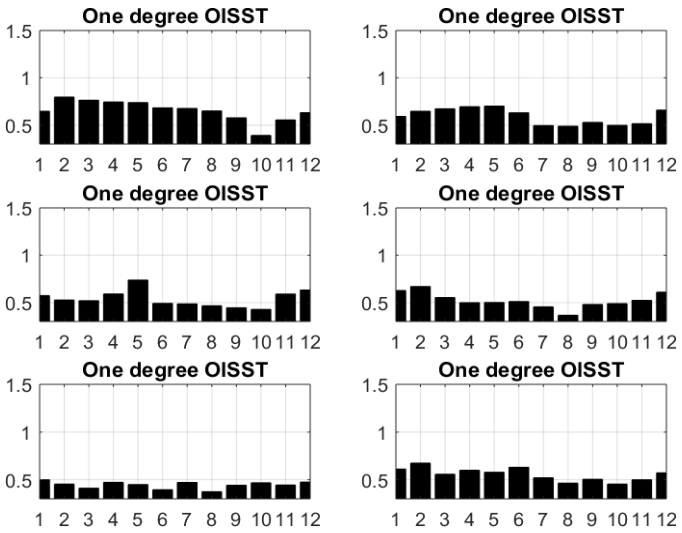


*Figure 4. 1982-2017 annual cycle of the standard deviation of SST (˚C) for 1˚x1˚ OIS ST for West Coast, South Coast, Port Elizabeth/Port Alfred, Transkei, KwaZulu-Natal and the Agulhas Current system domain (left to right and then top to bottom).*

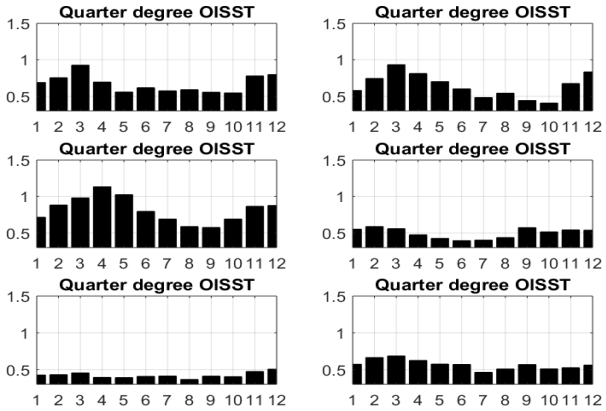


*Figure 5.1982-2017 annual cycle standard deviation of SST (˚C) for 0.25˚x0.25˚ resolution OI SST for West Coast, South Coast, Port Elizabeth/Port Alfred, Transkei, KwaZulu-Natal and the Agulhas Current system domain (left to right, top to bottom).*

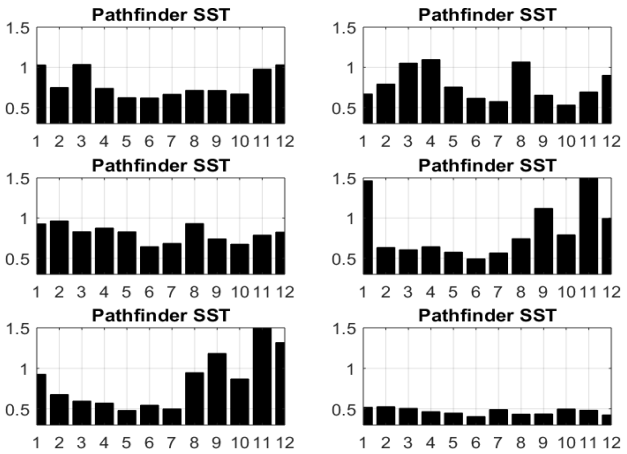


*Figure 6. 1982-2017 annual cycle standard deviation of SST (°C) for 4x4 km resolution AVHRR SST for West Coast, South Coast, Port Elizabeth/Port Alfred, Transkei, KwaZulu-Natal and the Agulhas Current system domain (left to right, top to bottom).*

The monthly annual cycles of standard deviation of SST are presented in Figures 4 to Figure 6 for the 3 datasets, respectively. In general, the standard deviations of the 0.25x0.25 OI SST are higher than the 1x1 degree OI SST and the Pathfinder SST has larger deviations probably because it is closer to the coast but also because there are many missing values which also explains the abrupt variation compared to neighboring months in standard deviations observed for instance in August for South Coast, or January for Transkei. For the large Agulhas Current domain all three datasets have similar standard deviations which seems logical given the large domain. For the 1x1 OI SST the West Coast has the highest standard deviation around 0.5 to 0.8 $^{o}$C with maximum in late summer (FMA) which is end of upwelling season and probably the most likely season to have a lot of variation. The 0.25$^{o}$ x 025$^{o}$ OI SST has a higher standard deviation because it can also represent the coast better than the 1$^{o}$ x 1$^{o}$ OI SST. The biggest difference between the two OI SST datasets is for PE/PA, again because the 1 degree is probably contaminated by the Agulhas Current as missing values are replaced by surrounding data in a 300 km radius. For Kwazulu-Natal and Transkei all datasets have similar annual cycles of standard deviation which is most probably due to the influence of the Agulhas Current, which has little interannual variation in those domains and because it is a deep warm current which is difficult to cool by the atmosphere (Rouault and Lutjeharms, 2003). The 0.25$^{o}$ x 0.25$^{o}$ OI SST has a more distinct annual cycle of standard deviation there. Focusing on the 0.25$^{o}$ x 0.25$^{o}$ OI SST, the West Coast minimum standard deviation is 0.1 $^{o}$C in March and the maximum is 0.5 $^{o}$C in October. For the South Coast, the maximum standard deviation is 0.9 $^{o}$C in March and the minimum is 0.25 $^{o}$C also in October. For PE/PA, the maximum standard deviation is 1.1 $^{o}$C in April and the minimum is 0.6 $^{o}$C in September. For the Transkei the maximum standard deviation is 0.6 $^{o}$C in February and the minimum is 0.25 $^{o}$C in June. For Kwazulu-Natal, the annual cycle is quite flat, the maximum standard deviation is 0.5 $^{o}$C in September and minimum is 0.2 $^{o}$C in August, For the Agulhas Domain, the maximum standard

deviation is 0.7$^0$C in March and the minimum is 0.5 $^o$C in July. The annual cycle of standard deviation provides some interesting information. First on the differences between datasets, second because the timing of maximum and minimum of standard deviation or the amplitude of the annual cycle provides information that is useful for forecasting. For instance, more variation is expected in late summer in upwelling regions than in winter and autumn. More variation in SST is also expected in upwelling regions than in regions affected by the Agulhas Current. The value of standard deviations will be kept in mind when looking at the rest of the document which presents normalised anomalies (anomalies divided by standard deviation). Third, the abrupt variation in Pathfinder SST could be an indication of too few valid data points near the coast for averaging the domains.

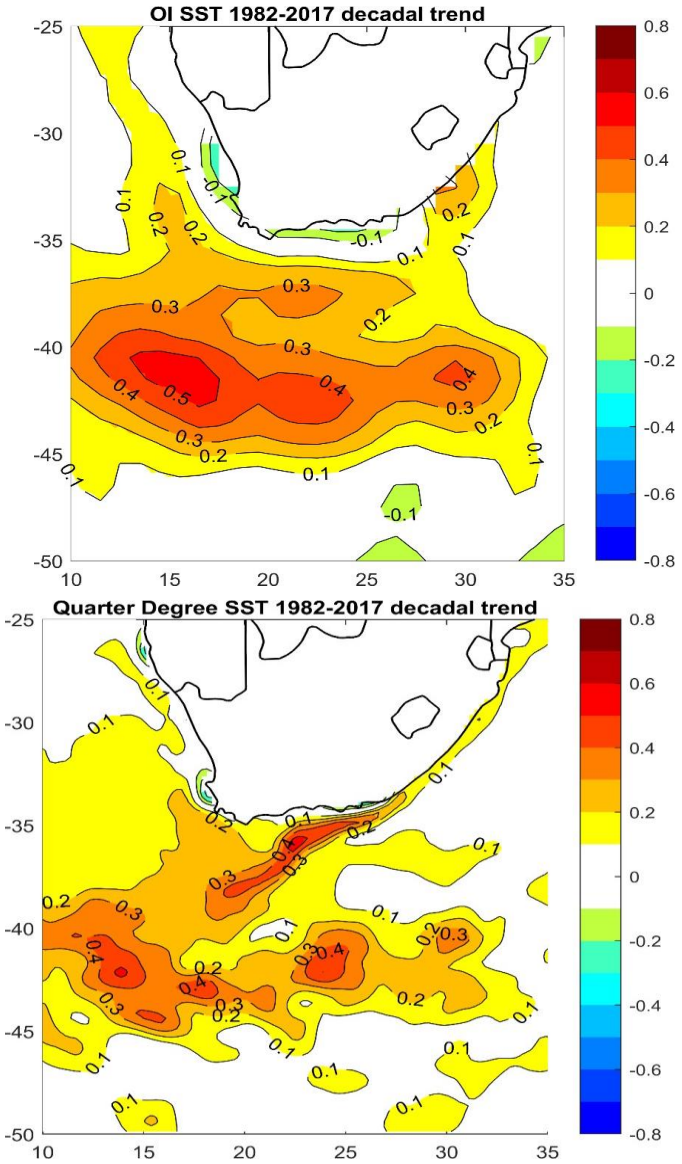


*Figure 7. Linear trends of sea surface temperature from 1982 to 2017 using 1˚x1˚ degree OI SST (top) and 0.25˚x 0.25˚ OI SST (left) in˚C per decade.*

Figure 7 shows the linear trend in SST in degrees per decade (10 years) using the 1 x 1˚OI SST and the 0.25˚x 0.25˚OI SST datasets available from 1982 to 2017. With 10 more years of data the regional trend using 1˚ x 1˚OI SST is similar to Rouault et al (2010) with cooling of about 0.3 ˚C per decade in the West Coast, South Coast and PE/PA areas and a warming in the Agulhas Current domain of up to 0.53 ˚C per decade in the retroflection region of the Agulhas Current. A warming of 0.5˚ C per decade corresponds to an increase of 1.8˚ C since1982. In Rouault et al. (2010) and Blamey et al. (2015) the maximum warming was 0.6˚ C per decade which is less than it was ten years ago. It is therefore possible that the warming of the Agulhas Current (Rouault et al., 2009, 2010) has stopped, reversed or slowed down. In this study, the 0.25˚x 0.25 OI SST is analysed for trends. There is not enough data in Pathfinder SST for a meaningful trend analysis as missing data make for a very patchy chart of trends. There is a strong warming trend reaching a maximum of approximately up to 1.8 °C per decade since 1982 which is present over the Agulhas Current System. The signature of the Agulhas Current is now quite distinct in the warming signal, more so than when using 1 x 1˚ OI SST. The warming signal is found along the Kwazulu-Natal and Transkei coastline where the Agulhas Current hugs the coast and then along the shelf that is away from the coast in PE/Pa and in the South Coast domain then in the Agulhas retroflection and in the Agulhas Return Current to the east. Maximum warming is in the retroflection area to the south west and then eastwards along 42˚S latitude at the location of the Agulhas Return Current. These results confirm that the Agulhas Current has warmed up and that the current may have accelerated bringing warm water further east and south. However, the coastal cooling is less marked with when using the 0.25 x0.25˚OI SST than when using 1 x 1˚OI SST especially in the South Coast domain but there is a cooling trend for PE/PA. Next, I look in the annual cycle of the trends in the 6 domains defined by Rouault et al. (2010) to compare with their results using 10 additional years of data and to better compare the different OI SSTs. It seems that using the 0.25 x0.25˚OI SST, the West Coast domain could have been extended further south in the Benguela upwelling region all the way to Cape Point, where most of the coastal warming occurs in the 0.25 x0.25˚OI SST. This is a very active upwelling cell (Dufois and Rouault, 2012, Pfaff et al., 2019) that cannot be picked up by the 1˚x1˚OI SST. Figure 8 shows the linear trend for all months of the year and all domains from 1982 to 2017 using Reynolds 1˚x 1˚OI SST, 0.25˚x 0.25˚OI SST and Pathfinder SST. This allows us to refine the charts presented previously. It is interesting to note that the trends are seasonal while global warming increase of temperature is not. This means that wind changes or current changes triggered by global warming or decadal variability of climate have a seasonal effect since all domains are largely forced by current and wind. There are also differences between datasets. There is a cooling trend below -0.1 °C per decade in the West Coast area, and it gets more pronounced in the

0.25 x0.25˚ resolution OI Reynolds SST.

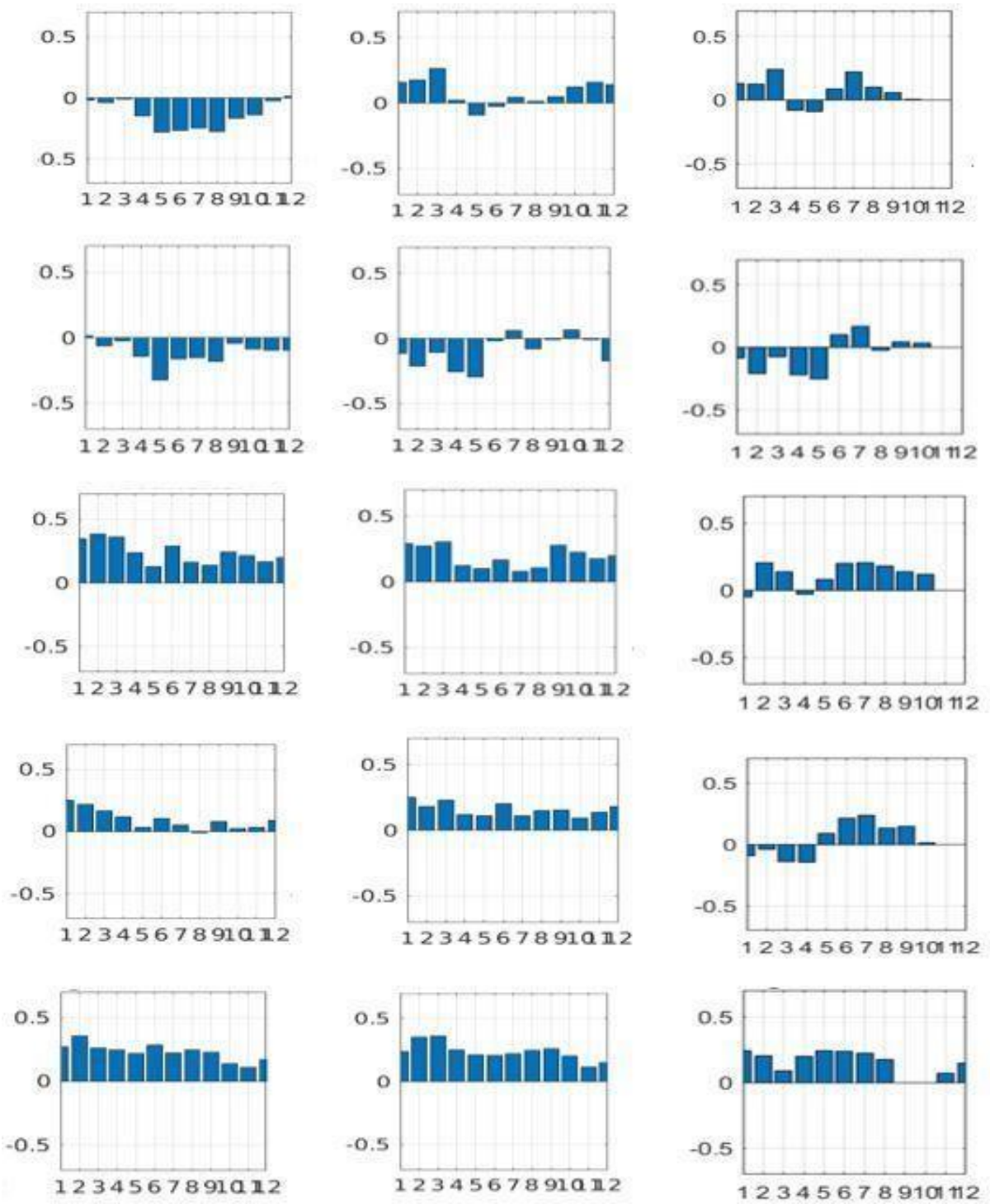


*Figure 8. Annual cycle of 1982–2017 SST linear trends in˚C per decade using (left to right) 1˚ x1˚ OI SST, 0.25 ˚x0.25˚ OI SST and AVHRR Pathfinder SST. From top to bottom West Coast, South Coast, Port Elizabeth/Port Alfred, Transkei, KwaZulu-Natal and the Agulhas Current system domain*

The pattern of the trends is similar amongst all three SST datasets analysed. For example, the warming trend in the Agulhas Current domain and in the Port Elizabeth/Port Alfred domain, is present in all the SST datasets used. The main difference between datasets is for West Coast where 1˚x1˚OI SST has a cooling trend mainly in winter and the two other datasets common warming trends in summer and no cooling trend. The reason for the discrepancy can be found in Figure 1 showing the domains and in Figure7 showing the map of trends. The cooling trend in the 0.25 x 0.25˚OI SST dataset is limited to the southern Benguela and is not captured by the domain used here (Figure 2). The reader is reminded that we want to compare the trends found by Rouault et al. (2010) and the 1˚x1˚OI SST cannot capture the very active and relatively narrow Cape Peninsula to Cape Columbine upwelling cell (Dufois and Rouault, 2012, figure 2) due to their low resolution. The difference in trend is a cause of concern because the southern Benguela is affected by similar wind systems of either west to east low-pressure systems, or the easterly to south easterly winds due to the South Atlantic High. However, the 0.25 x 0.25˚OI SST can sample further south than the 1˚x1˚ OI SST and Rouault et al.(2010) domains, and should be improved to include that 200 km long section of the upwelling area that shows a cooling trend of the same magnitude as the West Coast domain using 1˚x1˚ OI SST. Comparing the trend of 1˚x1˚OI SST done in the present study with 10 years more data than Rouault et al. (2010) in the same domain and same data, I find that the West Coast cooling trend has not increased or even stayed the same. It is about half that found by Rouault et al. (2010) with maximum cooling of 0.25℃ per decade in winter while Rouault et al. (2010) found cooling of about 0.25℃ per decade in spring. The cooling trend in the South Coast domain is similar in all datasets and like Rouault et al. (2010) but of smaller magnitude. A big difference is found for the PE/PA domain where there is a warming trend while Rouault et al (2010) found a cooling trend there in winter. The three Agulhas Current related domains, Transkei, Kwazulu-Natal and Agulhas Current domains show a similar warming trend throughout the year with a slight difference for Pathfinder SST in KwaZulu-Natal in summer. Again, the missing data in Pathfinder SST makes it less reliable for trend detection but it is comforting that it sometimes agrees with the other datasets when averaged over the domains. The KwaZulu-Natal trends are warmer that in Rouault et al (2010) but the Agulhas Domain trends are of a smaller magnitude by about 0.1 C per decade which suggests the warming has stopped, reversed or slowed down in the Agulhas Current. The same can be said for the cooling in the upwelling area. This suggest that the changes reported by Rouault et al. (2010) are not part of a trend but part of decadal variability or that the trend has slowed down. Dieppois et al. (2016) has shown evidence of decadal variability of rainfall? at the 10 year and 25 year scales in both the Western Cape and the interior of southern Africa which

could provide some guidance when studying the impact of global warming on trends and decadal variability of regional SST which is not the object of the present thesis. However, some of the trends are still large and they justify detrending the data in the remainder of the study. Next, we examine interannual variability by means of monthly anomalies in the 6 domains of interest.

### 3.2 Interannual variability

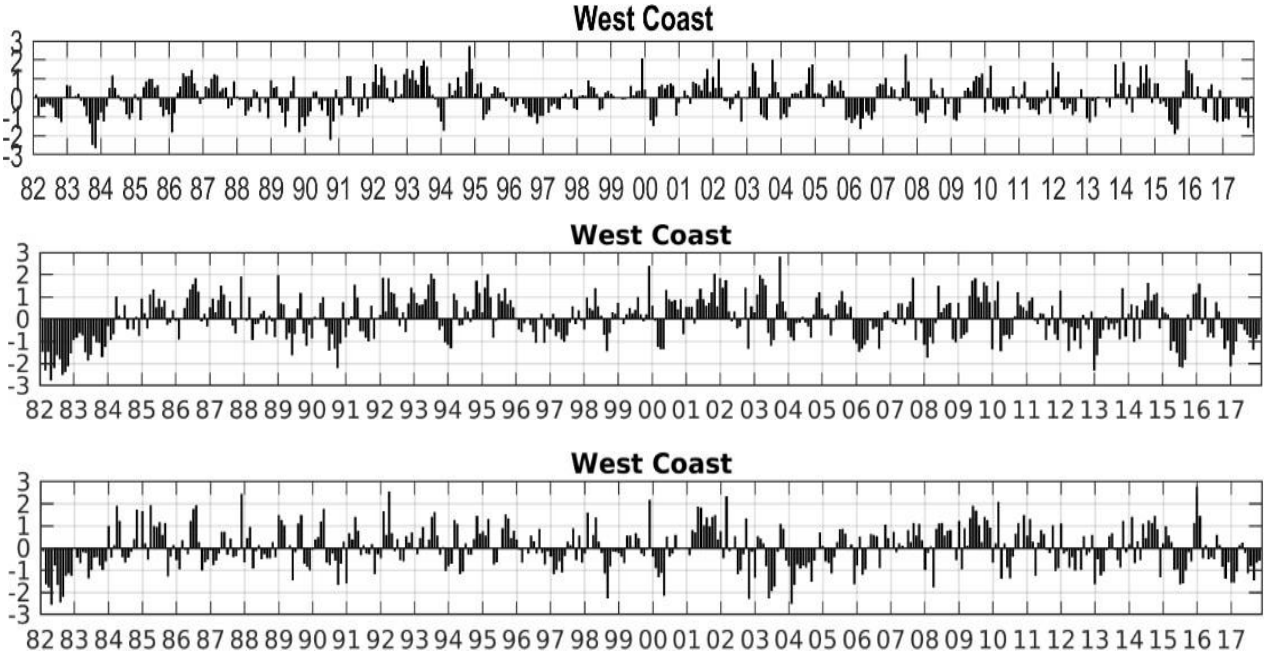


*Figure 9. Detrended normalised SST monthly anomaly from 1982 to 2017 using (from top to bottom) 1° x1° OISST, 0.25°x0.25° OISST and Pathfinder SST for West Coast.*

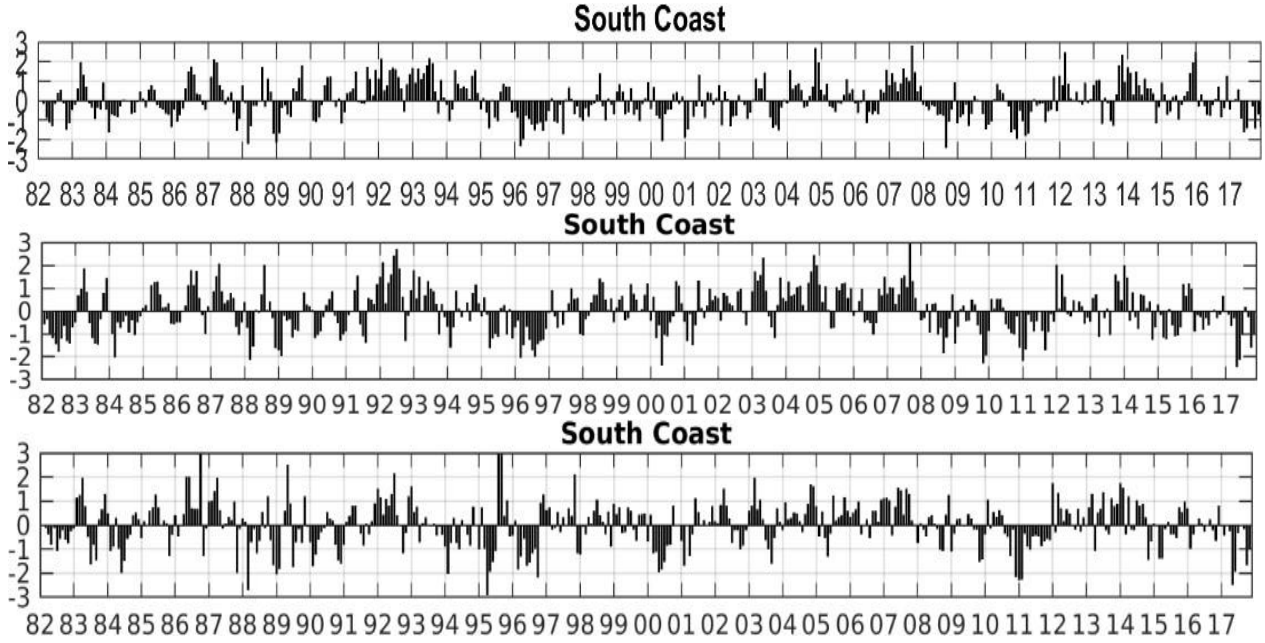


*Figure 10. Detrended normalised SST monthly anomalies from 1982 to 2017 using (from top to bottom) 1° x1° OI SST, 0.25°x0.25° OI SST and Pathfinder SST for the South Coast domain.*

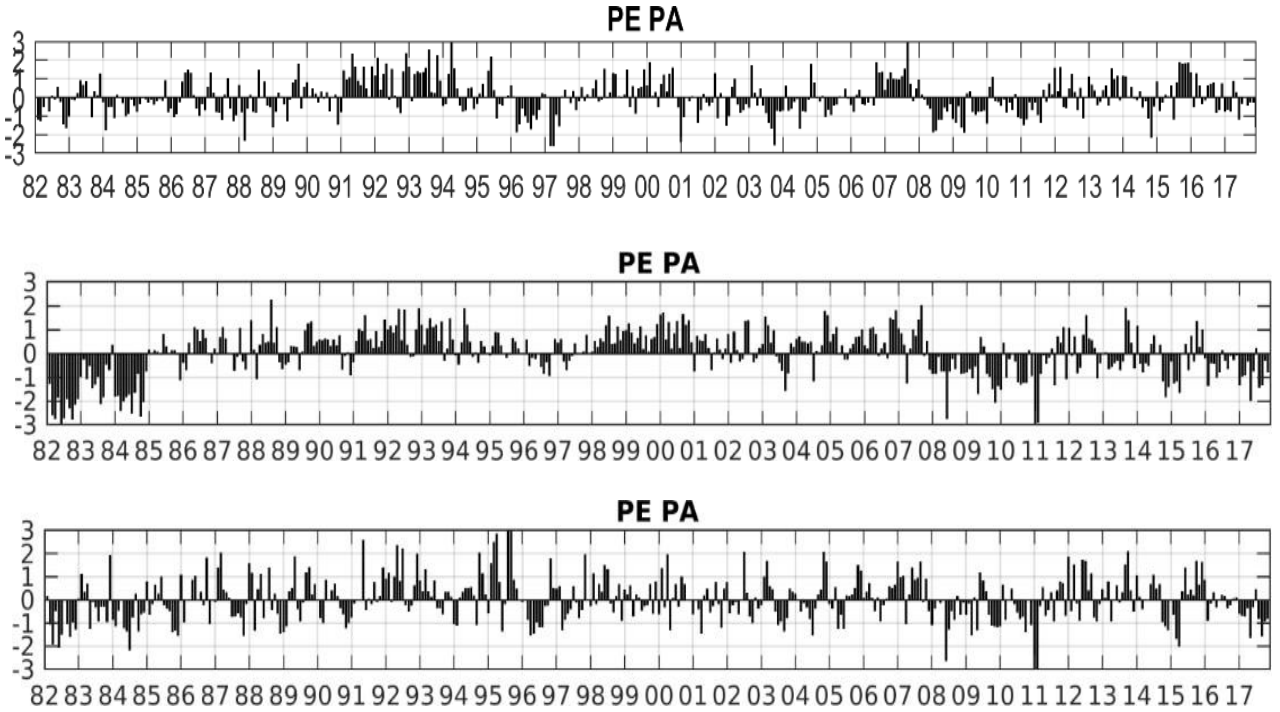


*Figure 11. Detrended normalised SST monthly anomalies from 1982 to 2017 using (from top to bottom) 1 x1˚ OI SST, 0.25˚x0.25˚ OI SST and Pathfinder SST for the Port Elizabeth/Port Alfred domain.*

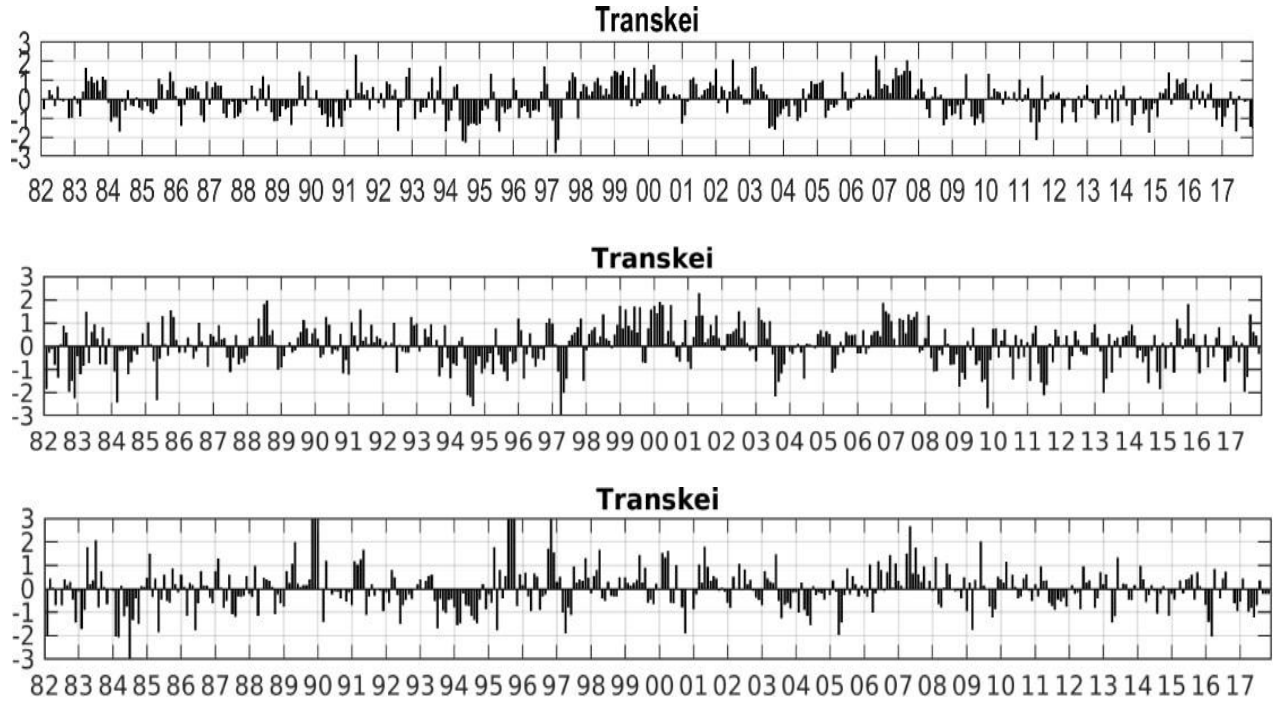


*Figure 12. Detrended normalised monthly anomalies from 1982 to 2017 using (from top to bottom) 1˚ x1˚ OI SST, 0.25˚x0.25˚ OI SST and Pathfinder SST for Transkei.*

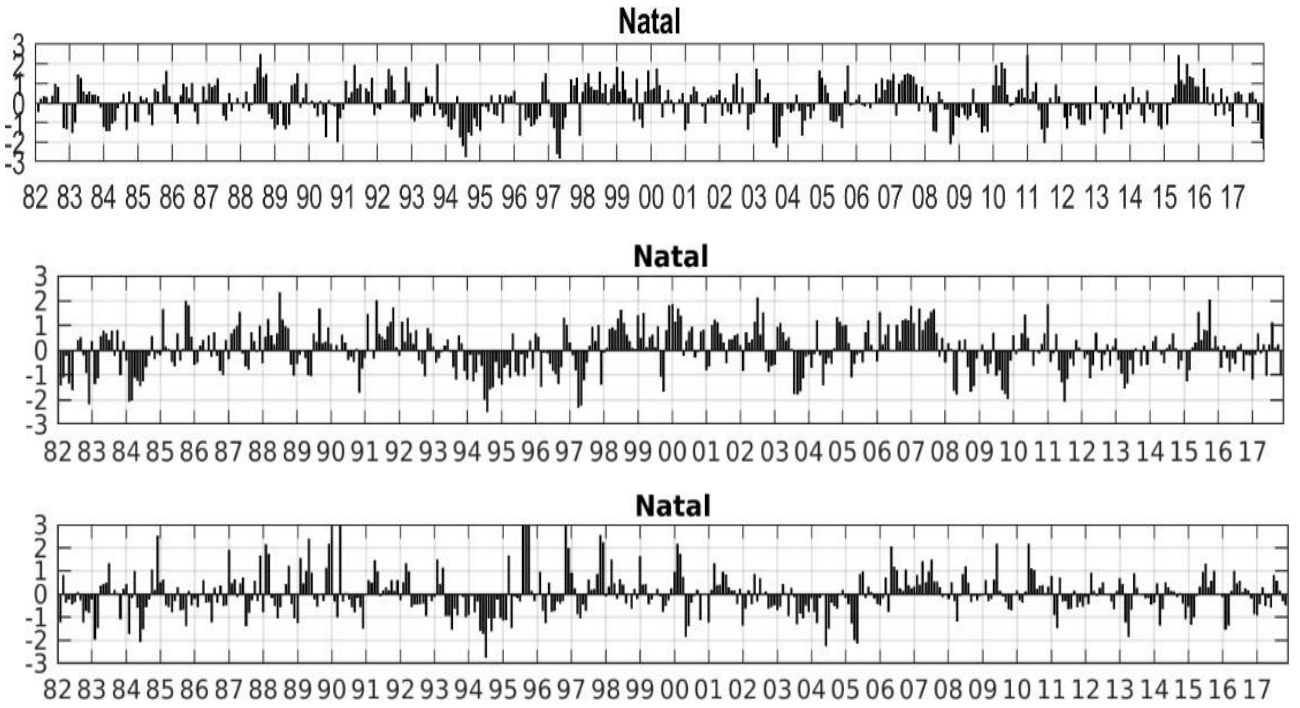


*Figure 13. Detrended normalised SST monthly anomaly from 1982 to 2017 using (from top to bottom) 1˚ x1˚ OI SST, 0.25˚x0.25˚ OI SST and Pathfinder SST for Kwazulu-Natal*

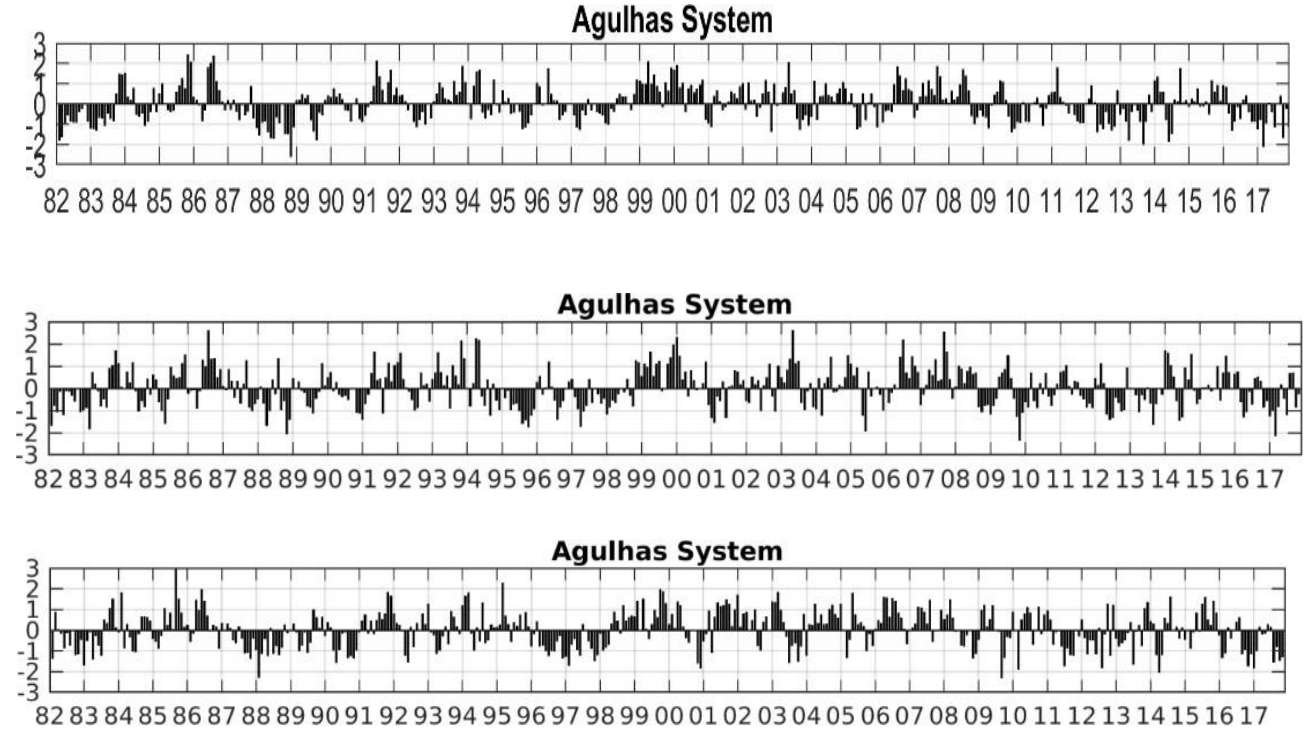


*Figure 14. Detrended normalised anomaly from the monthly mean, 1982–2017, using the 1˚ x1˚ OI SST, 0.25 ˚x0.25˚ OI SST and Pathfinder SST (from top to bottom) for the Agulhas Current system domain.*

The monthly normalized anomalies for the 6 regions (West Coast, South Coast, Port Elizabeth/Port Alfred, Transkei, KwaZulu-Natal and the Agulhas Current) are presented in Figures 9 to Figure 14 for the 3 datasets. 1 means the SST anomaly in C is above 1 standard deviation. This allow to objectively define a warm or cold event and compare dataset that have different standard deviation too. The interannual variability presented here is the history of warm and cold events around South Africa and could be used for various applications. For instance, to look at any anomalies in the marine ecosystem or for the Agulhas Current, rainfall and temperature anomalies at the coast. SST can inform on many natural processes which have strong societal impacts such as rainfall, red tides, ecosystems health and ocean acidification so any abnormal SST events are a symptom of disturbance in the ocean. Correlation between the two OI SST datasets for the 6 domains are 0.94, 0.97, 0.9, 0.98, 0.99, 0.98, respectively but correlation between the 1˚x1˚OI SST and pathfinder SST is lower at 0.86, 0.95, 0.88, 0.87, 0.88 and 0.47 respectively, the latest being a cause of concern, maybe due to the missing values in Pathfinder SST. Correlation between 0.25 x 0.25˚OI SST and Pathfinder is better at0.93, 0.97, 0.90, 0.89, 0.89 and 0.47. The SST is also detrended to remove any trends. In that respects the cold anomalies in West Coast in 1982 and 1983 for 0.25 x 0.25˚OI SST and Pathfinder SST seems odd with two years a cold anomalies in a raw which is suspicious when looking at the rest of the time series for all domain and all datasets and as the cooling is not present in 1983 in the 1˚x1˚OI SST. Same for PE/PA in 1982 1983 which a lot colder than the other datasets. This is a cause for concern. Other cold anomalies lasting for a year occurred in 1996 in South Coast in the three dataset and to some extent in West Coast, PE/PA and Transkei. Note that a strong La Niña occurred from 1995 to 1996 (Table 1 and Figure 15). Cold anomalies in summer occurred also in summer 2000 and 2001 in West Coast and South Coast also a La Niña year. Otherwise, warm anomalies seems to be also associated with El Niño like in 2003 but also warm anomalies occurs in 2002 which is an ENSO neutral year. The strong El Niño of 1997/1998 and 2015/2016 are also associated with warm anomalies in the West Coast and Agulhas Current domains. The Agulhas System Domain seems to show anomalies that are in opposite sign to the West Coast and sometimes are different to the Transkei and Kwazulu-Natal domain although they reflect the Agulhas current system. To conclude some monthly anomalies are above or below 2 standard deviation and some warming or cooling pattern can last for several months which suggest that the weather or ocean forcing of the coastal area can be anomalous for several months in a raw and the forcing is not totally random or chaotic. This means that wind forcing due to abnormal position of the South Atlantic and Indian Ocean can last for a few months or have some preferential position during the summer season. Knowing that ENSO can lead to warming of cooling I am now looking at the impact of ENSO on the SST of the 6 domains.

### 3.3 ENSO impact

| Year | FMA | DJF |
|---|---|---|
| 1980 | 0.3 | 0.6 |
| 1981 | -0.5 | -0.3 |
| 1982 | 0.2 | 0.0 |
| 1983 | 1.5 | 2.2 |
| 1984 | -0.3 | -0.6 |
| 1985 | -0.8 | -1.0 |
| 1986 | -0.3 | -0.5 |
| 1987 | 1.1 | 1.2 |
| 1988 | 0.1 | 0.8 |
| 1989 | -1.1 | -1.7 |
| 1990 | 0.3 | 0.1 |
| 1991 | 0.2 | 0.4 |
| 1992 | 1.5 | 1.7 |
| 1993 | 0.5 | 0.1 |
| 1994 | 0.2 | 0.1 |
| 1995 | 0.5 | 1.0 |
| 1996 | -0.6 | -0.9 |
| 1997 | -0.1 | -0.5 |
| 1998 | 1.4 | 2.2 |
| 1999 | -1.1 | -1.5 |
| 2000 | -1.1 | -1.7 |
| 2001 | -0.4 | -0.7 |
| 2002 | 0.1 | -0.1 |
| 2003 | 0.4 | 0.9 |
| 2004 | 0.2 | 0.4 |
| 2005 | 0.4 | 0.6 |
| 2006 | -0.5 | -0.8 |
| 2007 | 0.0 | 0.7 |
| 2008 | -1.2 | -1.6 |
| 2009 | -0.5 | -0.8 |
| 2010 | 0.9 | 1.5 |
| 2011 | -0.8 | -1.4 |
| 2012 | -0.5 | -0.8 |
| 2013 | -0.2 | -0.4 |
| 2014 | -0.2 | -0.4 |
| 2015 | 0.6 | 0.6 |
| 2016 | 1.7 | 2.5 |
| 2017 | 0.1 | -0.3 |

*Table 1. Oceanic Niño Index (ONI) of Climate Prediction Center, NOAA. The El Niño condition is in red, La Niña condition is in blue, neutral condition in black.*

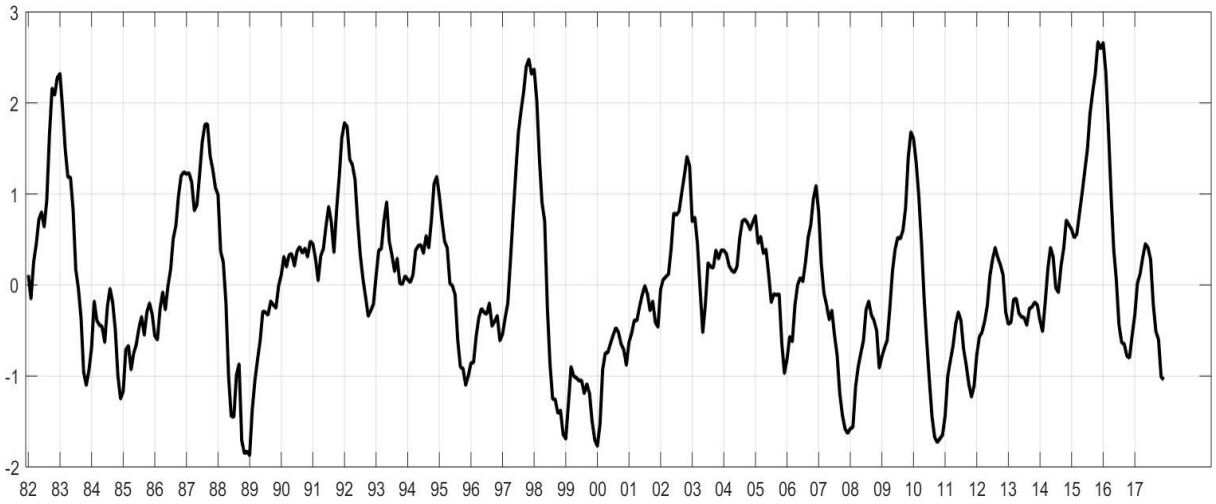


*Figure 15. Monthly values of the Oceanic Niño Index (ONI) from 1982 to 2017. El Niño (warmer than usual) conditions are present when the Oceanic Niño Index is greater than or equal to 0.5 for 3 consecutive months. La Niña conditions (cooler than usual) exist when the Oceanic Niño Index is lower than or equal to -0.5 for 3 consecutive months.*

In order to characterize abnormal events, their strength and duration, the Ocean Niño Index was used to assess the impact of ENSO on SST anomalies around the coast of South Africa The Niño 3.4 region has been correlated to ENSO in many other studies concerning rainfall and by Rouault et al (2010). It is presented in Figure 15 and Table 1. Figure 15 shows the monthly values of the Oceanic Niño Index (ONI) from 1982 to 2017. It is a 3-month running mean of SST anomalies in the Niño 3.4 region (5˚N-5˚S, 120˚-170˚W)]). El Niño conditions are present when the Oceanic Niño Index is greater than or equal to 0.5 for 3 consecutive months. La Niña conditions (cooler than usual) exist when the Oceanic Niño Index is lower than or equal to -0.5 for 3 consecutive months. Table 1 shows the ONI index in March (left) and January which are the means of the SST anomalies in FMA and DJF respectively. We focus on summer because this is when Rouault et al (2010) found correlation between SST and ENSO and it is also the time when ENSO is linked to rainfall in Southern Africa. The months of February, March and April (FMA) were extracted over the period of 1982 to 2017 and their seasonal means were calculated. FMA means from the monthly Ocean Niño Index (ONI) were also extracted and their association with the SST anomalies across the 6 coastal regions was assessed. Figures 10 to 15 show the association between the different warming and cooling events using 1 x 1˚OI SST 0.25 x 0.25˚OI SST as well as Pathfinder SST.

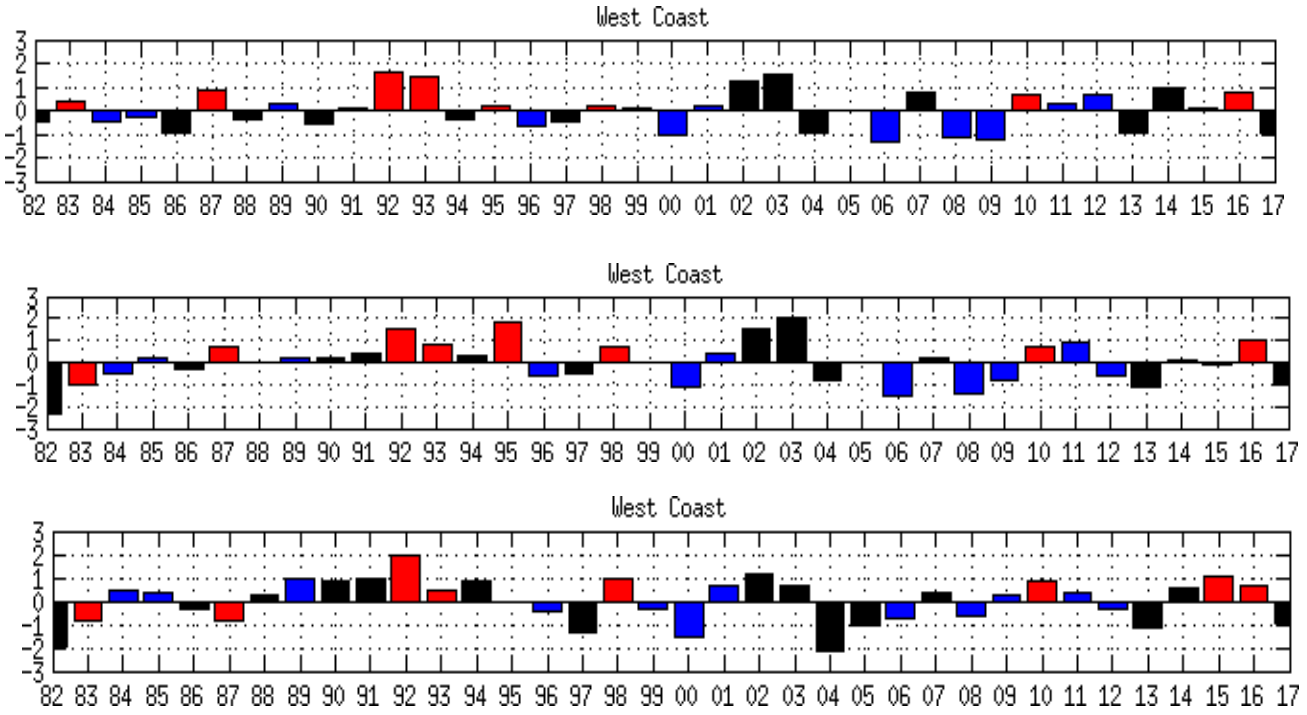


*Figure 16. Detrended normalised FMA anomalies from mean FMA 1982-2017 using (from top to bottom) 1X1° OISST; 0.25°X0.25° OISST and 4x4 km resolution AVHRR SST (Top to Bottom) for West Coast. Color code: Black (neutral years), Red (El Niño years) and Blue (La Niña Years).*

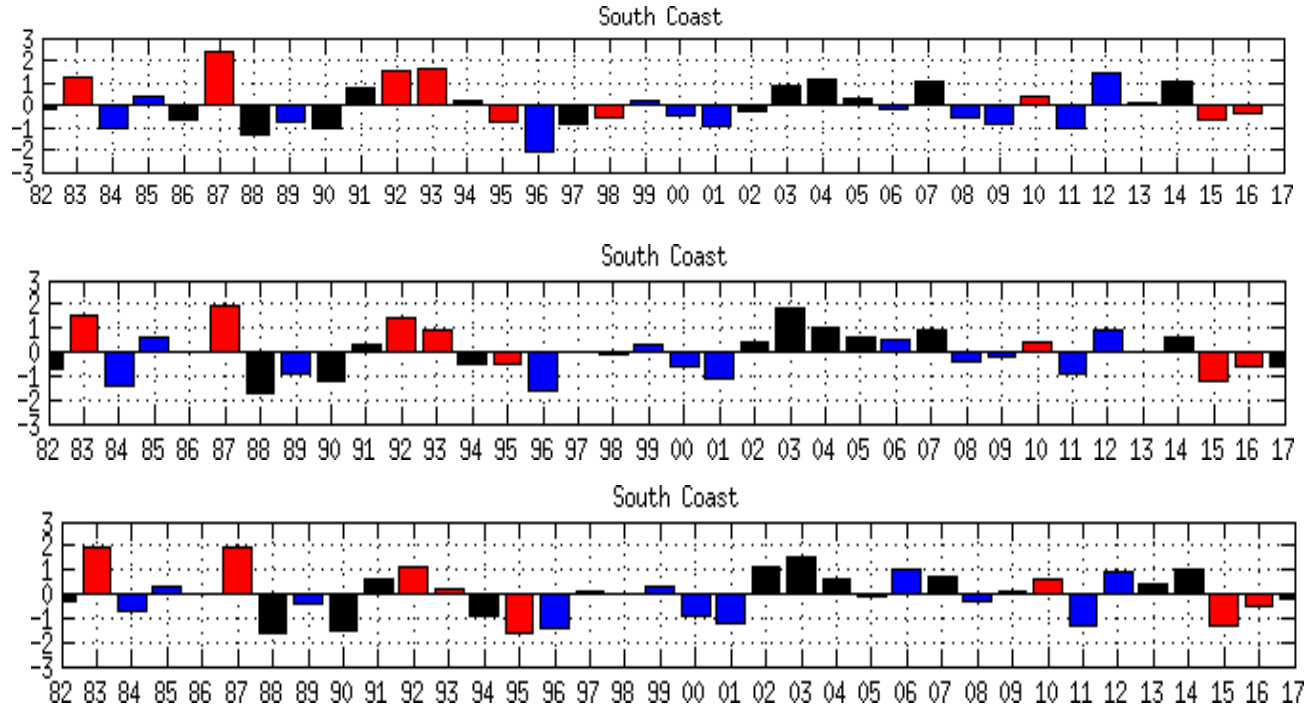


*Figure 17. Same as Figure 16 for South Coast.*

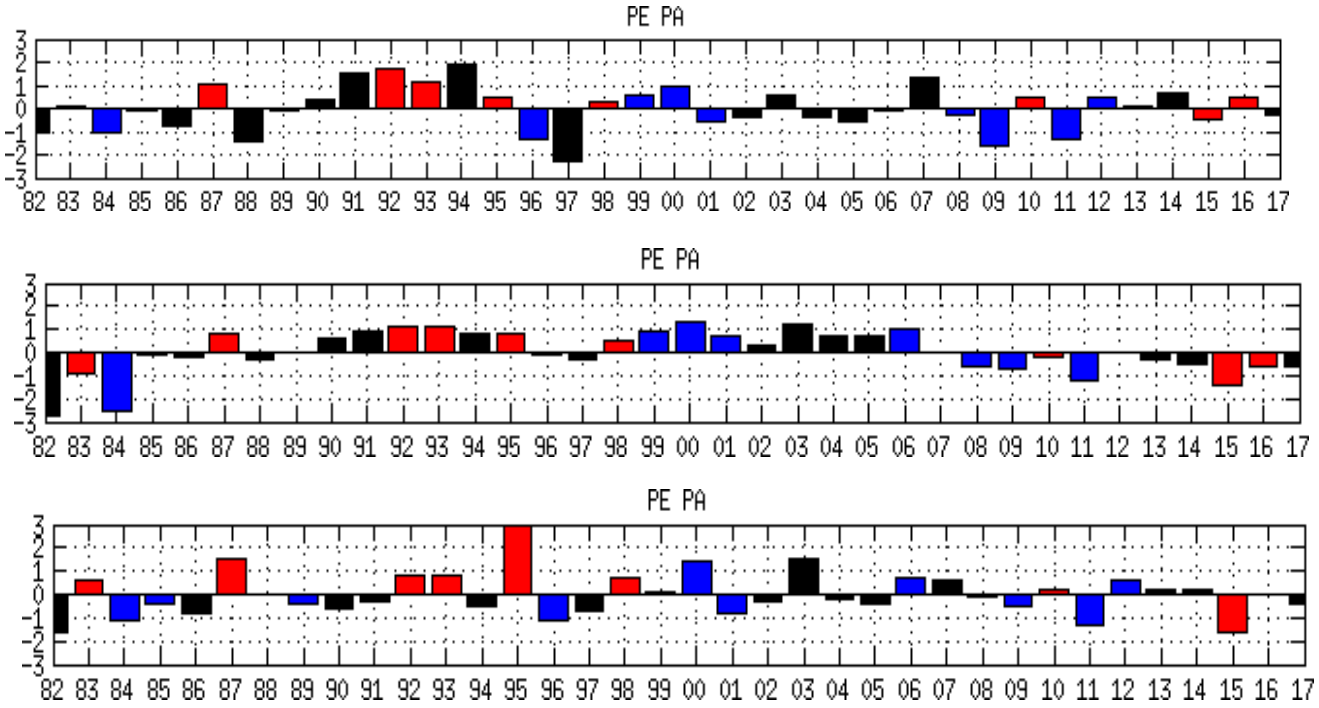


*Figure 18. Same as Figure 16 for the Port Elizabeth/Port Alfred domain.*

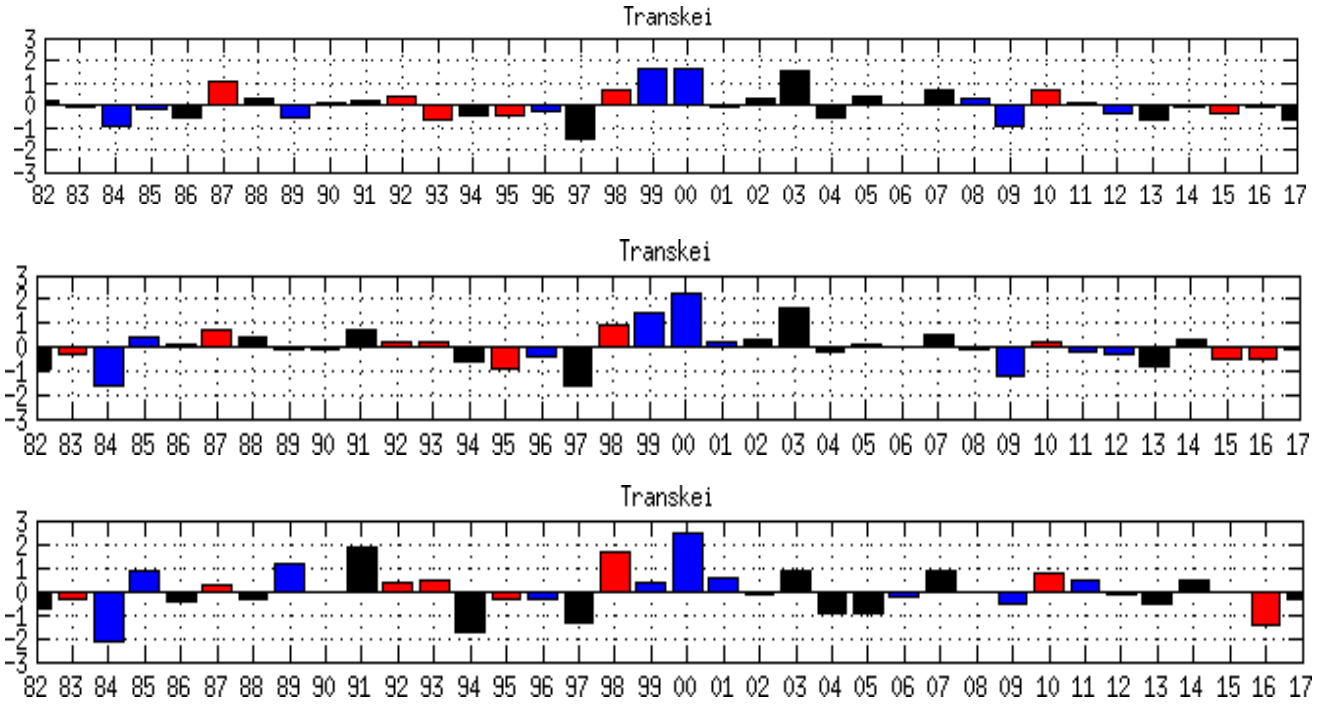


*Figure 19. Same as Figure 16 for the Transkei domain.*

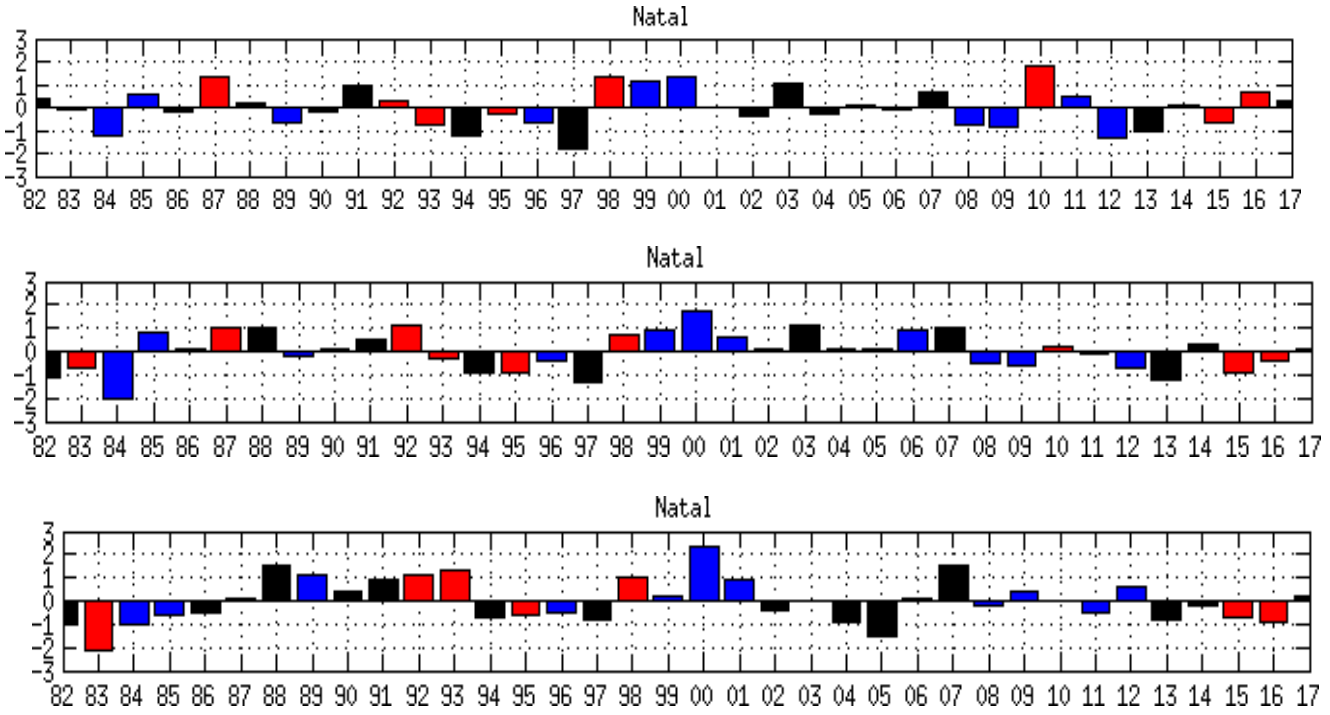


*Figure 20. Same as Figure 16 for the Kwazulu-Natal domain.*

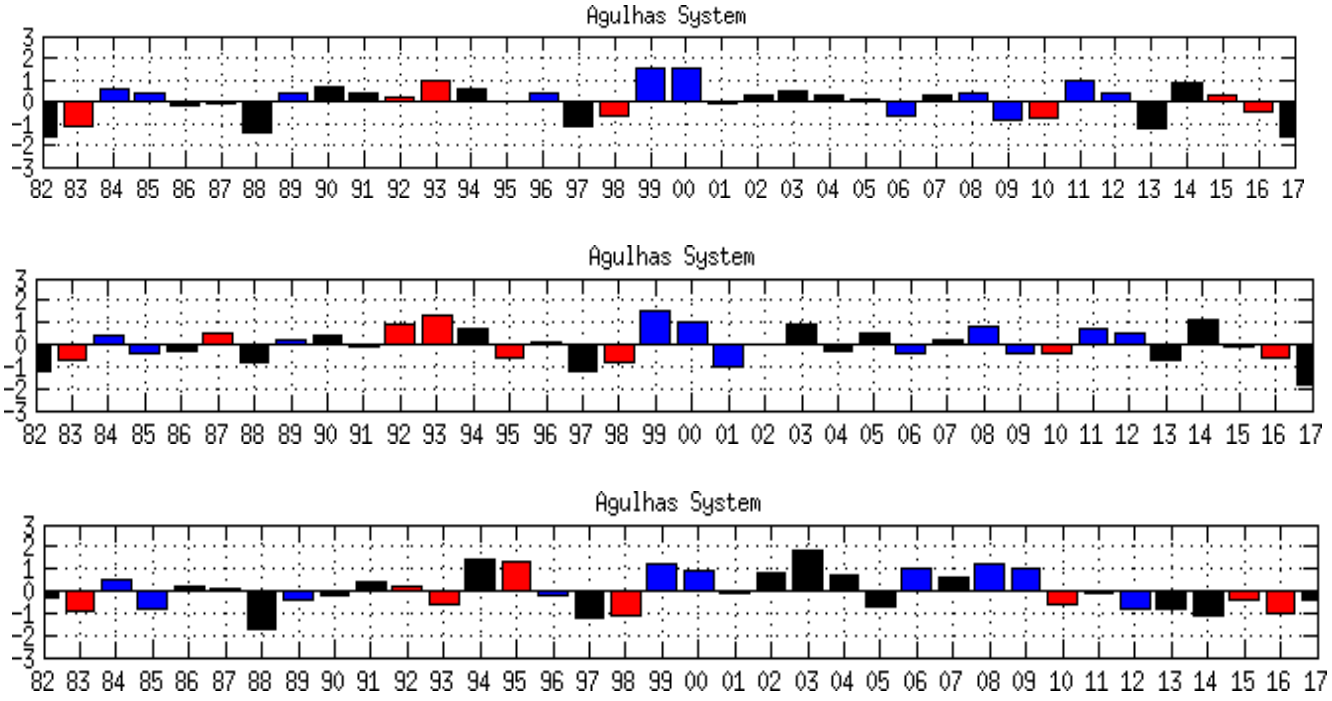


*Figure 21. Same as Figure 16 for Agulhas Current system domain.*

For this study, the criteria used to classify El Niño, La Niña and neutral years are as follows. Anomalies above 0.5 for a consecutive of 3 months are classified as El Niño year (extreme warming), anomalies below –0.5 are known as La Niña year (extreme cooling) and anomalies that lie between 0.5 and –0.5 are classified as Neutral years. To better characterize and simplify the results concerning the impact of ENSO, I present late summer seasonal anomalies

which is when ENSO was found to have the most impact on SST. Also, most of the studies concerning impact of ENSO on general atmospheric circulation and rainfall use seasonal averages, sometimes the full rainy season (NDJFM), sometimes the heart of the rainy season (DJF or JFM). This is because the ENSO impact is the not the same for each month of a season each year and sometimes one can have a normal month or above normal rainfall for a given month during ENSO. This could be the same for SST. Figures 16 to 21 present normalised seasonal anomalies for the average of FMA for the 6 domains and the 6 datasets. There is a clear relationship between the ONI ENSO index and coastal SST anomalies in the 6 regions, especially for West Coast and South Coast domains where many El Niño events are associated with warm anomalies and many La Niña associated with cold anomalies. However, not all El Niños or La Niñas lead to warm and cold anomalies respectively and there is no relationship between the values of the ENSO events and the value of the SST anomalies. There are also difference between datasets which is a source of concern and not necessarily due to the different offshore extent of each domain as can be seen in for the Agulhas Retroflection domain which has the same exact longitudinal and latitudinal extent for all datasets. In the West coast region, there is a warming of above 0.5 standard deviation occurring during the El Niño summer of 1987, 1992,1993, 1995 (only in 0.25 x 0.25 OI SST dataset), 2010, 2015 and 2016. The 3 SST datasets analysed in the West Coast domain show the same result except for 1995 and 1983 two strong El Niño years. The strong 97/98 El Niño has little effect on the West Coast and South Coast domains. The strong El Niño 1982/1983 is the only cool West Coast event in both 0.25 Oi SST and Pathfinder SST datasets but not for the one degree OI SST. There are cool anomalies in the West Coast occurring during La Niña in 1996, 2000, 2006, 2008. The West Coast experienced a cooler than normal season during an ENSO neutral year in 2004 and it is also warmer than normal for South Coast. A few years did not have the same relationship with ENSO. For example, a warming occurred in the 1989, 2001, 2011 and 2012 La Niñas in the West coast domain. This same pattern occurred in the one-degree OISST, 0.25 x 0.25 OI SST as well as Pathfinder datasets. However, 7 out of 11 cooling events occurred during La Niña in the West Coast and the South Coast. 4 out of 11 cooling events occurred during La Niña in PE/PA and Transkei. 5 out of 11 cooling events occurred in the KZN region and 4 out of 11 in the Agulhas current region. The FMA 2003 neutral year according to ONI has strong warm anomalies reaching a maximum of 2 standard deviation above normal. However, 2002/2003 is a well-known EL Niño event and the ONI index is above 0.5 until February and even in FMA the index is still positive and borderline El Niño at 0.4 instead of 0.5. I will consider that year as an El Niño Summer in the study because it is a typical El Niño case. Summer 2002 is inconsistent in the different datasets for the PE/PA, Transkei, KwaZulu-Natal domains. The Summer Niña year 2000 is quite interesting with warm anomalies reaching maximum of above 2 SD across the PE/PA, Transkei, KZN domains as

well as in the Agulhas Retroflection domain and cold anomalies in the West Coast and South Coast domains. In fact, the Agulhas Retroflection domain anomalies are often inverse to the West Coast anomalies. To have a spatial view of the impact of El Niño and La Niña on the region I present an El Niño and La Niña composite with the three datasets to study the average or canonical impact of ENSO on the region

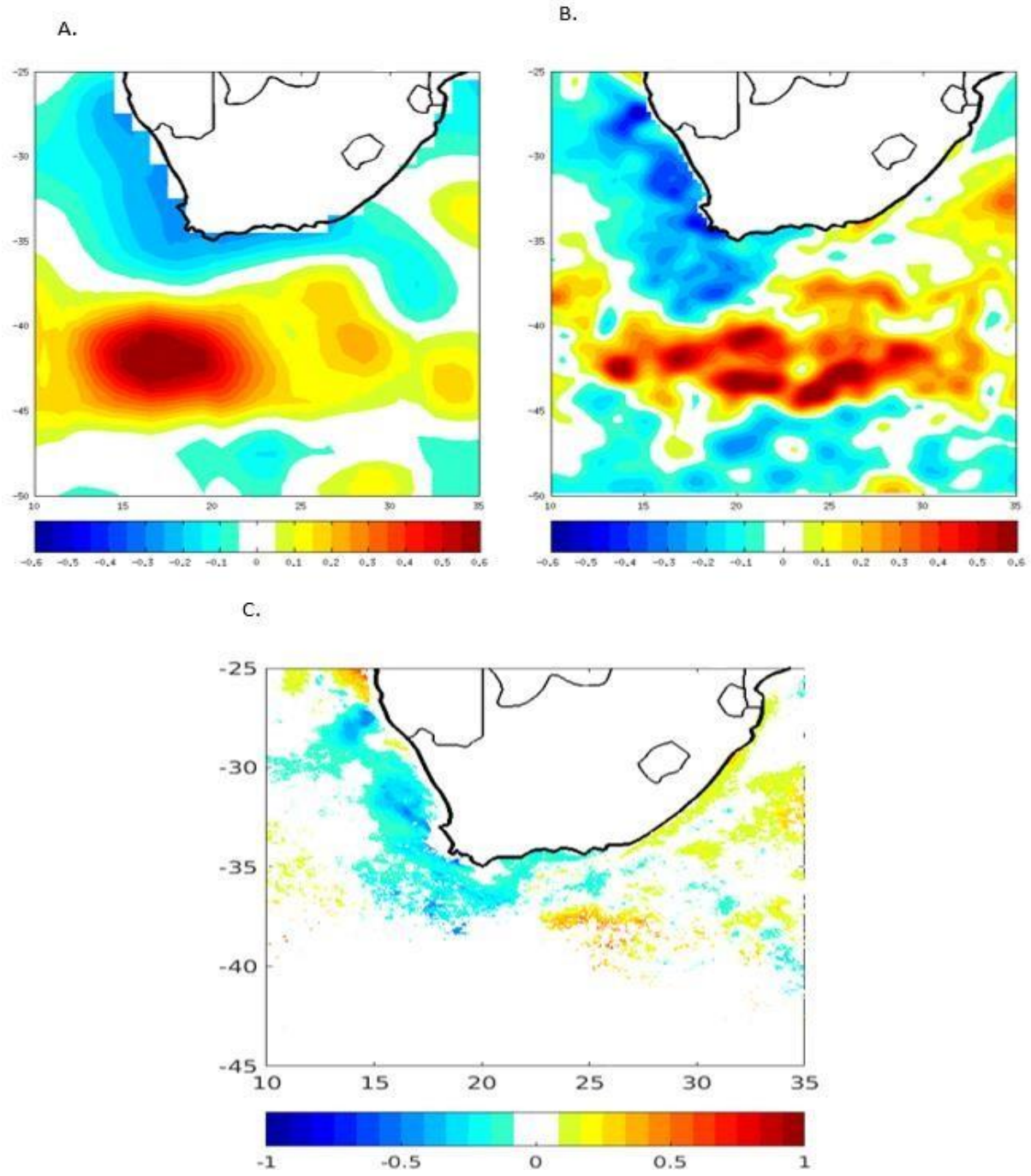


*Figure 22. La Niña FMA composite normalised map using 1˚ x1˚ OI SST, 0.25˚x0.25˚ OI SST and AVHRR Pathfinder SST. Years were selected using Ocean Niño Index FMA running mean. The La Niña FMA years are 1984, 1985, 1989, 1996, 1999, 2000, 2000, 2006, 2008, 2009, 2011, 2012, 2017.*

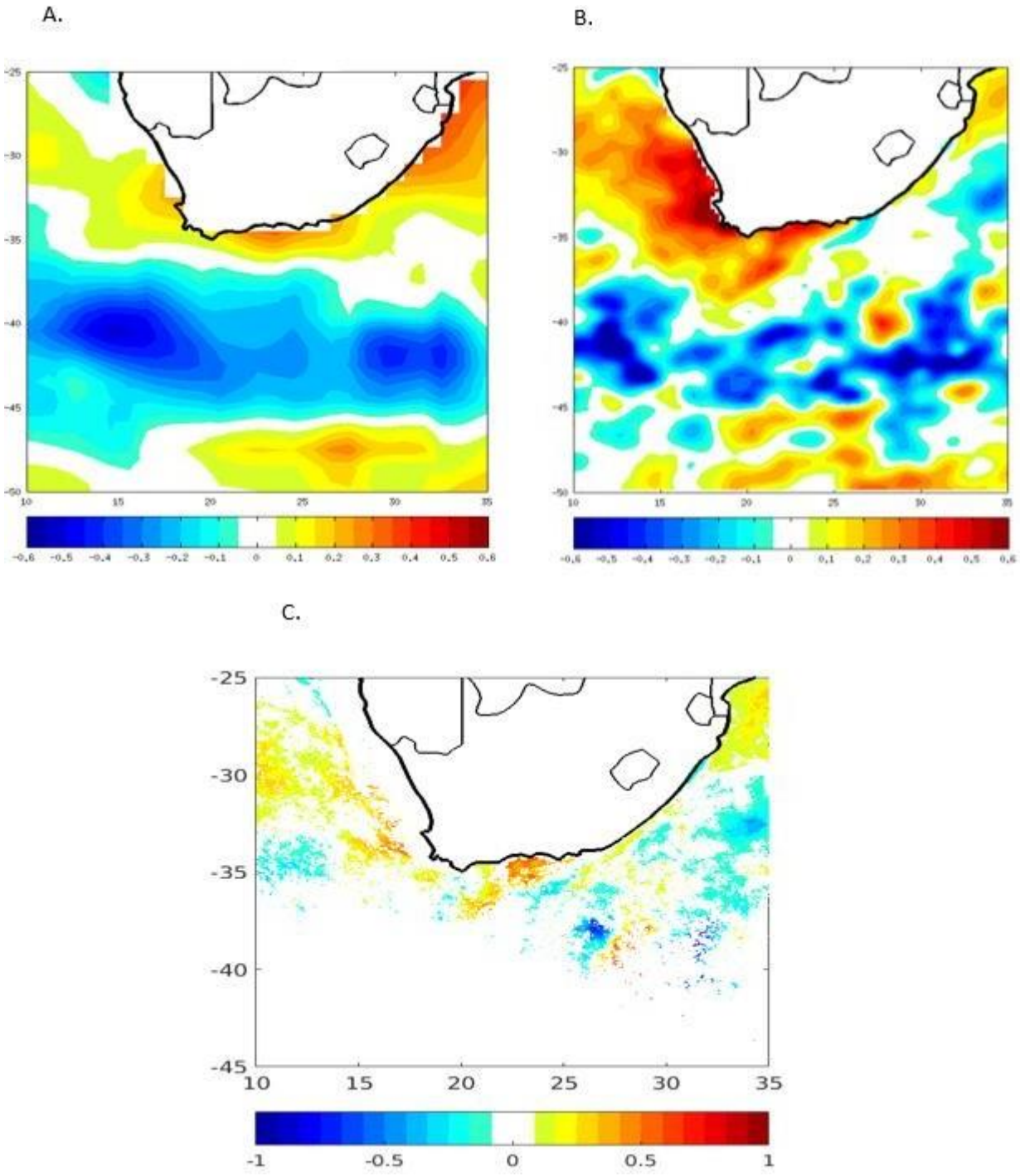


*Figure 23. El Niño FMA composite normalised anomaly map during El Niño using 1˚ x1˚ OI SST (a), 0.25˚x0.25˚ OI SST(b) and AVHRR Pathfinder SST(c). Years were selected using Ocean Niño Index FMA running mean (table 1). The El Niño years are 1983, 1987, 1988, 1992, 1995, 1998, 2003, 2005, 2007, 2010, 2015, 2016.*

Figures 22 and 23 show composites of sea surface temperature (1˚x1˚OI SST, 0.25 x 0.25 OI SST and Pathfinder SST) during El Niño and La Niña. The composites are made by averaging surface temperatures for the 12 La Niña years and 9 El Niño years

removing the corresponding seasonal mean and dividing g by the standard deviation. The El Niño years and La Niña years selected here are slightly different from the years used in the FMA time series based on the possibility that there is a delay between ENSO and its coastal impact. The same can be said for the La Niña year but inspection of Table 1 for DJF and FMA shows that the choice of El Niño years and La Niña summer years is not straight forward, but composites using the years in the FMA time series show little difference. The same can be said if I had used those years for the FMA anomaly time series: the general results concerning ENSO association, differences between datasets, differences of impact on domains and differences between values of ENSO and values of the coast perturbations are still valid.

The results of the composite analyses are quite interesting. They show important differences between datasets especially in the coastal regions impacted by Agulhas Current. They also show a more intense West Coast warming during El Niño using 0.25 x 0.25 OI SST, especially in the part of the south Benguela upwelling that is missed by the 0.25 x 0.25 OI SST West Coast domain (the Cape Columbine to Cape Point upwelling cell). The Pathfinder SST is patchy but seems to support the quarter degree OI SST rather than the 1 degree OI SST especially in the South Coast to Agulhas Current domains. The La Niña composites show cold anomalies along the West Coast and the South Coast of South Africa, with warm anomalies to the south. The causes of the change will be studied below. The cold anomalies in 0.25 x 0.25˚OISST stopped in the location of the Agulhas Current. The AVHRR SST dataset is patchy but is quite like 0.25 x 0.25˚OI SST except at the border between Namibia and South Africa. The main differences are found between 1˚x1˚OI SST and 0.25 x 0.25˚OI SST east of the tip of Africa which suggests a possible limitation in the 1˚x1˚OI SST when close to the Agulhas Current. The 1˚x1˚OI SST also seems to have cold anomalies further north than the 0.25 x 0.25˚OI SST and Pathfinder SST areas covered. The coldest anomalies along the coast are from Cape Columbine to Cape Point in the 0.25 x 0.25˚OI SST, the area that is not captured in the West Coast domain. The use of the same domains as Rouault et al. (2010) was to compare with 1˚x1˚OI SST a dataset that does not allow sampling close to the coast in this narrow upwelling that is bordered offshore by the warm Agulhas Jet and the Agulhas Leakage. The large scale La Niña composite presented in Figure 25 shows that the West Coast cooling and the warming to the south is part of a large-scale basin-wide signal. It seems to be congruent with a warming to the north in Namibia and Angola reminiscent of a Benguela Niño (Rouault et al., 2003, Florenchie et al.; 2003; 200; Imbol Koungue et al.; 2010). The impact of El Niño presented in Figure 23 also shows stronger warming in the south Benguela upwelling region and differences between 1˚x1˚OI SST and 0.25˚x0.25˚In the Agulhas current system. The 0.25 x 25˚OI SST also shows the presence of the Agulhas Current.

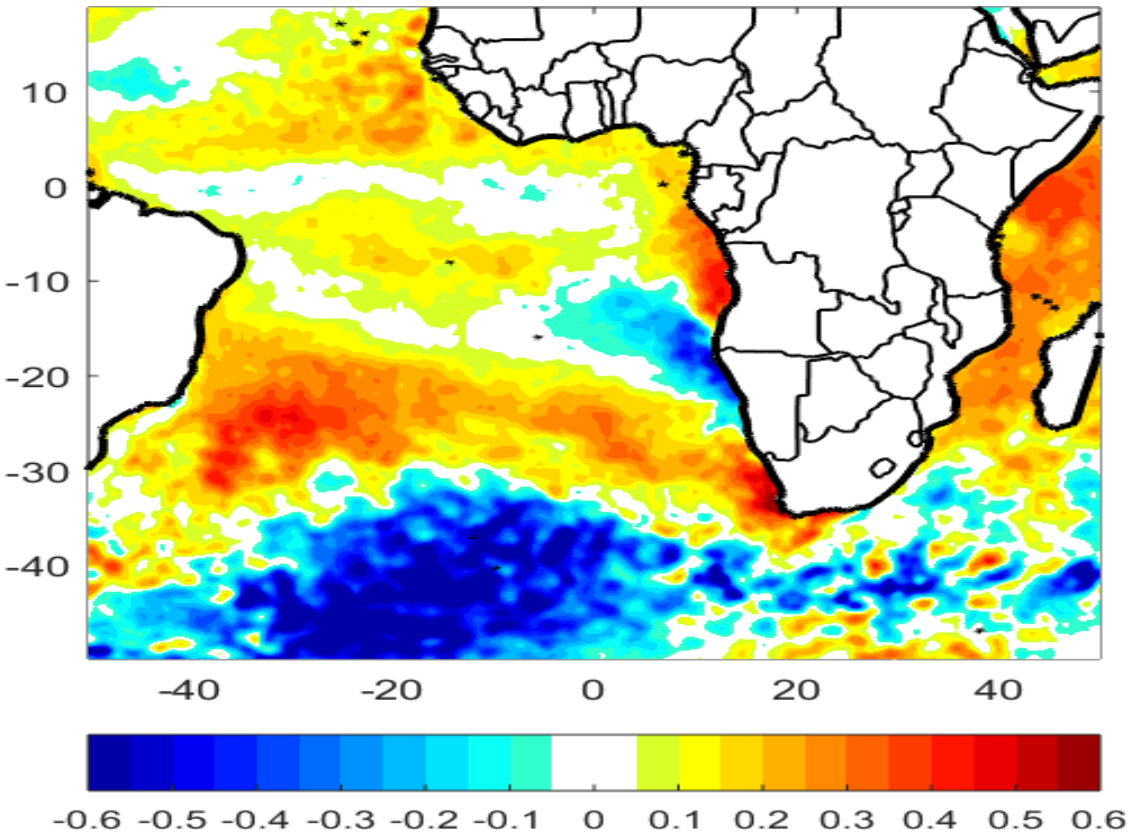


*Figure 24. Same as figure 23 for large scale using 0.25°x0.25° OISST during El Niño.*

The warm SST anomalies map shown in Figure 24 for El Niño also shows the same opposite sign large scale signal which suggests a shift in the South Atlantic High pressure system and associated trade wind and upwelling favorable south easterly winds all the way to the Angolan Border leading to cooling in the Northern Benguela and warming off Angola. It also suggests stronger westerly winds, or a shift of the low-pressure system associated to the westerly wind belt in the South Atlantic. Some places get cooler and other places get warmer. There is warming in the Mozambique channel and South of Madagascar that can bring warmer water into the Agulhas Current and explain why the large-scale cooling, possibly wind driven, is not seen in the Agulhas Retroflection domain. The opposite argument could be used for the La Niña composite shown in Figure 25. Comparing, the La Niña and Niño composites, it seems that the all high-pressure and low-pressure atmospheric systems to the south are shifted. The modification at the coast is part of a coherent and relatively homogeneous large-scale system.

Next, I will look at El Niño, La Niña years seasons and warm and cold years in West Coast happening in ENSO neutral years.

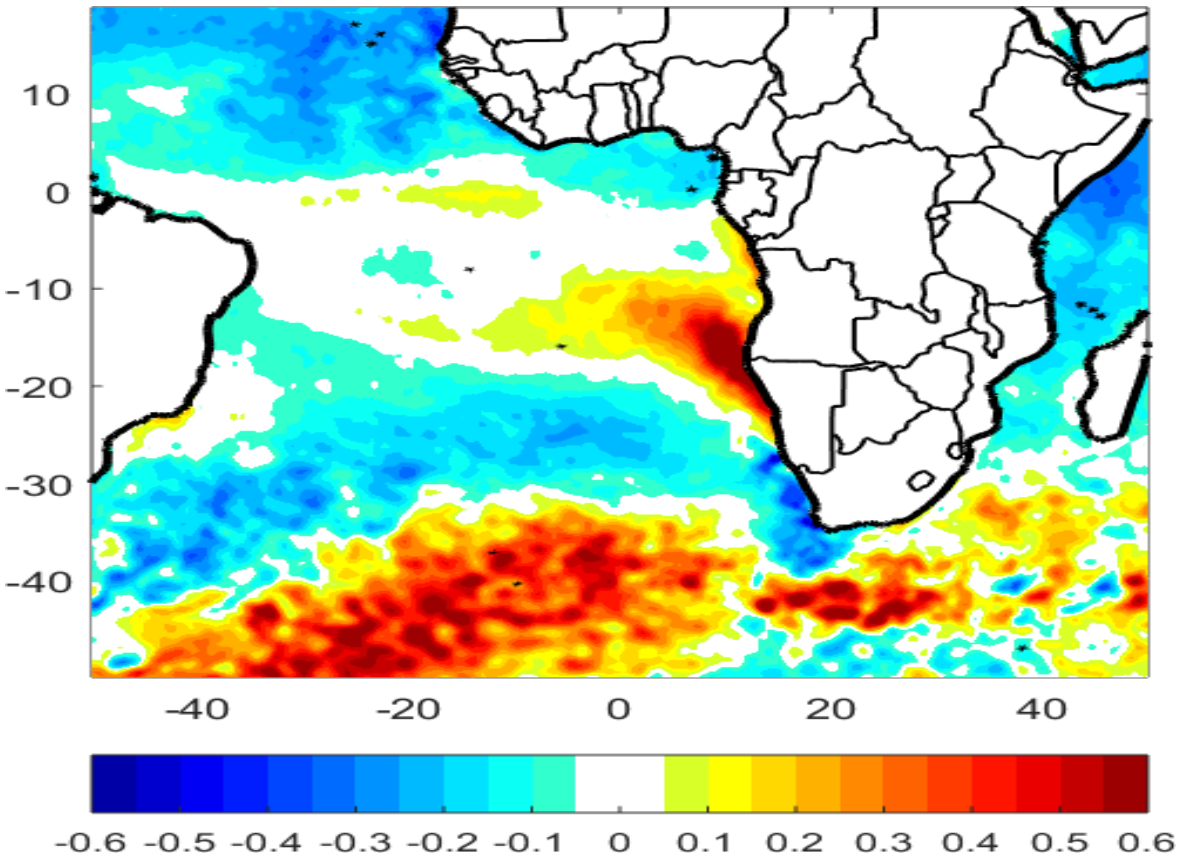


*Figure 25. Same as Figure 24 but for large scale using 0.25°x0.25° OISST during La Niña.*

I start with La Niña years that led to a cooling in West Coast. I pick up FMA 2000, 2006, 2008 and 2009 which are presented in figure 26. Not much happen in South Coast during those Niña years. 2008 has a warmer than normal clear Agulhas Current signal. Namibia is not warm in 2000 but it is for the other years. No sign of warmer than normal Agulhas Current in 2009. Looking at the large-scale basin wide equivalent in figure 27, FMA 2000 shows a clear extension of cold anomaly basin wide like what happen in in the La Niña composite anomaly (Figure25) while in 2006 the cold anomalies does not extend to far towards Brazil. The warm anomalies south of the South Atlantic high-pressure system is also present with less spatial extension. The warming off Northern Namibia has a difference from the average situation in spatial extension and intensity and situation in the Tropical Atlantic is either colder or warmer and decoupled from the Northern part of the South Atlantic high-pressure system. In conclusion, the impact of La Niña for a colder than normal east coast FMA season has some commonality, but regional basin wide difference can happen.

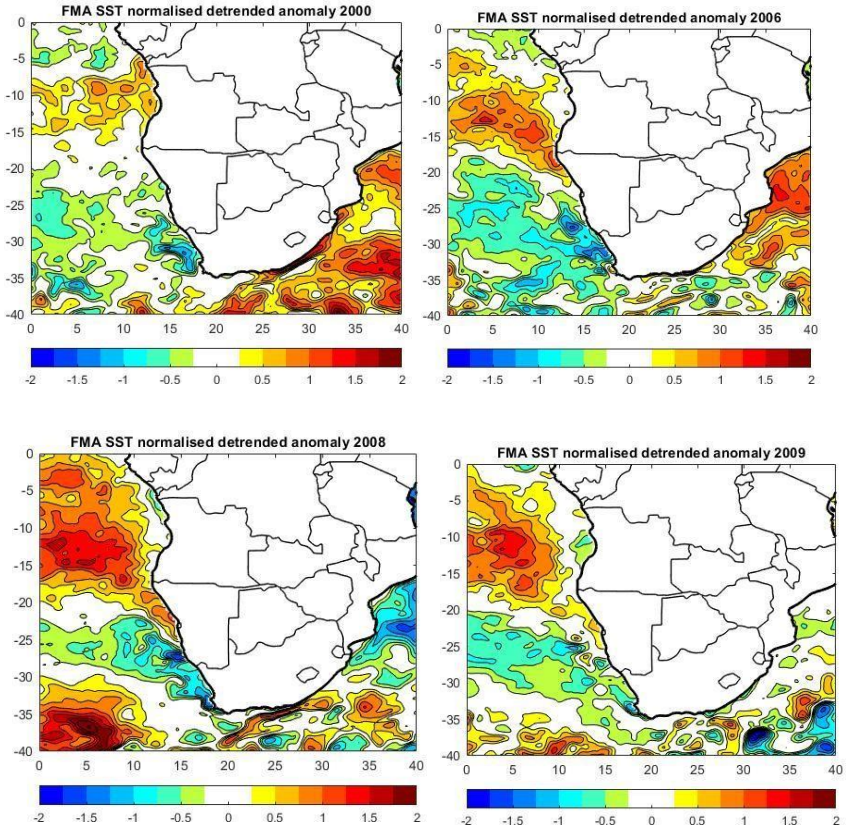


*Figure 26. Cold West Coast FMA SST normalised anomalies during 2000 (top left) , 2006 (top right) , 2008 (bottom left) and 2009 (bottom right) FMA La Niña season (Top to bottom, left to right).*

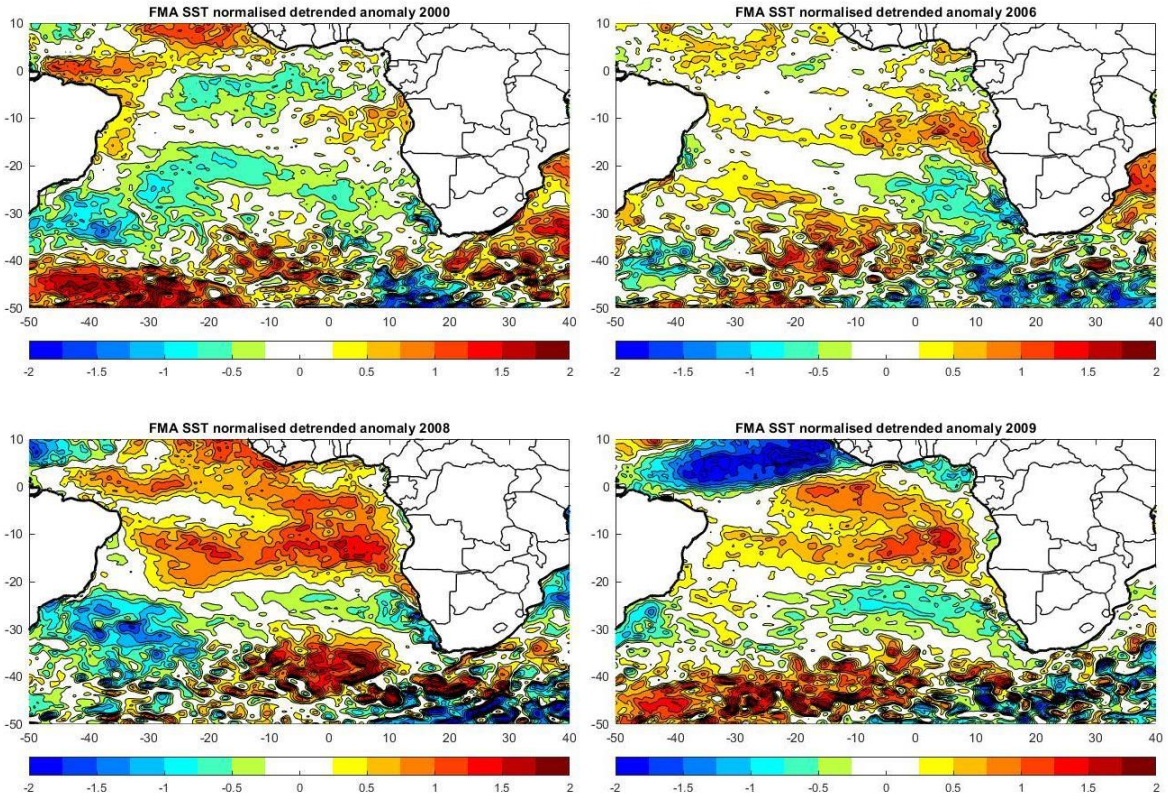


*Figure 27. Same as figure 26 but for large scale conditions. during 2000 (top left) , 2006 (top right) , 2008 (bottom left) and 2009 (bottom right) FMA La Niña season (Top to bottom, left to right).*

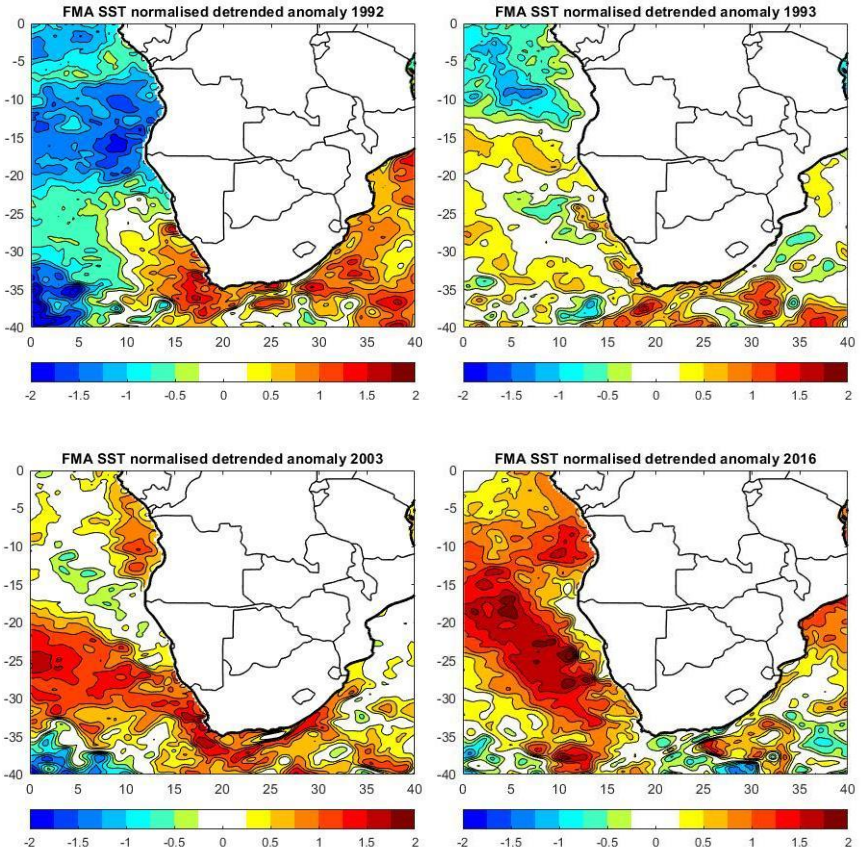


*Figure 28. Selected warm West Coast FMA during El Niño FMA season of 1992 (top left) , 1993 (top right), 2003 (bottom left) and 2016 (bottom right)*

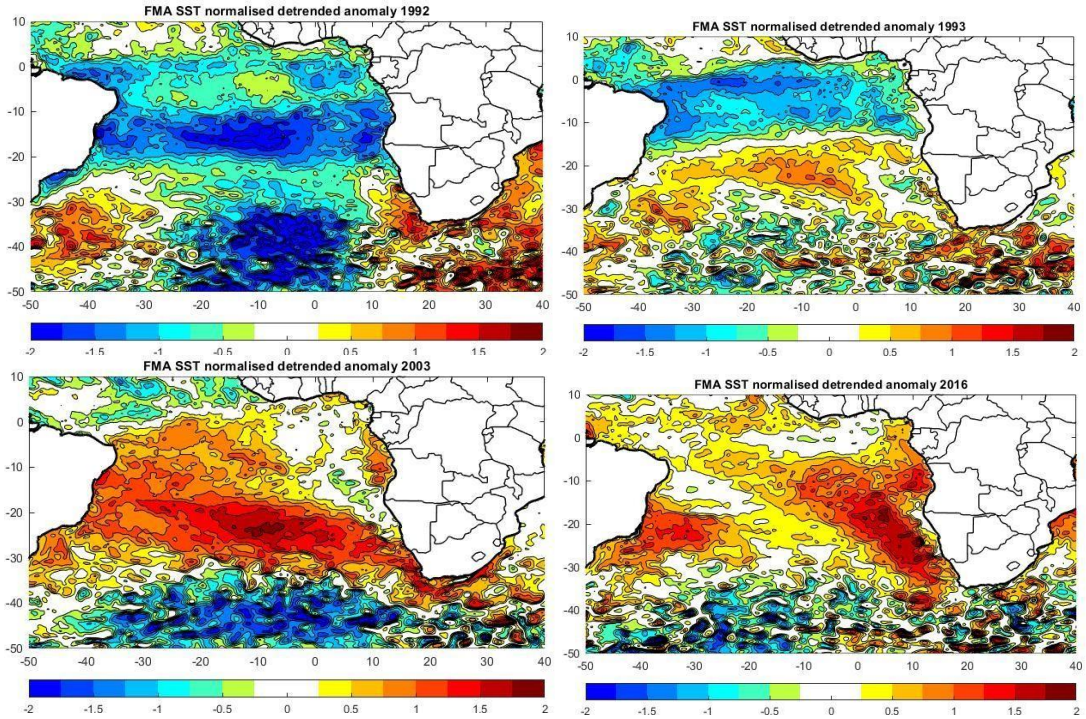


*Figure 29. Same as figure 28 for large scale. 1992 (top left), 1993 (top right), 2003 (bottom left) and 2016 (bottom right)*

Next, I look at El Niño FMA season of year 1992, 1993, 2003, and 2016. 2015/2016 is one of the strongest El Niño on record. SST detrended anomalies around South Africa are presented in Figure 28 while large scale anomalies are presented in Figure 29. The year 2003 is very similar to the El Niño composite anomaly. 1992 is quite different when the West Coast warming does not extend towards Brazil. In fact, cold anomalies occurs where the El Niño composite anomalies show a warm anomaly. The cold anomalies in the mid-latitude does extend just west of the Agulhas Current system that is warmer than normal. It could be that the Agulhas Current was very intense that year. 1993 is more like the El Niño composite anomaly average but less intense. The 2016 large-scale signal is quite strong but from the west coast, it is oriented more to the north-west than the El Niño composite anomaly. The Namibian coast is not cooler than normal and is different from expected according to the canonical El Niño composite and is normal. Still, it is not warm and stands out as different from a classic West Coast warming. The South Coast and Agulhas Retroflection domains are cooler than normal. The mid-latitude cooling extends throughout the mid-latitudes of the South Atlantic and South Indian Ocean. All years but 2016 have a warm South Coast. Rouault et al. (2010) showed that the West Coast and South Coast domains are correlated in summer. The correlation between the two regions is because when the southerly wind is stronger than normal off the West Coast it is often stronger than normal and easterly along the South Coast, both regions being under the influence of the South Atlantic high with interference from cold fronts that stop the upwelling from occurring. El Niño wind composite anomalies will be presented below. The same conclusion can be drawn here as for La Niña which involves mainly regional differences in the basin-wide modifications in the South Atlantic and Tropical Atlantic Ocean and along the coast. There is also a hint that the Agulhas Current may interfere with that system. One hypothesis beyond the scope of the study is that the intensity of the Agulhas Current, which depends on oceanic and atmospheric conditions in the Indian Ocean, interferes with the impact of El Niño on SST. Strong winds lead to stronger transfer of energy between the ocean and the atmosphere via the turbulent flux of sensible heat fluxes leading to cooling of the se surface. As it is very difficult to cool the Agulhas Current, stronger wind there will not necessarily lead to negative SST anomalies at the ocean surface South of Africa all the way to 40 45 S. In the tropical Atlantic and off Angola where Kelvin waves can propagate leading to Atlantic Niño and Benguela Niños or Niñas and along the equator, SST is more correlated to modification of the thermocline that to the turbulent latent and sensible heat fluxes that are well correlated to SST anomalies in subtropics and mid-latitudes (Yu et al., 2006). Maps of turbulent fluxes will also be been shown below to verify that hypothesis. Next, I examine ENSO neutral years that led to cooling or warming in West Coast and South Coast domains to find out whether the anomalies are also part of basin-wide modifications or more locally produced.

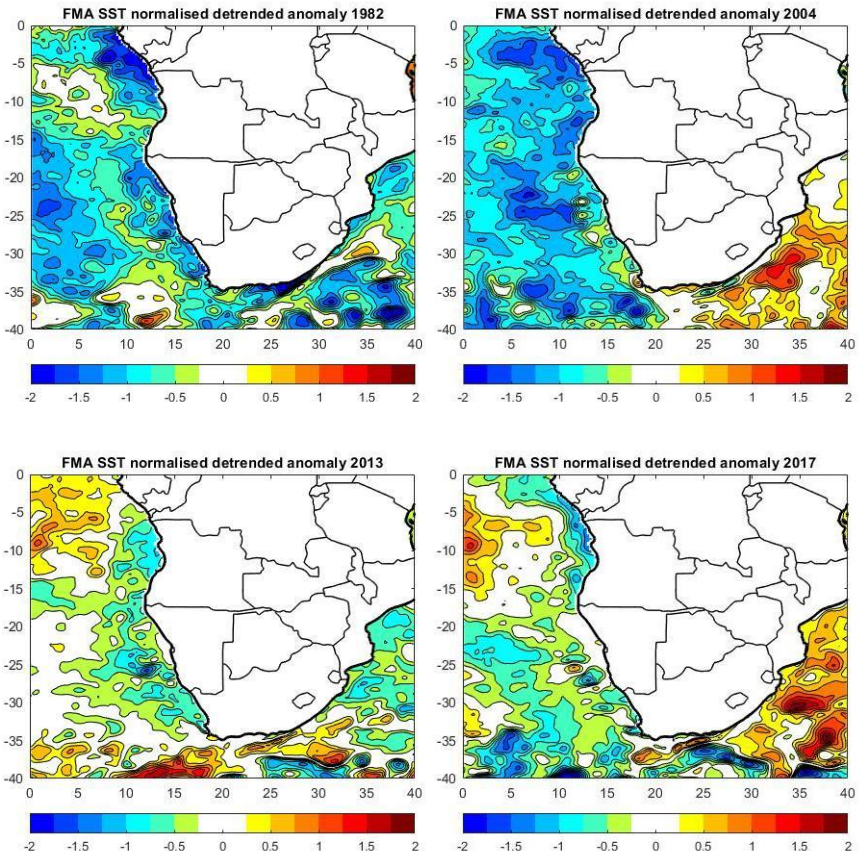


*Figure 30. Cooler than Normal West coast years in FMA not happening during La Niña. 1982, top left, 2004, top right, 2013, bottom left and 2017 bottom right.*

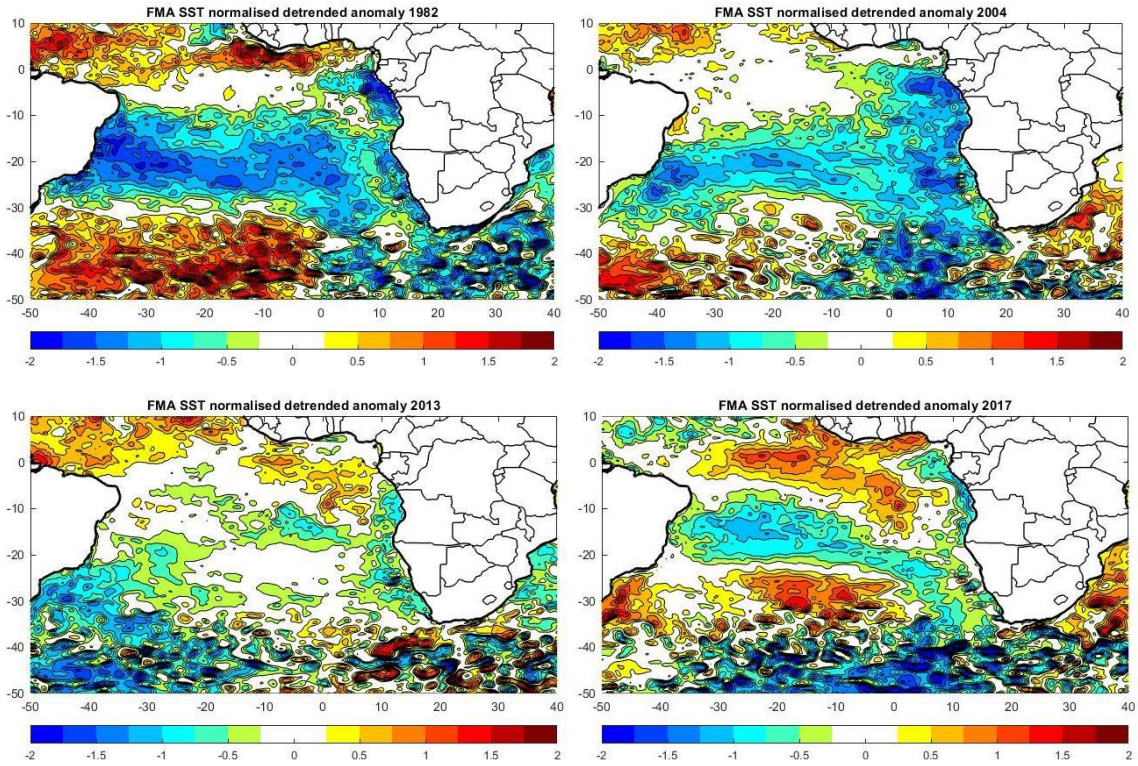


*Figure 31. Same as figure 30 but on a large scale.*

The cooler than normal late summer FMA West Coast years happening during neutral ENSO conditions is presented in Figures 30 and 31. They show a clear difference from the cold West Coast cases happening during La Niña . The cooling extends along the coast of southern Africa, which is different from the La Niña composite where cooling shows alternating zones of warming and cooling. However, the cooling is also part of large-scale basin-wide forcing which means this basin wide change can also happen in ENSO neutral years either randomly or forced by a phenomenon other than ENSO. This may indicate a random but persistent intensification of the South Atlantic high-pressure and trade wind system in the tropical Atlantic at least for 1982 and 2004, rather than a shift in the high pressure system that would lead to regions experiencing weaker or stronger than normal wind speeds in alternating bands while intensification would lead to stronger winds everywhere. There may also be a continental effect: if low pressure occurs over the continent, then the pressure gradient with the ocean increases and upwelling favorable winds increase. As for the cooling off Angola and Northern Namibia, this can be forced locally but also remotely by increased trade wind along the Equator, a phenomenon leading to Benguela Niñas (Florenchie et al., 2004, Imbol Koungue et al., 2018, 2019). In 1982 and to some extent in 2004, the South Coast and PE/PA and the 3 Agulhas Current related domains (Transkei, Kwazulu-Natal and Agulhas Current) are cooler than normal, which is not the case in 2004 and 2013. This provides another example of potential interference by the Agulhas Current which is forced by the Indian Ocean wind stress curl leading to changes in transport of water masses and changes in current speed. Due to its high heat capacity, the atmosphere has less effect in generation sea surface anomalies than the open ocean despite large air sea fluxes there (Rouault and Lutjeharms, 2003, Imbol Nkwinkwa et al., 2019)

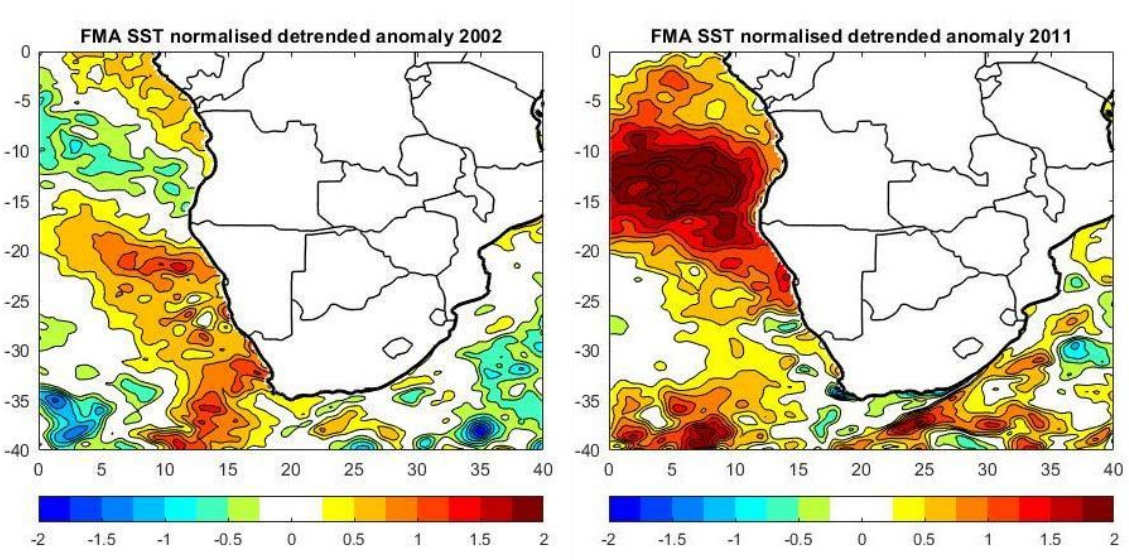


*Figure 32. Typical FMA warming in the West Coast domain during non-El Niño years in 2002 (left) and 2011 (right).*

There are not many warm west coast years occurring in neutral or La Niña years. Those late summer FMA are presented in Figure 32 and are in FMA 2002 and 2011. Note that 2020/2011 was mostly a La Niña year. The 2011 FMA was a very warm and well documented Benguela Niño and was forced remotely along the Equator (Rouault et al., 2018). Wind were also weaker in Namibia leading to addition warming that are typical of the impact of El Niño on the region. The large-scale impact of both years is quite different with 2011 and is quite like the La Niña impact except for the warming in west Coast. South Coast was colder than normal which is expected during la Niña . Usually Benguela effect stop at around 25 S but it was one of the stronger Benguela Niño and maybe the impact was felt further South by way of Kelvin wave that have shown to propagate all the way to Cape Town at least (Bachelery et al. 2020). The 2002 warming is all the way to Northern Namibia which is different than the average El Niño effect The Agulhas Current was clearly stronger in 2011. Concerning 2011 there is still a cooling in the West Coast Benguela upwelling that is not captured by my West Coast domain.

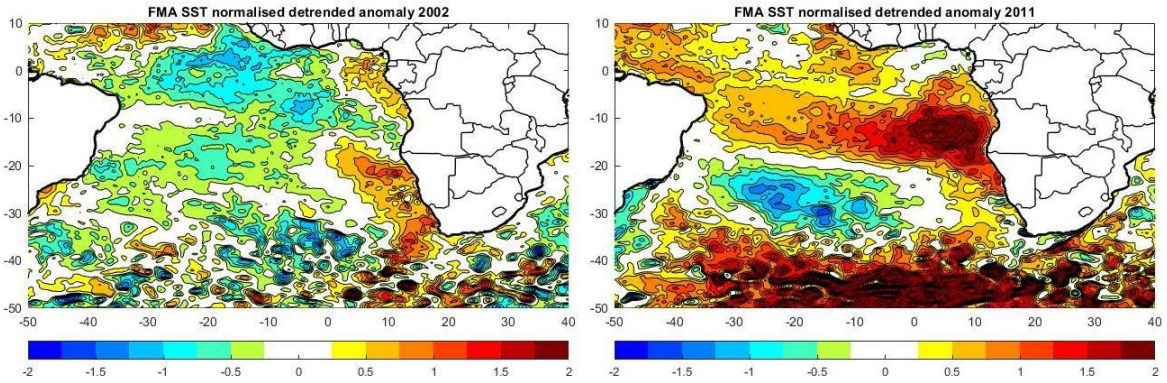


*Figure 33. Same as figure 32 but for large scale.*

Correlations between the El Niño Southern Oscillation using the Ocean Niño Index (ONI) and both OI SST are presented in Table 2. Significant correlations (95%) are highlighted in bold. The West Coast, South Coast and Agulhas Retroflection domains have the most frequent significant correlations. Better correlations occur with 2 to 3 months lag rather without lags. There are also differences in timing and value and even sign of correlation using the two datasets. For the West Coast significant correlations occur mostly from December to May at 0 lag. Better correlations are found using 1 x 1˚OI SST which is surprising because 0.25 x 0.25˚ OI SST can go closer to the coast into the upwelling area and I was expecting a stronger impact of the change in wind speed during ENSO or during normal years closer to the coast where upwelling is stronger. It may be due do the fact that the domain is smaller or there are too many missing data near the coast in 0.25 x 0.25˚OI SST. The closer to the coast the colder the water and the stronger the upwelling and the wind effect. Another concern is that sometimes there

is a lack of correlation during a month when there is significant correlation before and after or with various lags. For instance, there is no correlation for the West Coast in January while significant correlation exists in in December in February using 1˚x1˚OI SST. This may be due to the limited duration of the dataset with only 35 data points and since 1982 we had one third neutral years, one third la Niña years and one third El Niño years. A seasonal correlation over 3 months would use 3 times more points. Other significant correlations in the West Coast domain occur between lag 1 up to lag 5 reaching a maximum of R=0,43. Best correlations are found at 2 to 3 months' lag?? for DJF which is encouraging. The most frequent correlations occur in the West Coast using 1˚x1˚OI SST and confirmed by 0.25 x 0.25˚OI SST with most consistent correlations in late summer and highest correlations at 3 months lag. This is a very good result which opens the door to forecasting SST in the West coast in late summer. This shows the potential for statistics to be used to forecast at the seasonal scale with three months lag. Since the wind drives the SST and the upwelling, there could be an impact on marine ecosystems too.

An intriguing feature of both the 1˚x1 OI SST and using 0.25 x 0.25 OI SST is the significant lag correlation in early summer with up the 6 months lag in November while there is little or no correlation in November at zero lag. This suggest that the ENSO impact can take a while to propagate. ENSO matures in the austral summer and sometimes starts months or years before its maturation. One can also have a protracted El Niño lasting for up to nearly three years or a La Niña year sharply followed by El Niño or not, complicating the problem. However, it seems that the important number of significant correlations at various lag in the austral summer in the West Coast domain could be used for seasonal forecasting when some of the caveats mentioned above are resolved and mechanisms for the lags are better understood. For the South Coast, 1˚x1˚OI SST and 0.25 x 0.25˚OI SST have similar numbers of cases with significant correlation with ENSO. Correlations are slightly lower than the West Coast when using 0.25 x 0.25˚OI SST. The 1˚x1˚OI SST that has the highest correlation with R=0.48 at 5 months lag in December. Lag correlations seem higher than with zero lag and I observed the same diagonal pattern of lag correlation in Table 1. There is relatively good correlation in the austral summer at lags of up to 6 months. Late summer is better correlated at zero lag in both datasets and early summer at 4 to 6 months lag which is also puzzling. The PE/PA domain has weaker positive correlations also in a diagonal pattern as the two previous domains with less correlation and various lags, but late summer is relatively well correlated. However, the PE/PA domain is not correlated with ENSO except for the odd negative correlation in May. Transkei does not show much correlation except for a few of negative correlations for the 0.25 x 0.25˚OI SST and a neat diagonal pattern of positive significant correlations using the 1˚x1˚OI SST. KwaZulu-Natal has a few of negative correlation at various

lag while it is positive in the 0.25 x 0.25˚ OI SST. The Agulhas domain has an almost symmetric negative pattern of correlation at the same time and lag than for the West Coast and South Coast domains which is less marked in the 0.25x 0.25˚OI SST. This suggest a shift in weather system, and this will be investigated in the next section.

*Table 2: Correlation between the Ocean Niño Index and SST normalised detrended anomalies using one degree OI SST and quarter degree OI SST in the six domains: West Coast, South Coast, PE/PA, Transkei KwaZulu Natal and the Agulhas Retroflection Domain. The correlations are calculated at lag 0 to 6 with ONI leading. All values in bold blue are significant at a 95% confidence level.*

WEST COAST (1˚x1˚OI SST)

| LA G | JUL | AUG | SEP | OC T | NO V | DEC | JAN | FEB | MAR | APR | MAY | JUN |
|---|---|---|---|---|---|---|---|---|---|---|---|---|
| 0 | -0,19 | -0,19 | -0,14 | 0,08 | 0,13 | **0,38** | 0,16 | **0,39** | **0,31** | **0,40** | **0,30** | -0,04 |
| 1 | -0,21 | -0,13 | 0,00 | 0,10 | **0,38** | 0,13 | **0,39** | **0,34** | **0,41** | **0,34** | 0,06 | -0,20 |
| 2 | -0,10 | -0,02 | 0,04 | **0,33** | 0,12 | **0,39** | **0,30** | **0,43** | **0,40** | 0,01 | -0,09 | -0,19 |
| 3 | -0,04 | 0,02 | **0,30** | 0,10 | **0,36** | **0,30** | **0,35** | **0,42** | 0,01 | -0,11 | -0,12 | -0,12 |
| 4 | 0,02 | 0,28 | 0,11 | **0,30** | 0,26 | **0,35** | **0,36** | -0,03 | -0,12 | -0,11 | -0,21 | -0,16 |
| 5 | 0,27 | 0,08 | 0,25 | 0,19 | **0,30** | **0,35** | -0,04 | -0,15 | -0,10 | -0,19 | -0,31 | -0,04 |
| 6 | 0,07 | 0,21 | 0,18 | 0,27 | 0,32 | -0,06 | -0,12 | -0,13 | -0,14 | -0,30 | -0,08 | 0,23 |

WEST COAST (0.25x0.25 OI SST)

| LA G | JUL | AUG | SEP | OCT | NOV | DEC | JAN | FEB | MAR | APR | MAY | JUN |
|---|---|---|---|---|---|---|---|---|---|---|---|---|
| 0 | -0,25 | -0,22 | -0,25 | 0,01 | -0,03 | 0,22 | -0,14 | **0,44** | 0,28 | 0,23 | -0,15 | -0,24 |
| 1 | -0,25 | -0,21 | -0,05 | -0,07 | 0,23 | -0,16 | **0,39** | **0,32** | 0,29 | -0,05 | -0,21 | -0,31 |
| 2 | -0,21 | -0,01 | -0,11 | 0,13 | -0,14 | **0,40** | **0,30** | **0,34** | 0,04 | -0,20 | 0,3-0 | -0,25 |
| 3 | 0,02 | -0,10 | 0,12 | -0,22 | **0,38** | **0,35** | **0,28** | 0,11 | -0,19 | -0,28 | -0,22 | -0,28 |
| 4 | -0,10 | 0,16 | -0,19 | 0,28 | **0,32** | **0,31** | 0,06 | -0,19 | -0,28 | -0,18 | -0,39 | -0,10 |
| 5 | 0,17 | -0,19 | 0,25 | 0,23 | 0,28 | 0,08 | -0,20 | -0,27 | -0,15 | -0,37 | -0,23 | -0,17 |
| 6 | -0,23 | 0,26 | 0,24 | 0,23 | 0,08 | -0,24 | -0,26 | -0,17 | -0,29 | -0,23 | -0,16 | 0,07 |

SOUTH COAST (1˚x1˚OI SST)

| | JUL | AUG | SEP | OCT | NOV | DEC | JAN | FEB | MAR | APR | MAY | JUN |
|---|---|---|---|---|---|---|---|---|---|---|---|---|
| 0 | -0.01 | 0.22 | 0.18 | 0.04 | -0.07 | 0.10 | **0.31** | 0.27 | 0.27 | **0.35** | **0.31** | -0.01 |
| 1 | 0.18 | 0.20 | 0.04 | -0.09 | 0.09 | **0.30** | **0.30** | 0.26 | **0.32** | 0.41 | 0.11 | 0.11 |
| 2 | 0.25 | 0.01 | -0.06 | 0.07 | **0.31** | **0.34** | 0.22 | **0.33** | **0.42** | 0.18 | 0.26 | 0.24 |
| 3 | -0.07 | -0.05 | 0.08 | **0.31** | **0.34** | 0.20 | 0.28 | **0.44** | 0.21 | 0.26 | 0.29 | 0.30 |
| 4 | -0.05 | 0.11 | **0.31** | **0.30** | 0.17 | 0.27 | **0.43** | **0.23** | 0.18 | **0.30** | 0.21 | -0.06 |
| 5 | 0.12 | 0.33 | 0.23 | **0.14** | 0.23 | **0.48** | 0.22 | 0.18 | 0.17 | 0.18 | -0.13 | -0.06 |
| 6 | **0.39** | 0.22 | 0.10 | 0.23 | **0.44** | 0.24 | 0.18 | 0.14 | 0.08 | -0.14 | -0.01 | 0.15 |

SOUTH COAST (0.25x0.25 OI SST)

| LAG | JUL | AUG | SEP | OCT | NOV | DEC | JAN | FEB | MAR | APR | MAY | JUN |
|---|---|---|---|---|---|---|---|---|---|---|---|---|
| 0 | -0.14 | -0.06 | 0.06 | 0.13 | -0.13 | 0.11 | 0.25 | 0.28 | 0.19 | **0.31** | 0.14 | -0.14 |
| 1 | -0.08 | 0.08 | 0.11 | -0.12 | 0.11 | 0.24 | 0.29 | 0.19 | 0.34 | 0.24 | -0.07 | -0.09 |
| 2 | 0.10 | 0.08 | -0.10 | 0.12 | 0.21 | **0.34** | 0.16 | **0.37** | 0.31 | 0.04 | 0.05 | -0.02 |
| 3 | -0.02 | -0.09 | 0.13 | 0.21 | **0.34** | 0.17 | **0.32** | **0.36** | 0.15 | 0.11 | 0.11 | 0.13 |
| 4 | -0.08 | 0.15 | 0.19 | **0.32** | 0.18 | **0.33** | **0.36** | 0.19 | 0.16 | 0.22 | 0.11 | -0.08 |
| 5 | 0.12 | 0.21 | 0.20 | 0.16 | **0.30** | **0.40** | 0.17 | 0.19 | 0.25 | 0.13 | -0.19 | -0.10 |
| 6 | 0.28 | 0.21 | 0.09 | **0.34** | **0.40** | 0.19 | 0.17 | 0.24 | 0.13 | -0.20 | -0.07 | 0.12 |

PE/PA (1˚x1˚OI SST)

| LA G | JUL | AUG | SEP | OCT | NOV | DEC | JAN | FEB | MAR | APR | MAY | JUN |
|---|---|---|---|---|---|---|---|---|---|---|---|---|
| 0 | -0.04 | 0.13 | 0.08 | -0.07 | -0.03 | -0.02 | 0.03 | 0.18 | 0.26 | **0.30** | 0.24 | -0.04 |
| 1 | 0.08 | 0.07 | -0.04 | -0.04 | -0.05 | 0.01 | 0.20 | 0.29 | 0.26 | **0.38** | 0.03 | 0.14 |
| 2 | 0.08 | -0.09 | -0.01 | -0.09 | 0.02 | 0.27 | 0.26 | 0.26 | **0.33** | 0.12 | 0.26 | 0.13 |
| 3 | -0.14 | 0.01 | -0.06 | 0.01 | **0.25** | **0.26** | 0.23 | **0.33** | 0.11 | 0.30 | 0.15 | 0.13 |
| 4 | 0.04 | -0.03 | 0.00 | 0.22 | 0.22 | 0.23 | **0.36** | 0.14 | 0.23 | 0.17 | 0.07 | -0.08 |
| 5 | 0.01 | 0.04 | 0.14 | 0.19 | 0.18 | **0.40** | 0.15 | 0.24 | 0.13 | 0.06 | -0.03 | 0.05 |
| 6 | 0.16 | 0.11 | 0.18 | 0.16 | **0.34** | 0.18 | 0.23 | 0.11 | 0.03 | -0.09 | 0.16 | 0.12 |

PE/PA (0.25x0.25 OI SST)

| LAG | JUL | AUG | SEP | OCT | NOV | DEC | JAN | FEB | MAR | APR | MAY | JUN |
|---|---|---|---|---|---|---|---|---|---|---|---|---|
| 0 | -0.09 | 0.01 | -0.16 | -0.15 | -0.13 | 0.08 | 0.06 | 0.11 | 0.01 | 0.07 | -0.06 | -0.08 |
| 1 | -0.08 | -0.14 | -0.13 | -0.15 | 0.08 | 0.08 | 0.14 | 0.03 | 0.07 | 0.07 | -0.05 | -0.01 |
| 2 | -0.16 | -0.13 | -0.15 | 0.07 | 0.11 | 0.19 | 0.00 | 0.08 | 0.07 | -0.01 | 0.02 | -0.14 |
| 3 | -0.15 | -0.12 | 0.09 | 0.15 | 0.20 | 0.02 | 0.04 | 0.09 | -0.01 | 0.01 | -0.17 | -0.22 |
| 4 | -0.08 | 0.12 | 0.16 | 0.22 | 0.02 | 0.05 | 0.10 | 0.03 | -0.02 | -0.12 | -0.32 | -0.15 |
| 5 | 0.13 | 0.16 | 0.18 | 0.03 | 0.05 | 0.15 | 0.02 | 0.00 | -0.12 | -0.31 | -0.14 | -0.07 |
| 6 | 0.16 | 0.16 | -0.02 | 0.08 | 0.15 | 0.05 | 0.00 | -0.11 | -0.29 | -0.10 | -0.02 | 0.15 |

TRANSKEI (1˚x1˚OI SST)

| LA G | JUL | AUG | SEP | OCT | NOV | DEC | JAN | FEB | MAR | APR | MAY | JUN |
|---|---|---|---|---|---|---|---|---|---|---|---|---|
| 0 | -0.06 | -0.18 | -0.08 | -0.01 | -0.02 | -0.18 | -0.10 | -0.01 | 0.03 | 0.12 | 0.15 | -0.08 |
| 1 | -0.24 | -0.07 | 0.04 | -0.03 | -0.17 | -0.11 | 0.04 | 0.02 | 0.25 | **0.32** | -0.05 | 0.01 |
| 2 | -0.03 | 0.01 | -0.01 | -0.20 | -0.08 | 0.10 | 0.02 | 0.24 | **0.37** | 0.04 | 0.03 | **-0.23** |
| 3 | -0.04 | 0.02 | -0.21 | -0.08 | 0.11 | 0.05 | 0.26 | **0.39** | 0.13 | 0.03 | -0.15 | 0.06 |
| 4 | 0.04 | -0.18 | -0.14 | 0.10 | 0.08 | 0.28 | **0.45** | 0.16 | 0.07 | -0.13 | 0.01 | 0.06 |
| 5 | -0.19 | -0.13 | 0.03 | 0.08 | 0.26 | **0.49** | 0.21 | 0.08 | -0.04 | -0.02 | 0.12 | 0.07 |
| 6 | -0.06 | 0.00 | 0.07 | 0.24 | **0.47** | 0.23 | 0.12 | -0.03 | 0.01 | 0.04 | 0.15 | -0.12 |

TRANSKEI (0.25x0.25 OI SST)

| LAG | JUL | AUG | SEP | OCT | NOV | DEC | JAN | FEB | MAR | APR | MAY | JUN |
|---|---|---|---|---|---|---|---|---|---|---|---|---|
| 0 | -0.18 | -0.09 | 0.03 | -0.01 | -0.15 | -0.29 | -0.19 | -0.15 | -0.02 | 0.04 | -0.06 | -0.23 |
| 1 | -0.16 | 0.00 | 0.01 | -0.14 | -0.26 | -0.18 | -0.13 | -0.05 | 0.16 | 0.09 | -0.21 | -0.14 |
| 2 | -0.01 | 0.05 | -0.13 | -0.28 | -0.19 | -0.07 | -0.04 | 0.18 | 0.11 | -0.14 | -0.09 | -0.16 |
| 3 | 0.02 | -0.10 | -0.28 | -0.22 | -0.06 | -0.01 | 0.17 | 0.14 | -0.05 | -0.05 | -0.14 | 0.02 |
| 4 | -0.12 | -0.25 | -0.26 | -0.05 | 0.03 | 0.18 | 0.17 | -0.01 | 0.03 | -0.14 | -0.02 | 0.05 |
| 5 | -0.28 | -0.28 | -0.05 | 0.04 | 0.17 | 0.17 | 0.01 | 0.05 | -0.12 | -0.03 | 0.04 | -0.15 |
| 6 | -0.21 | -0.04 | 0.01 | 0.16 | 0.12 | 0.02 | 0.11 | -0.14 | 0.01 | 0.01 | -0.10 | -0.33 |

KWAZULU-NATAL (1˚x1˚OI SST)

| LA G | JUL | AUG | SEP | OCT | NOV | DEC | JAN | FEB | MAR | APR | MAY | JUN |
|---|---|---|---|---|---|---|---|---|---|---|---|---|
| 0 | -0.09 | -0.15 | -0.20 | -0.07 | 0.08 | 0.04 | -0.10 | -0.38 | -0.03 | 0.11 | 0.03 | 0.08 |
| 1 | -0.05 | -0.17 | -0.02 | 0.07 | 0.08 | -0.10 | -0.34 | -0.02 | 0.10 | 0.02 | 0.05 | 0.02 |
| 2 | -0.08 | 0.01 | 0.04 | 0.13 | -0.10 | -0.32 | 0.00 | 0.16 | 0.02 | 0.03 | 0.01 | 0.00 |
| 3 | 0.04 | 0.06 | 0.16 | -0.12 | -0.29 | 0.00 | 0.10 | 0.08 | 0.07 | -0.01 | -0.01 | -0.01 |
| 4 | 0.03 | 0.22 | -0.15 | **-0.26** | 0.01 | 0.09 | 0.07 | 0.08 | 0.04 | 0.07 | 0.00 | 0.03 |
| 5 | 0.03 | -0.18 | -0.19 | 0.02 | 0.02 | 0.06 | -0.10 | 0.07 | 0.04 | 0.12 | 0.04 | -0.03 |
| 6 | -0.17 | -0.16 | 0.04 | 0.00 | 0.05 | 0.13 | 0.12 | 0.05 | 0.14 | 0.16 | -0.08 | 0.06 |

KZN (0.25x0.25 OI SST)

| LAG | JUL | AUG | SEP | OCT | NOV | DEC | JAN | FEB | MAR | APR | MAY | JUN |
|---|---|---|---|---|---|---|---|---|---|---|---|---|
| 0 | -0.21 | -0.17 | 0.14 | 0.09 | -0.06 | -0.20 | -0.14 | -0.14 | 0.00 | 0.13 | 0.20 | -0.02 |
| 1 | -0.19 | 0.11 | 0.14 | -0.07 | -0.19 | -0.14 | -0.11 | -0.01 | 0.25 | **0.35** | 0.04 | -0.13 |
| 2 | 0.08 | 0.17 | -0.11 | -0.22 | -0.14 | -0.06 | -0.01 | 0.26 | **0.39** | 0.14 | -0.04 | -0.10 |
| 3 | 0.13 | -0.08 | -0.21 | -0.15 | -0.04 | 0.02 | 0.27 | **0.43** | 0.19 | 0.06 | -0.04 | 0.16 |
| 4 | -0.07 | -0.17 | -0.20 | 0.01 | 0.06 | 0.28 | 0.43 | 0.22 | 0.16 | -0.02 | 0.11 | 0.16 |
| 5 | -0.21 | -0.26 | -0.01 | 0.07 | 0.26 | **0.45** | 0.26 | 0.17 | -0.02 | 0.07 | 0.20 | -0.09 |
| 6 | -0.22 | 0.01 | 0.05 | 0.26 | **0.42** | 0.29 | 0.22 | -0.02 | 0.08 | 0.14 | -0.08 | -0.25 |

AGHULAS RETROFLECTION (1˚x1˚OI SST)

| LA G | JUL | AUG | SEP | OCT | NOV | DEC | JAN | FEB | MAR | APR | MAY | JUN |
|---|---|---|---|---|---|---|---|---|---|---|---|---|
| 0 | -0.04 | -0.09 | 0.24 | 0.23 | -0.01 | -0.13 | -0.33 | -0.31 | -0.25 | -0.32 | -0.09 | -0.27 |
| 1 | -0.14 | 0.28 | 0.16 | -0.01 | -0.12 | -0.36 | -0.35 | -0.23 | -0.36 | -0.18 | -0.36 | -0.18 |
| 2 | 0.30 | 0.16 | -0.06 | -0.17 | -0.37 | -0.35 | -0.27 | -0.34 | -0.24 | -0.31 | -0.27 | -0.16 |
| 3 | 0.12 | -0.05 | -0.21 | -0.39 | -0.37 | -0.28 | -0.36 | -0.21 | -0.28 | -0.31 | -0.18 | 0.32 |
| 4 | -0.02 | -0.20 | -0.39 | -0.39 | -0.32 | -0.35 | -0.22 | -0.24 | -0.30 | -0.21 | 0.20 | 0.16 |
| 5 | -0.17 | -0.35 | -0.41 | -0.37 | -0.38 | -0.18 | -0.20 | -0.26 | -0.23 | 0.06 | 0.10 | 0.03 |
| 6 | -0.30 | -0.40 | -0.38 | -0.41 | -0.20 | -0.15 | -0.23 | -0.22 | -0.01 | -0.04 | 0.10 | -0.12 |

AGULHAS RETROFLECTION (0.25x0.25 OI SST)

| LAG | JUL | AUG | SEP | OCT | NOV | DEC | JAN | FEB | MAR | APR | MAY | JUN |
|---|---|---|---|---|---|---|---|---|---|---|---|---|
| 0 | -0.30 | -0.18 | -0.21 | -0.16 | -0.03 | -0.31 | 0.00 | -0.11 | 0.21 | 0.15 | -0.10 | -0.05 |
| 1 | -0.20 | -0.22 | -0.17 | -0.13 | -0.33 | -0.17 | -0.19 | 0.24 | 0.12 | -0,1 | -0.04 | -0.28 |
| 2 | -0.23 | -0.15 | -0.13 | -0.15 | -0.33 | -0.15 | 0.27 | 0.11 | -0.1 | -0.1 | -0.30 | -0.19 |
| 3 | -0.17 | -0.10 | -0.16 | -0.33 | -0.09 | **0.31** | 0.07 | -0.14 | -0.1 | -0.3 | -0.21 | -0.22 |
| 4 | -0.09 | -0.09 | -0.37 | 0.14 | 0.23 | 0.12 | -0.12 | -0.07 | -0.3 | -0.2 | -0.24 | -0.15 |
| 5 | -0.09 | -0.34 | 0.00 | 0.06 | 0.09 | -0.07 | -0.04 | -0.28 | -0.2 | -0.3 | -0.20 | -0.05 |
| 6 | -0.31 | -0.03 | 0.10 | -0.11 | 0.03 | -0.01 | -0.24 | -0.23 | -0.3 | -0.2 | -0.07 | -0.04 |

.

## CHAPTER 4: ENSO atmospheric forcing

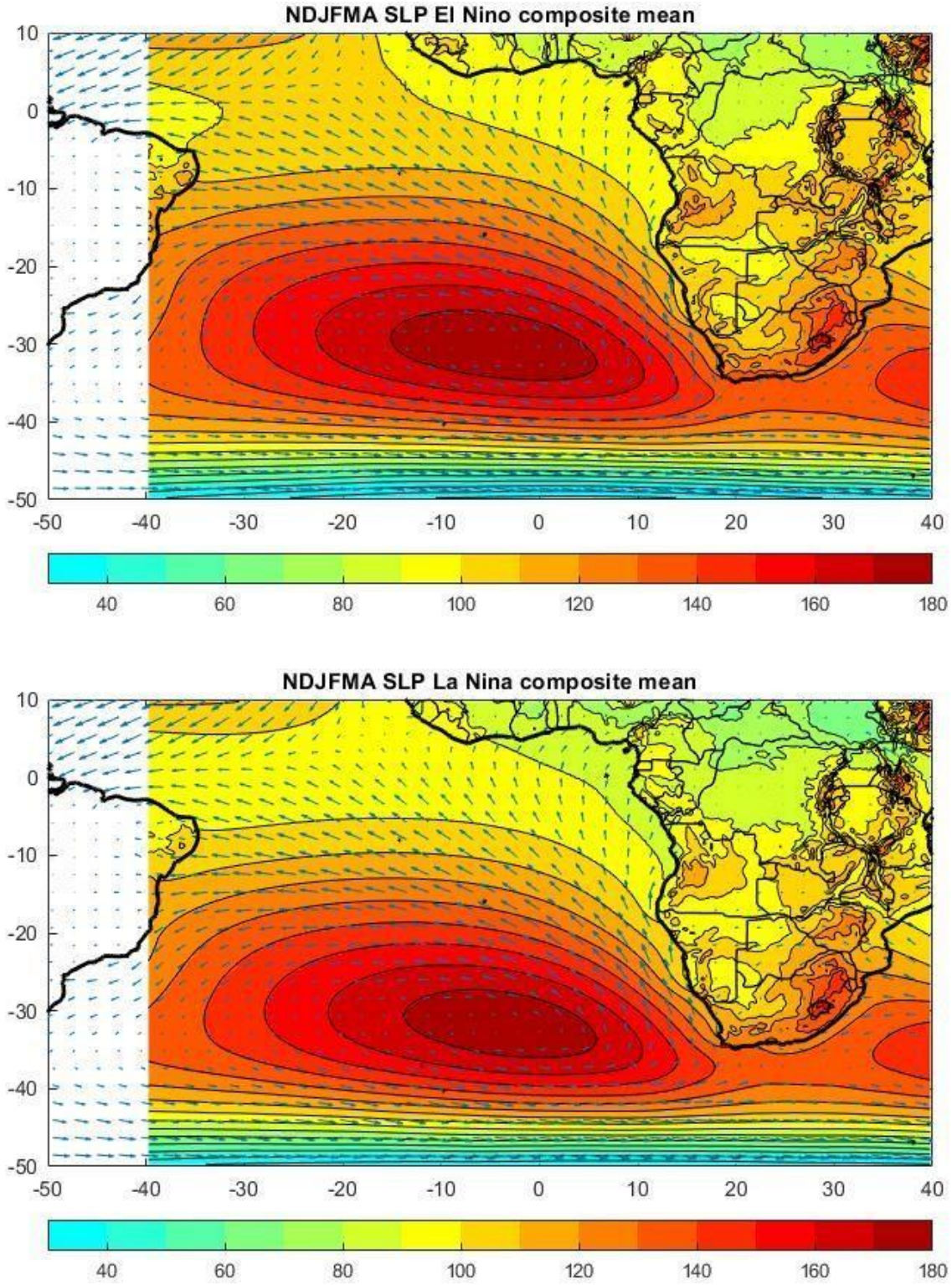


*Figure 34. mean NDJFMA surface wind speed and direction (arrow) and 1000 hPa geopotential height(color) during an average El Niño (top) and La Niña (bottom) for summer (average of November to April*

Figure 34 shows surface pressure and the wind speed and direction in summer (November to April) at the 1000 hPa geopotential height for the 1982-2017 climatological average of average of November to April. It clearly shows the relation between wind and pressure and the southern extent of the South Atlantic high-pressure system. This will the basis upon which anomalies from the mean will be discussed. At first, there does not seem much difference between the two but close inspection and anomalies for seasonal means presented in Figure 35 for El Niño and Figure 36 for La Niña show slight differences. This also shows that winds do not reverse from El Niño to La Niña , they just decrease or increase. Those differences explain most of the SST anomalies previously shown for ENSO also presented for NDJFMA in Figures 35 and 36. Distinctions between early summer (NDJF) and late summer (FMA) will be explored below.

The rationale for showing the whole summer (NDJFM) and NDJ and FMA separately is that ENSO is correlated in early summer to some domains studied, and we need to know whether there is any difference between early summer and late summer due to the differences in correlation. The South Atlantic High pressure occupies the whole Atlantic basin from South Africa to South America with strong south easterly to easterly winds from 10 S to 30 S. South of the high pressure center, quite far South, from 40 S, the wind is westerly and further south the mid-latitude low pressure system generates winds whose average is mostly westerly. During a storm the wind goes from north westerly to south westerly. South of Africa the pressure is lower, as it is situated in between the Atlantic and the Indian Ocean Highs with relatively low pressure and weaker winds south of Africa. The South Indian Ocean high pressure system is visible to the east. The weak winds south of Africa from the coast to about 40 S are an artefact of the averaging, because the wind is either easterly or westerly there and the averages reduce the absolute wind speed. Along the Equator, the wind is easterly. From 10 N to 10 S, low pressure and easterly winds prevail in the austral summer as part of the Inter Tropical Convergence Zone (ITCZ) which creates the easterly winds. North of Namibia to the equator the wind is southerly to south-westerly and influenced by the West African Monsoon and the Central African ITCZ low pressure system. The southern African continent has a lower pressure than the Ocean which contributes to increase the pressure gradient between ocean and continent and to intensify the southerly to south easterly winds along the coast. The upwelling favorable wind is therefore created by the high-pressure isobar gradient and the pressure contrast with the continent. Close examination of figure 34 show that the South Atlantic high-pressure system is shifted to the south by a few degrees during La Niña when compared to El Niño . This explains the wind anomalies along the coast of South Africa presented in Figures 35 and 36 with north-westerly anomalies during El Niño and south-easterly anomalies during La Niña in the West Coast and South Coast domains. It also explains warm SST anomalies around South Africa during El Niño and the cold anomaly during

La Niña . Another feature in Figure 34 is that the pressure is higher in the tropical Atlantic and above the continent during El Niño than during La Niña which will modify the pressure gradient and the wind speed too. All of that is clearer in the El Niño and Composite anomalies shown below. The association between anomaly of geopotential and wind speed is during La Niña and El Niño is presented in Figure 36 and it clearly show the basin wide association between geopotential gradient anomalies and wind speed and direction anomalies most of it linked to the large-scale SST anomalies. The winds do not change direction between el Niño and La Niña , they are just weaker or stronger, leading to the SST anomalies. The change in wind speed changes the flux of latent and sensible heat at the surface contributing to the large-scale basin-wide warming or cooling and contributing to the coastal SST anomalies that are usually increased or reduced anomalies.

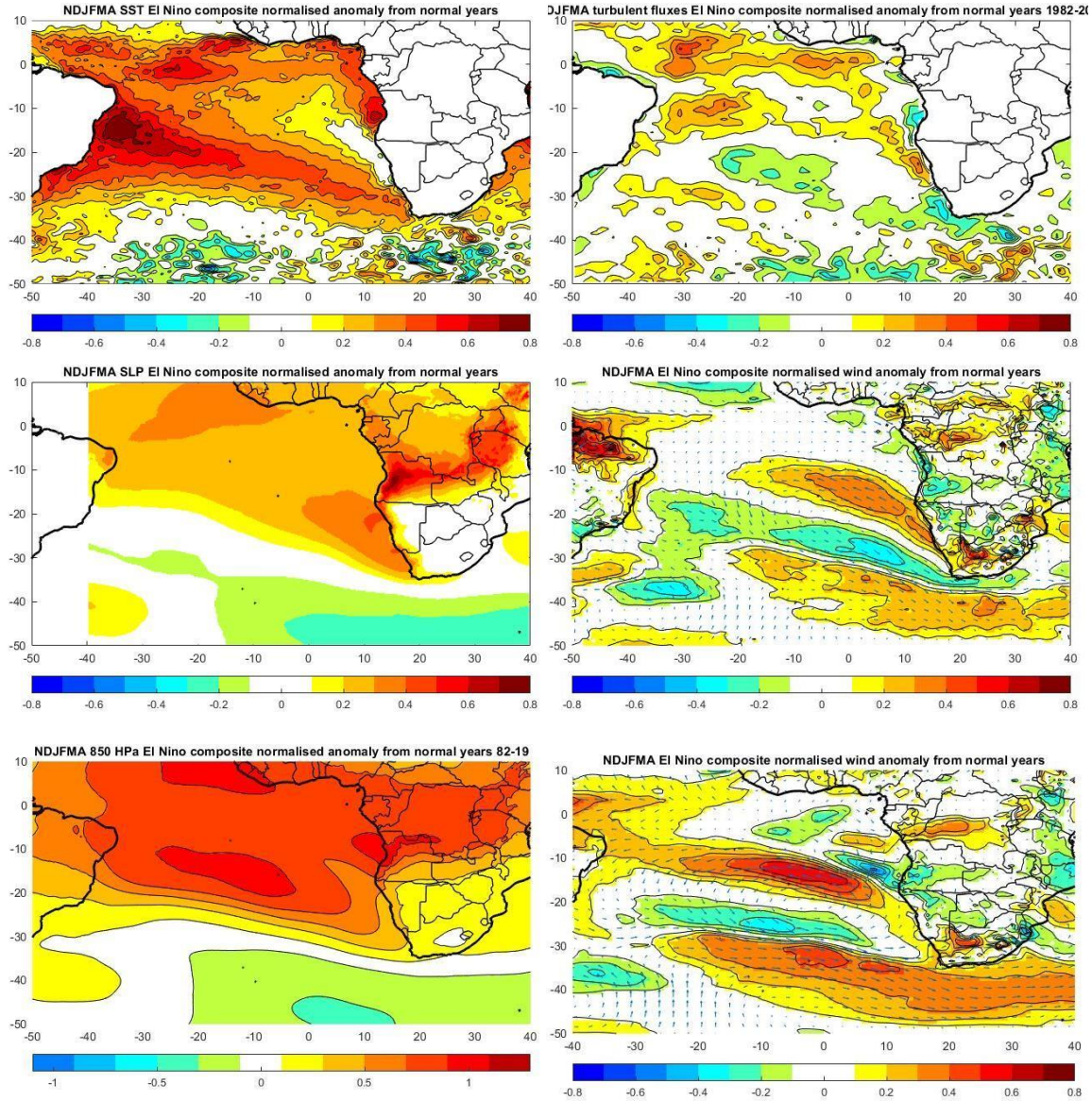


*Figure 35. Composite El Niño NDJFMA normalised detrended anomalies for (left to right top to bottom) SST, ERA 5 turbulent latent and sensible heat flux, 1000 geopotential height anomaly, 1000 hPa wind speed and direction, 850 geopotential height and 850 geopotential wind speed and direction.*

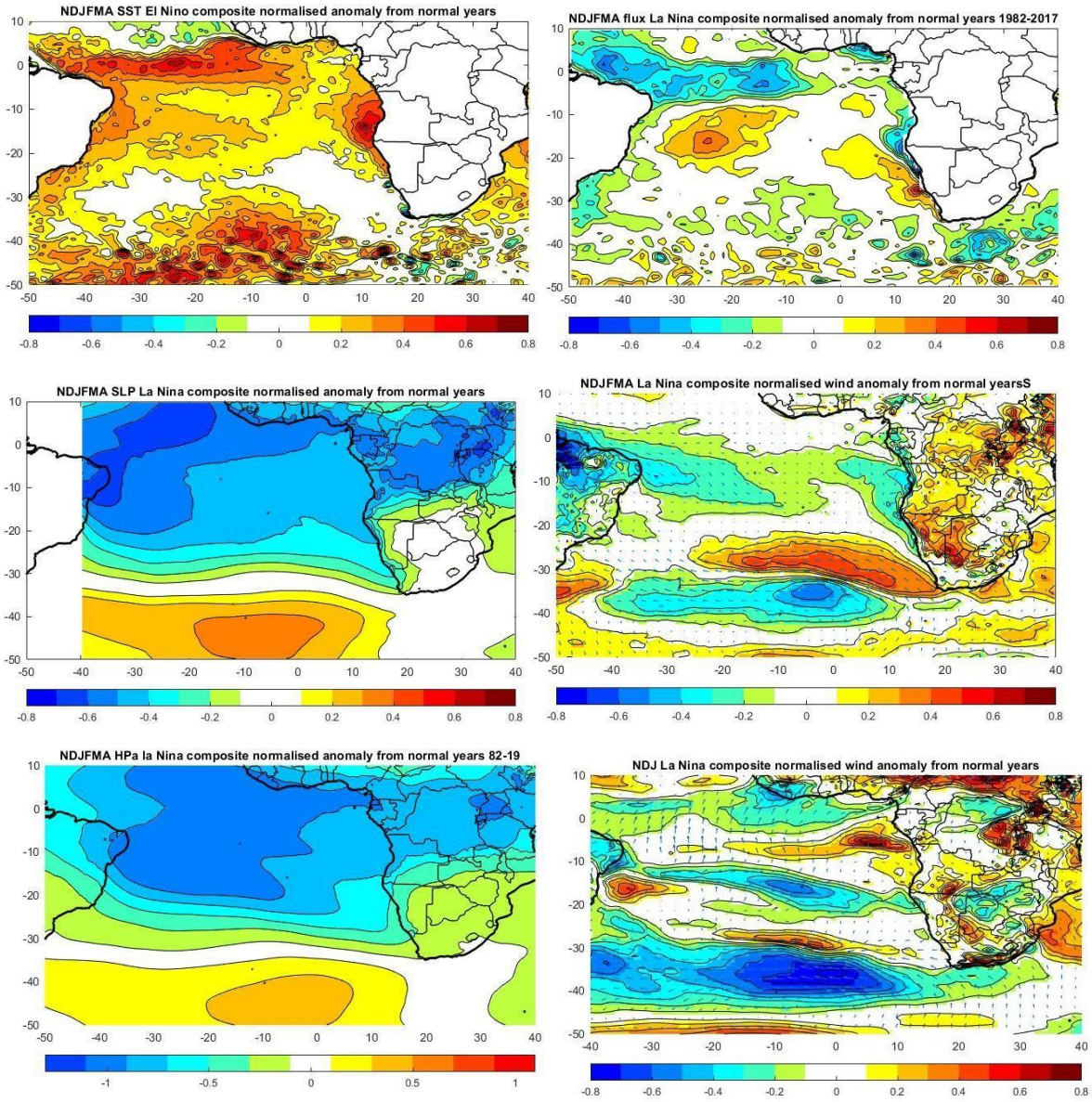


*Figure 36. Composite La Niña NDJFMA normalised detrended anomalies for (left to right top to bottom) SST, ERA 5 turbulent latent and sensible heat flux, 1000 geopotential height anomaly 1000 hPa wind speed and direction 850 geopotential height and 850 geopotential wind speed and direction.*

The Tropical Atlantic is complicated because of the remote impact of wind anomalies along the equator and along the African coast all the way to the Northern Benguela which is at the origin of Atlantic Niños and Niñas (Imbol Koungue et al., 2018, 2019). The NDF SST anomalies during early summer (NDJ) during El Niño presented in Figure 38 are like the FMA La Niño composite (Figure 40) in terms of regional SST around South Africa. A major difference, basin wide, is that the basin-scale warming is less in NDJ than FMA. The high-pressure anomalies in the mid-latitudes in DJF are larger than in FMA leading to weaker wind anomalies and lower heat fluxes anomalies in FMA than DJF. Large-scale patterns at 850 and 1000 HPa are quite different and weaker in late summer than early summer which may explain the basin-wide

SST warming. The north-westerly wind anomalies leading to the SST warming all the way to South Africa are not as marked in FMA as in DJF, but weaker latent heat fluxes occur in FMA than in DJF contributing to maintaining the warming around South Africa. The ocean has a large heat capacity. The atmospheric forcing is therefore stronger in DJF than in FMA but due to the high heat capacity of the ocean, SST anomalies probably persist and increase in FMA. Also, the warming decreases the latent and sensible fluxes as the differences in temperature between ocean and atmosphere decrease.

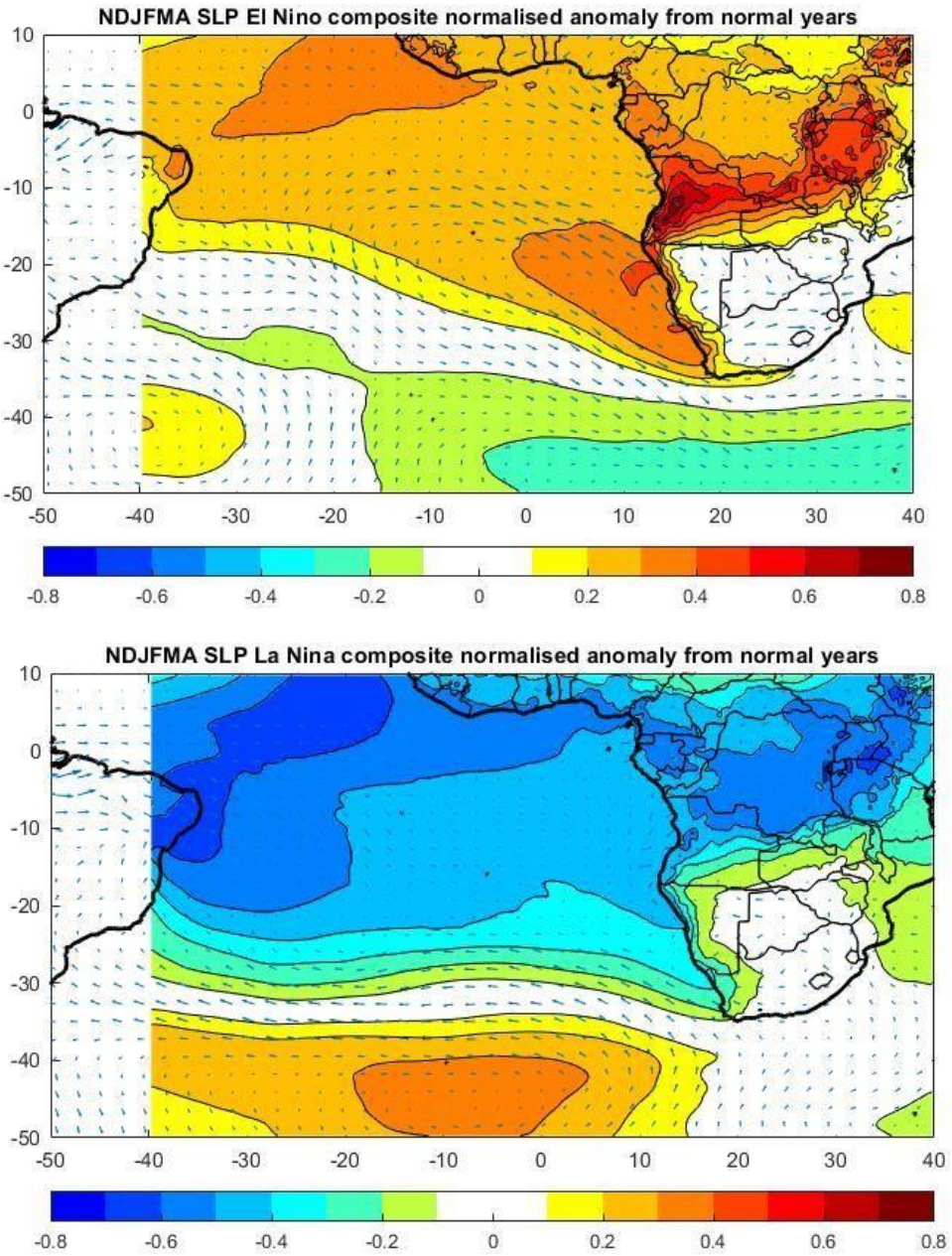


*Figure 37. Composite El Niño and La Niña NDJFMA normalised detrended anomalies for 1000 geopotential height anomaly (color) and wind speed and direction (arrows).*

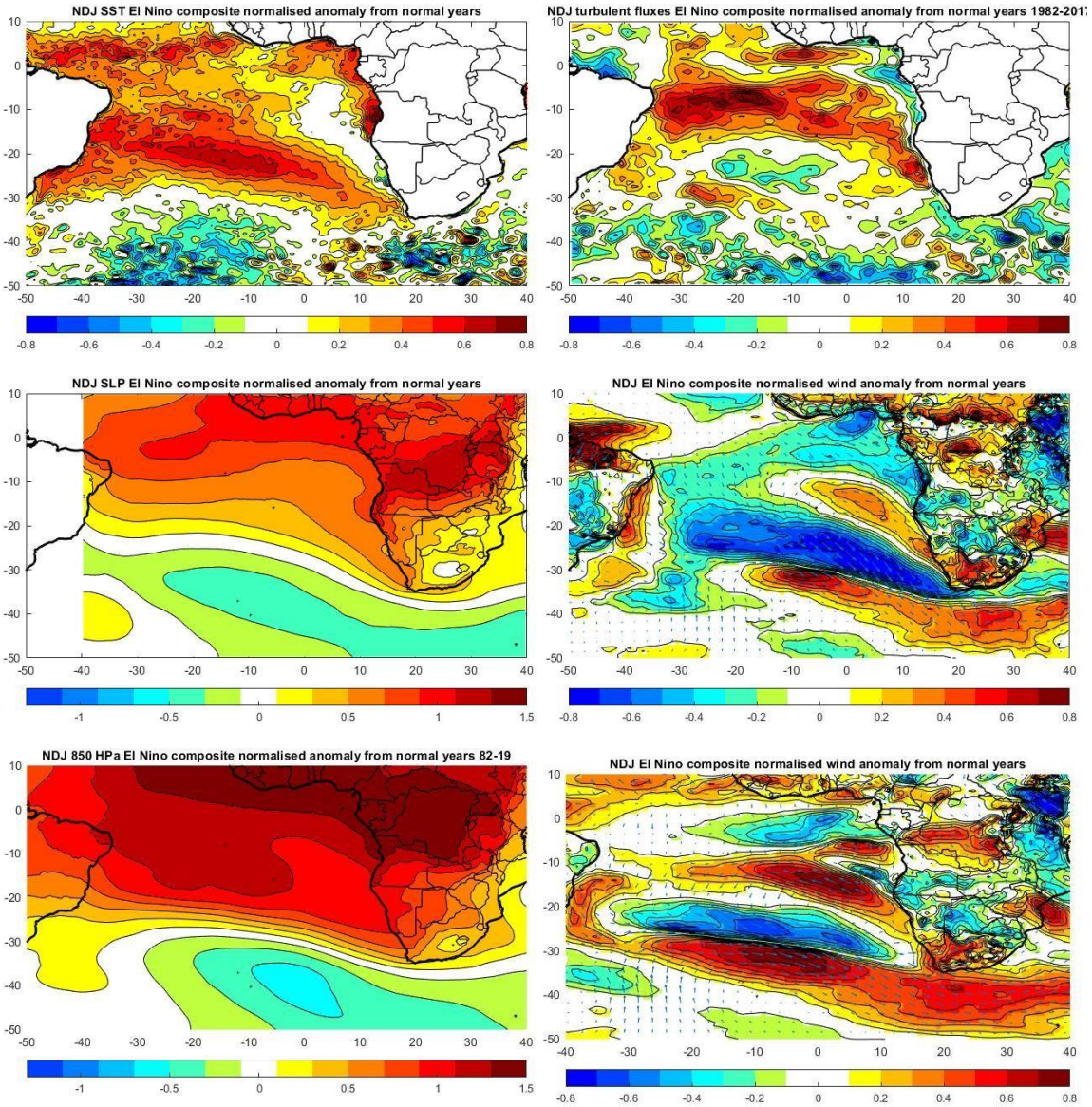


*Figure 38. Composite El Niño NDJFMA normalised detrended anomalies for (left to right top to bottom) for SST, ERA 5 turbulent latent and sensible heat flux, 1000 geopotential height anomaly 1000 hPa wind speed and direction 850 geopotential height and and 850 geopotential wind speed and direction.*

The NDF SST anomalies during early summer (NDJ) La Niña presented in Figure 39 are quite like FMA La Niña composites (Figure 40). A major basin-wide difference is that the basin-scale warming is lower in NDJ than FMA. The high-pressure anomalies in the mid-latitudes in DJF are larger than in FMA, leading to weaker wind anomalies and lower heat flux anomalies to the north in FMA than DJF. Large-scale patterns are quite similar, with regional differences especially in the Tropical Atlantic. The band of higher than normal south-east wind speed in the West Coast domain is quite similar leading to the cold anomalies in the upwelling. The atmospheric geopotential is lower above land in DJF than in FMA but in the Tropical Atlantic it is the opposite. All in all, there is little difference in SST anomalies and anomalous atmospheric forcing between the West Coast and South Coast domains in both DJF and

FMA. Similar large-scale forcing occurs in both seasons with more basin wide warming leading to lower geopotential anomalies in the tropics and subtropics. All in all, there are regional differences and the atmospheric forcing is stronger in DJF than in FMA but not different enough to prevent the SST warming from increasing in FMA. Since ENSO generally starts to develop in June and grow from then on in time, space and in intensity and strength, the lag correlation can be explained by the fact that the impact of ENSO is in early summer or late summer during the mature phase of ENSO, but ENSO has had enough time to influence the globe.

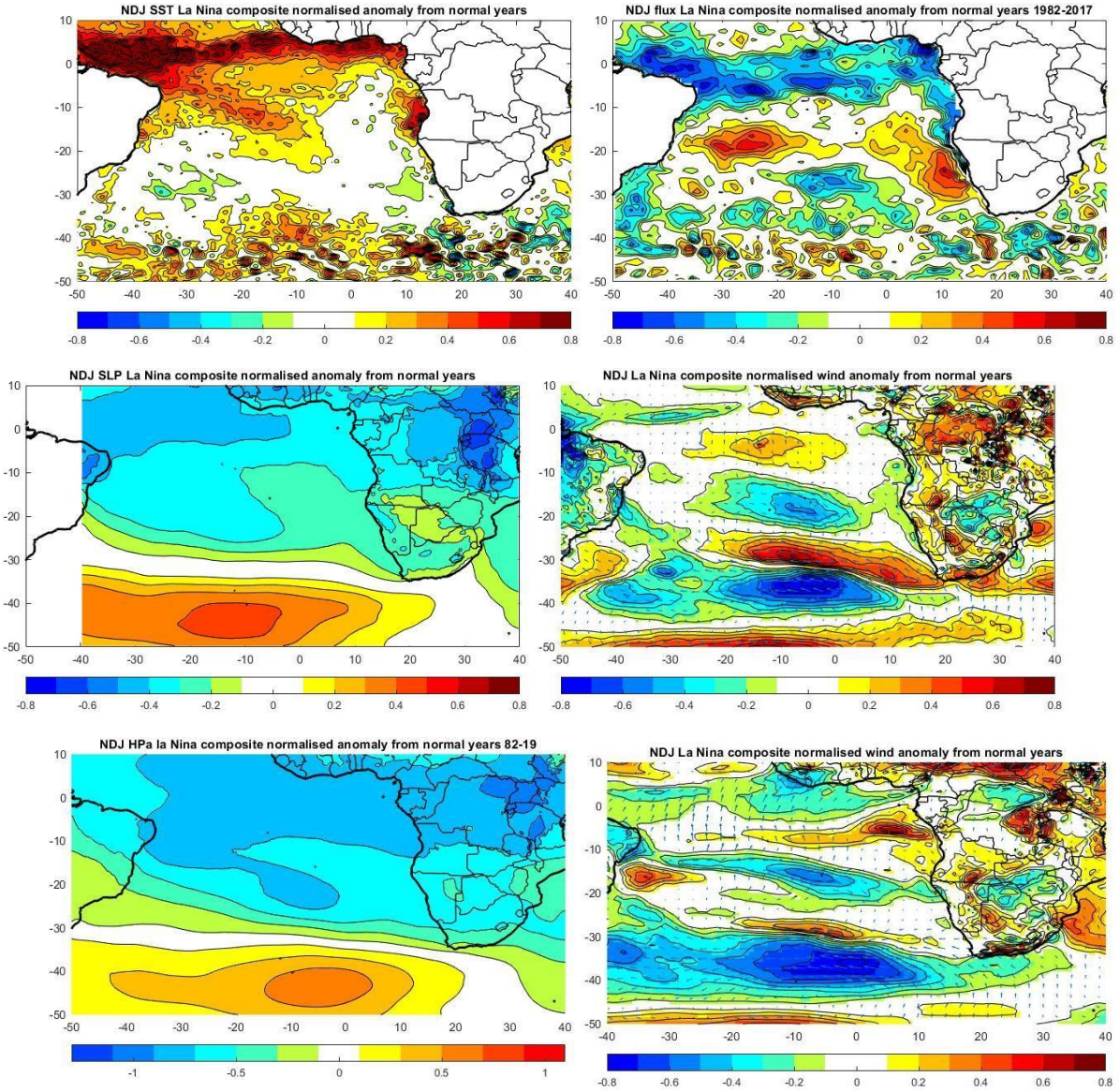


*Figure 39. La Niña Composite NDJ normalised detrended anomalies for (left to right top to bottom) for SST, ERA 5 turbulent latent and sensible heat flux, 1000 geopotential height anomaly 1000 hPa wind speed and direction 850 geopotential height and 850 geopotential wind speed and direction.*

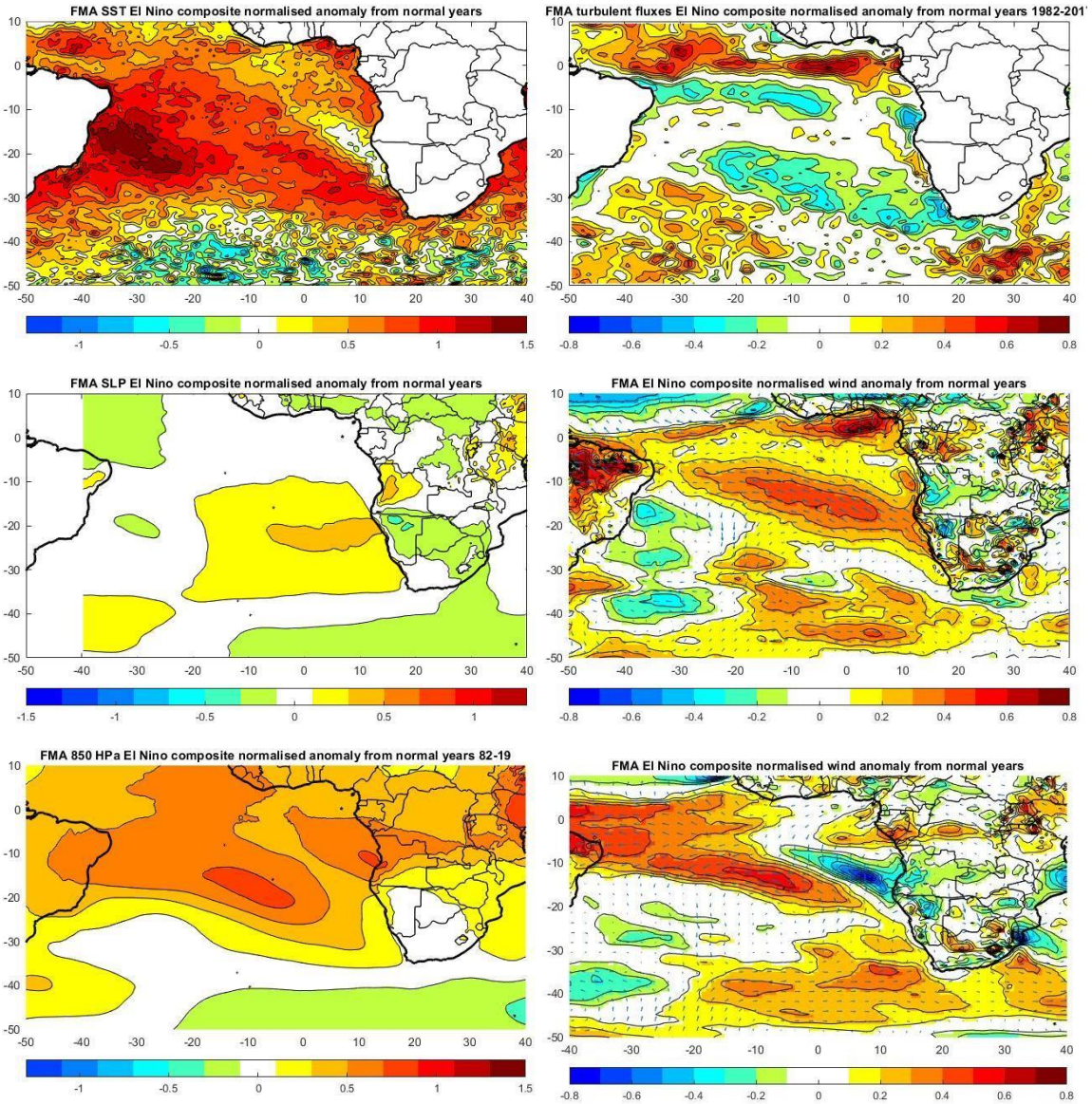


*Figure 40. Composite El Niño FMA normalised detrended anomalies for (left to right top to bottom) for SST, ERA 5 turbulent latent and sensible heat flux, 1000 geopotential height anomaly 1000 hPa wind speed and direction 850 geopotential height and 850 geopotential height and 850 geopotential wind speed and direction.*

The perturbation created in the atmosphere over the Pacific depends on ocean-atmosphere interaction. There must be a delay between the Pacific Ocean-atmosphere interaction and its propagation to southern Africa. Another effect is that the Pacific interaction influences the SST of the Tropical Atlantic and the Indian Ocean which in turn will influence southern Africa and the South Atlantic Ocean. The small correlations at zero lag could be due to the time the ENSO perturbation takes to warm the Indian Ocean or the Tropical Atlantic that in turn also influences the southern African climate. The effect of ENSO is quite persistent and consistent during summer with slight regional differences and slight differences in intensity of the atmospheric forcing.

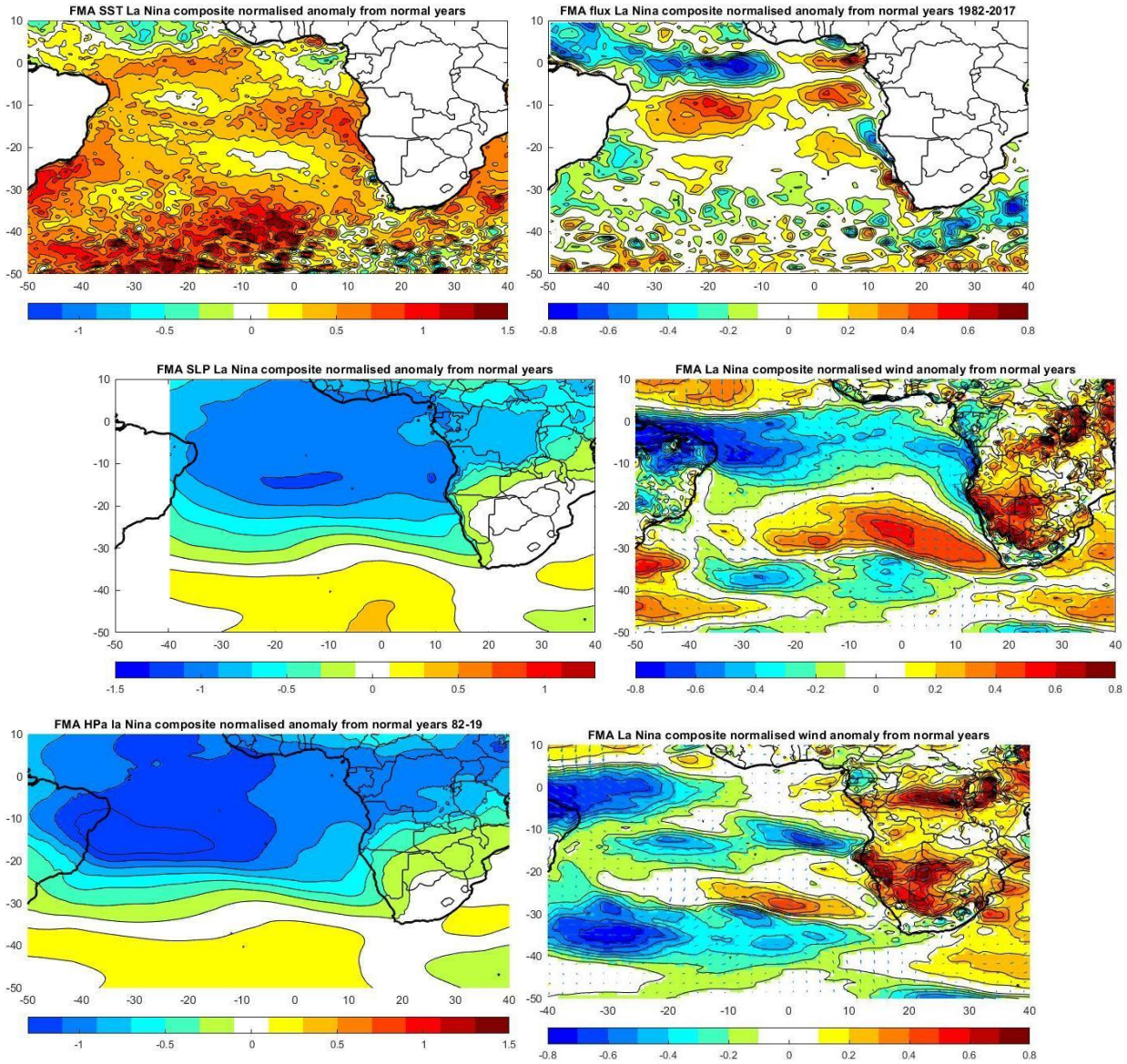


*Figure 41. La Niña Composite FMA normalised detrended anomalies for (left to right top to bottom) for SST, ERA 5 turbulent latent and sensible heat flux, 1000 geopotential height anomaly 1000 hPa wind speed and direction 850 geopotential height and 850 geopotential height and 850 geopotential wind speed and direction.*

## CHAPTER 5: DISCUSSION

Three datasets were used in this study to improve and update results concerning SST trends and correlations with ENSO presented ten years ago by Rouault et al (2010). I first looked at the annual cycle of SST and compared results among the 3 SST datasets that allow one to go closer to the coast according to greater resolution of datasets. The trends in SST around South Africa from 1982 to 2017 were also updated but Pathfinder SST could not be used because of too much missing data. SST anomalies were then detrended and normalised for time series analysis of the interannual variability of SST around the coast of South Africa at monthly and seasonal scales. Correlations showed a moderate effect of ENSO on the Coast of South Africa as part of large-scale basin-wide effect of ENSO on the South Atlantic. The results also showed an interesting lag in the correlations with ENSO is leading by a few months. This study looked at a period of 35 years. This study is the first to use 3 different datasets to examine the effect of ENSO on SST and it is very useful to see how the spatial resolution of each dataset gives different and robust results and to show which one performs best in showing SST anomalies along the coast, as well as robust correlation results. The use of different SST datasets allows us to validate the results from 1˚x1˚resolution OI SST which was used by Rouault et al (2010). Differences in trends and correlation among the 3 datasets are cause for concern. The results of 0.25x 0.25˚OI SST and Pathfinder SST are disappointing as correlation with ENSO is not improved with those two datasets which sample closer to the coast. The issue of missing values in the 4x4 km resolution AVHRR SST was a constraint, but Pathfinder SST is useful to validate the 0.25 x 0.25˚OI SST, especially for the ENSO composites as it is a very high-resolution dataset and we were able to extract SST even closer to the coast. It seems that 0.25 x 0.25˚OI SST is better than 1˚x1˚OI SST for the south coast and eastwards for the ENSO composites. Differences in trends pose a problem. Rouault et al. (2010) and Blamey et al. (2015) expressed the limitations and some concerns related to the use of the 1 x 1˚resolution Optimally Interpolated Reynolds SST; using the 0.25 x 0.25˚OI SST did not solve the problem although it probably improves results for the Port Alfred upwelling cell and the South Peninsula- Cape Columbine upwelling cell, which were not well defined in the 1˚x1˚OI SST and Rouault et al. (2010) datasets. For the South Coast, PE/PA, Transkei and KwaZulu-Natal trends and impacts of ENSO should be taken with caution and studied further with other more recent datasets such as MODIS or with in situ data that I did not have time to investigate. The proximity of the Agulhas Current to those latter domains may have interfered with the coastal domains as the interpolation scheme of the 1 x1˚OI dataset uses data interpolation and correlation in a radius of 300 Km for 1˚x1˚resolution OI SST to replace missing data, and the Agulhas Current is quite close to those coastal areas. There are also some differences in time

series especially from 1982 to 1985 that seem artificial and maybe those years should be removed altogether. All the above may explain the differences in trends and in interannual variability. Another concern is the lack of correlation within certain months when the preceding and following months are significantly correlated. Also, the lack of correlation at zero lag while there are significant correlations at longer lags are concerning and possibly the dataset (35 years) is not long enough or that it takes a few months for the signal to reach southern Africa or to warm the Indian and Atlantic Oceans which in turn could influence the global atmospheric circulation. However, no lag correlation has ever been attempted for the SST relationship with ENSO for the South African coastline. It is possible that several mechanisms are responsible for the ENSO correlation at different times of the year and with different mechanisms. The large-scale forcing has not been shown before and shows that the upwelling regions and the domains are quite small compared to the large-scale forcing; a small shift in latitude and longitudinal in the large-scale forcing could effect a change. The smaller the region, the lower the correlation. The same can be said for the time scale. In general climatologists use large regions to correlate rainfall to ENSO in southern Africa over periods of several months, sometimes 3 to 5 months. The results show that monthly scales and small regions may lead to relatively weak correlations. There are also sometimes slight discrepancies in the ERA 5 composites and the OI SST composites, but in general stronger than normal winds lead to cold anomalies and weaker than normal winds lead to higher than normal SST.

## CHAPTER 6: CONCLUSION

Results show significant positive correlations with El Niño for the West Coast and South Coast in summer at the monthly scale, reaching a maximum up to R=0.45 with up to 3 months lag. Correlation is higher in late summer. There is an also a symmetric negative correlation in the Agulhas Retroflection domain south of Africa mostly in the retroflection area and in the Agulhas Return Current. The ENSO impact on the coast of South Africa, especially West Coast and South Coast is due to changes in wind speed with weaker upwelling-favorable winds during El Niño, leading to warmer than normal coastal waters; during la Niña there are stronger than normal south-easterly winds leading to colder than normal coastal waters. The wind perturbation is part of a large-scale basin-wide perturbation in the tropical Atlantic and in the South Atlantic High-pressure system, as well as changes in the westerly wind pattern to the South. Non-ENSO related impacts on the South African coastline can be as important as ENSO-related SST perturbations and are also linked to large-scale perturbations in the South Atlantic. There is no relation between the strength of ENSO and the strength of the perturbation, and some ENSO events do not lead to the expected canonical change. The large-scale SST perturbations seem to be caused by anomalous surface turbulent flux of latent

and sensible heat and abnormal wind speeds and directions. This study opens the road for seasonal forecasting of SST in the Benguela upwelling system because of the positive lag correlation between ENSO and SST, with ENSO leading SST particularly for the West Coast. Differences between the SST datasets and missing data due to clouds near the coast are a concern and coastal observing and measuring systems need to be upgraded properly and calibrated and long time-series maintained. The origins of discrepancies in the datasets need to be understood and datasets improved. More needs to be done to understand the large scale forcing during ENSO events or during ENSO-neutral years by examining the impact of other modes of natural variability such as the AMO and SAM. The SST trends in West Coast and Agulhas Retroflection domains have decreased, suggesting that decadal variability is at work, or that trends have stopped or slowed down. This should also be examined further. To conclude, the use of 0.25 x 0.25˚OI SST should be extended further south inthe West Coast domain and maybe in a larger offshore domain than in the present thesis. The Agulhas Retroflection domain used by Rouault et al. (2010) can be improved and it seems that 0.25 x 0.25˚OI SST represents the Agulhas Current better. Further work should look at the large scale atmospheric and ocean forcing in more detail and include other coastal areas of southern Africa (Namibia and Angola) as well as the core of the Agulhas Current. Further work needs also to integrate other satellite products and in situ data to look at specific ENSO events described and examine the impact of these changes on marine ecosystems.

## REFERENCES


Banzon, V., Smith, T.M., Chin, T.M., Liu, C.Y. and Hankins, W., (2016) A long-term record of blended satellite and in situ sea-surface temperature for climate monitoring, modeling and environmental studies.

Blamey, L. K., L. J. Shannon, J. J. Bolton, R. J. M. Crawford, F. Dufois, H. Evers King, C. L. Griffiths, L. Hutchings, A. Jarre, M. Rouault, K. Watermeyer, H. Winker (2015) Ecosystem change in the southern Benguela and the underlying processes. Journal of Marine Systems. 144: 9-29

Chiang, J. & Sobel, A. (2001) Tropical Tropospheric Temperature Variations Caused by ENSO and Their Influence on the Remote Tropical Climate*. Journal of Climate. 15 DOI:10.1175/1520- 0442(2002)015.

Dieppois B, M Rouault and M New (2015) "The impact of ENSO on Southern African rainfall in CMIP5 ocean atmosphere coupled climate models." Climate Dynamics,45,9, 2425-2442. DOI 10.1007/s00382-015-2480-x

Crétat, J., Richard, Y., Pohl, B., Rouault, M., Reason, C. and Fauchereau, N. (2012) Recurrent daily rainfall patterns over South Africa and associated dynamics during the core of the austral summer. International Journal of Climatology. doi: 10.1002/joc.2266

Dieppois, B., Pohl, B., Rouault, M., New, M., Lawler, D. & Keenlyside, N. (2016) Interannual to interdecadal variability of winter and summer southern African rainfall, and their teleconnections. Journal of Geophysical Research: Atmospheres. 121(11):6215-6239. doi: 10.1002/2015JD024576

Dijkstra, H. (2006) The ENSO phenomenon: Theory and mechanisms. Advances in Geosciences. 6 DOI:10.5194/adgeo-6-3-2006.

Dufois, F. and Rouault, M. (2012) Sea surface temperature in False Bay (South Africa): Towards a better understanding of its seasonal and inter-annual variability. Continental Shelf Research. 43:24-35. DOI: 10.1016/j.csr.2012.04.009

Dufois, F., Penven, P., Whittle, C.P. and Veitch, J. (2012) On the warm nearshore bias in Pathfinder monthly SST datasets over Eastern Boundary Upwelling Systems. *Ocean Modelling*, *47*, pp.113-118.

Fauchereau; B. Pohl, CJR Reason, M Rouault and Y. Richard (2009) Recurrent daily OLR patterns in the Southern Africa / Southwest Indian Ocean region, implications for South African rainfall and teleconnexions. Climate Dynamics. DOI: 10.1007/s00382-008-0426-2

Florenchie, P., CJC Reason, JRE Lutjeharms, M. Rouault, C. Roy and S. Masson (2004) Evolution of Interannual Warm and Cold events in the South-East Atlantic Ocean, Journal of Climate. 17, 2318–2334

Fauchereau N., S. Trzaska , M. Rouault , Y. Richard (2003) Rainfall Variability and Changes in Southern Africa during the 20th Century in the Global Warming Context, Natural Hazards, Volume 29, Issue 2, pp. 139

Florenchie, P., JRE Lutjeharms, C.J.C Reason, S. Masson and M. Rouault (2003) Source of the Benguela Niños in the Atlantic Ocean, Geophysical Research Letter, Vol. 30 No. 10 10.1029/2003GL017172

Hutchings, L., Van der Lingen, C.D., Shannon, L.J., Crawford, R.J.M., Verheye, H.M.S., Bartholomae, C.H., Van der Plas, A.K., Louw, D., Kreiner, A., Ostrowski, M. and Fidel, Q., (2009) The Benguela Current: An ecosystem of four components. *Progress in Oceanography*, *83*(1-4), pp.15-32.

Imbol Koungue R.A., Illig S. and M Rouault 2017 Role of interannual Kelvin wave propagations in the equatorial Atlantic on the Angola Benguela Current system. Geophys. Res. Oceans, 122, 4685–4703, doi:10.1002/2016JC012463

Imbol Nkwinkwa N., A.S.; Rouault, M.; Johannessen, J.A. Latent Heat Flux in the Agulhas Current 2020 Remote Sens. 2019, 11, 1576.

Imbol Koungue, R. A., Rouault, M.,Illig, S., Brandt, P., & Jouanno, J. (2019) Benguela Niños and Benguela Niñas in forced ocean simulation from 1958 to 2015.Journal of Geophysical Research:Oceans,124.

Johnston P. A., E. R. M. Archer, C. H. Vogel, C. N. Bezuidenhout, W. J. Tennant and R. Kuschke. (2004) Review of seasonal forecasting in South Africa. Climate Research. 28(1):67-82. DOI:10.3354/cr028067

Kainge, P., Kirkman, S., Estevão, V., van der Lingen, C.D., Uanivi, U., Kathena, J.N., van der Plas, A., Githaiga-Mwicigi, J., Makhado, A., Nghimwatya, L. and Endjambi, T., 2020. Fisheries yields, climate change, and ecosystem-based management of the Benguela Current Large Marine Ecosystem. *Environmental Development*, p.100567.

Krug M and J. Tournadre (2012) Satellite observations of an annual cycle in the Agulhas Current. Geophys. Res. Lett., 39, L15607, doi:10.1029/2012GL052335

Landman , W.A and S.J. Mason. (2001) Forecasts of Near-Global Sea Surface Temperatures Using Canonical Correlation Analysis. Journal of Climate. 14(18):3819-3833.

Landman, W.A., Barnston, A.G., Vogel, C. and Savy, J., (2019) Use of El Niño–Southern Oscillation related seasonal precipitation predictability in developing regions for potential societal benefit. *International Journal of Climatology*, *39*(14), pp.5327-5337.

Lakhraj-Govender, R. and Grab, S.W., (2019) Assessing the impact of El Niño–Southern Oscillation on South African temperatures during austral summer. *International Journal of Climatology*, *39*(1), pp.143-156.

Mead A, C L Griffiths, G M Branch, C D McQuaid, L K Blamey, J J Bolton, R J Anderson, F Dufois, M Rouault, P W Froneman, A K Whitfield, L R Harris, R Nel, D Pillay, J B Adams (2013) Human- mediated drivers of change: impacts on coastal ecosystems and marine biota of South Africa, 35, 3, 403-425

Meneghesso, C., Seabra, R., Broitman, B.R., Wethey, D.S., Burrows, M.T., Chan, B.K., Guy-Haim, T., Ribeiro, P.A., Rilov, G., Santos, A.M. and Sousa, L.L., (2020) Remotely sensed L4 SST underestimates the thermal fingerprint of coastal upwelling. *Remote Sensing of Environment*, *237*, p.111588.

Philander SG (1990) El Niño, La Niña, and the Southern Oscillation. Academic Press, London, p 289

Pohl B, Dieppois B, Crétat J, Lawler D, Rouault M. 2018, From synoptic to interdecadal variability in southern African rainfall: towards a unified view across timescales. Journal of Climate, 31, 5845-5872, DOI:10.1175/JCLI-D-17-0405.

Pfaff, MC, Logston, RC, Raemaekers, SJPN, Hermes, JC, Blamey, LK, Cawthra, HC, Colenbrander, DR, Crawford, RJM, Day, E, du Plessis, N, Elwen, SH, Fawcett, SE, Jury, MR, Karenyi, N, Kerwath, SE, Kock, AA, Krug, M, Lamberth, SJ, Omardien, A, Pitcher, GC, Rautenbach, C, Robinson, TB, Rouault, M, Ryan, PG, Shillington, FA, Sowman, M, Sparks, CC, Turpie, JK, van Niekerk, L, Waldron, HN, Yeld, EM and Kirkman, SP. 2019. A synthesis of three decades of socio-ecological change in False Bay, South Africa: setting the scene for multidisciplinary research and management. Elem Sci Anth, 7: 32. DOI: https://doi.org/10.1525/elementa.367

Phillipon N, Rouault M Richard Y, Favre (2012) on the impact of ENSO on South Africa winter rainfall International Journal of Climatology, DOI: 10.1002/joc.3403

Reynolds, R.W., Rayner, N.A., Smith, T.M., Stokes, D.C. and Wang, W. (2002) An improved in situ and satellite SST analysis for climate. *Journal of climate*, *15*(13), pp.1609-1625.

Reynolds, R.W., Smith, T.M., Liu, C., Chelton, D.B., Casey, K.S. and Schlax, M.G. (2007) Daily high-resolution-blended analyses for sea surface temperature. *Journal of Climate*, *20*(22), pp.5473-5496.

Rouault M. and Y. Richard, (2003) Spatial extension and intensity of droughts since 1922 in South Africa, Water SA 29, 489-500

Rouault M and Y Richard (2005) Intensity and spatial extent of droughts in Southern Africa. Geophysical Research Letters 32, L15702, 4 PP., 2005 doi:10.1029/2005GL022436

Rouault, M., S. Illig, C. Bartholomae, C.J.C. Reason and A. Bentamy (2007) Propagation and origin of warm anomalies in the Angola Benguela upwelling system in 2001. J. Mar. Syst., 68, 477-488

Rouault M, P Penven and B Pohl, Warming of the Agulhas Current since the 1980's (2009) Geophys. Res. Lett., 36, L12602, doi:10.1029/2009GL037987

Rouault, M., Pohl, B. & Penven, P. (2010) Coastal oceanic climate change and variability from 1982 to 2009 around South Africa. African Journal of Marine Science. 32(2):237-246. DOI:10.2989/1814232X.2010.501563

Rouault, M., Illig, S., Lübbecke, J. and Koungue, R.A.I., (2018) Origin, development and demise of the 2010–2011 Benguela Niño. Journal of Marine Systems. 188, 39-48 https://doi.org/10.1016/j.jmarsys.2017.07.007

Smit, A.J., Roberts, M., Anderson, R.J., Dufois, F., Dudley, S.F., Bornman, T.G., Olbers, J. and Bolton, J.J., (2013) A coastal seawater temperature dataset for biogeographical studies: large biases between in situ and remotely sensed data sets around the coast of South Africa. *PLoS One*, *8*(12).

Veitch, J., Penven, P. and Shillington, F., (2009) The Benguela: A laboratory for comparative modeling studies. *Progress in Oceanography*, *83*(1-4), pp.296-302.

Yulaeva, E. & Wallace, J.M. (1994) The Signature of ENSO in Global Temperature and Precipitation Fields Derived from the Microwave Sounding Unit. Journal of Climate. 7(11):1719- 1736. DOI:10.1175/1520-0442(1994)007.

Yu, L., X. Jin, and R. A. Weller (2006) Role of net surface heat flux in the seasonal evolution of sea surface temperature in the Atlantic Ocean. *Journal of Climate*, **9(**23**)**, 6153-6169, https://doi.org/10.1175/JCLI3970.1.

Wang, Chunzai, Clara Deser, Jin-Yi Yu, Pedro DiNezio, and Amy Clement (2017) "El Niño and southern oscillation (ENSO): a review." In *Coral reefs of the eastern tropical Pacific*, pp. 85-106. Springer, Dordrecht.